

The Maragheh bovids (Mammalia, Artiodactyla): systematic revision and biostratigraphic-zoogeographic interpretation

Dimitrios S. KOSTOPOULOS

University of Thessaloniki, Department of Geology,
GR-54124 Thessaloniki (Greece)
dkostop@geo.auth.gr

Raymond L. BERNOR

College of Medicine, Department of Anatomy,
Laboratory of Evolutionary Biology, Howard University,
520 W St. Northwest, Washington, DC 20059 (USA)
rbernor@comcast.net

Kostopoulos D. S. & Bernor R. L. 2011. — The Maragheh bovids (Mammalia, Artiodactyla): systematic revision and biostratigraphic-zoogeographic interpretation. *Geodiversitas* 33 (4): 649-708. DOI: 10.5252/g2011n4a6.

ABSTRACT

A comprehensive systematic review of the Bovidae from the fossiliferous sites of Maragheh, Iran, based mainly on the collections stored in the Muséum national d'Histoire naturelle, Paris and the Laboratory of Evolutionary Biology in Howard University, Washington, DC, is undertaken here. We identify 18 species, including the newly nominated genus *Demecquenemia* n. gen. We further recognize two species of *Gazella* Blainville, 1816, four species of *Prostrepsiceros* Major, 1891, including *Pr. cf. vinayaki* (Pilgrim, 1939) that is documented for the first time in Maragheh, as well as the presence of *Palaeoryx* Gaudry, 1861 and the possible presence of *Palaeoreas* Gaudry, 1861. Our revision includes new material and improved systematic understanding of both *Urmiatherium polaki* Rodler, 1889 and of the boselaphines from Maragheh. The biostratigraphic distribution of Maragheh Bovidae is discussed in the light of the new data and a thorough comparison of the Maragheh bovid assemblage with those of Pikermi, Samos and other sites in the region is conducted. We demonstrate that Maragheh was a biogeographic crossroads of several Late Miocene zoogeographic provinces of Eurasia.

KEY WORDS

Mammalia,
Artiodactyla,
Bovidae,
Turolian,
Maragheh,
biostratigraphy,
palaeozoogeography,
large mammals,
new genus.

RÉSUMÉ

Bovidés de Maragheh (Mammalia, Artiodactyla): révision systématique et interprétation biostratigraphique et zoogéographique.

Un ré-examen exhaustif de la systématique des bovidés des sites fossilifères de Maragheh, Iran, basé principalement sur les collections du Muséum national d'Histoire naturelle, Paris et du Laboratory of Evolutionary Biology, Howard University, Washington, DC permet d'identifier 18 espèces, l'une d'entre elles

MOTS CLÉS

Mammalia,
Artiodactyla,
Bovidae,
Turolien,
Maragheh,
systématique,
biostratigraphie,
paléozoogéographie,
grands mammifères,
genre nouveau.

rattachée à un nouveau genre, *Demecquenemia* n. gen. Deux espèces de *Gazella* Blainville, 1816 et quatre espèces de *Prostrepsiceros* Major, 1891 sont reconnues, y compris *Pr. cf. vinayaki* (Pilgrim, 1939) qui est documenté pour la première fois à Maragheh, ainsi que les genres *Palaeoryx* Gaudry, 1861 et probablement *Palaeoreas* Gaudry, 1861. De plus, le matériel nouveau et révisé précise la systématique d'*Urmiatherium polaki* Rodler, 1889 et des boselaphinés de Maragheh. La répartition biostratigraphique des bovidés de Maragheh est examinée à la lumière des nouvelles données et une comparaison approfondie de l'assemblage des bovidés de Maragheh avec ceux de Pikermi, Samos et d'autres sites dans la région est menée, aboutissant à des conclusions paléogéographiques généralisées et à l'identification de Maragheh comme un carrefour de plusieurs provinces zoogéographiques du Miocène supérieur d'Eurasie.

INTRODUCTION

Early and later expeditions in the famous Maragheh fossil-site complex (Iran; 37°22'N, 46°14'40"E; Fig. 1) led to one of the most impressive Eurasian fossil mammal collections, housed today by several museums and institutions across the world (Mecquenem 1908, 1925; Bernor 1978, 1986; Watabe & Nakaya 1991; Bernor *et al.* 1996). Bernor (1986), Bernor *et al.* (1996) and Mirzae Ataabadi *et al.* (in press) presented evidence for a chronological range of nearly 9.0 to less than 7.6 Ma for the Maragheh fauna, which is regarded as representing the easternmost boundary of the late Miocene Greco-Iranian Province of Bonis *et al.* (1979) or the approximate geographic center of the Sub-Paratethyan zoogeographic province (Bernor *et al.* 1979; Bernor 1983).

As in several late Miocene mammal assemblages, bovids are amongst the most abundant and diversified mammal groups in the Maragheh fauna. The existing faunal lists (Table 1) record up to 23 bovid taxa but in the most recent review, Bernor *et al.* (1996) recognized 14 bovid species (including *O. atropatenes* (Rodler & Weithofer, 1890) mistakenly omitted from their list) (Table 1). Most of these taxa are thought to come from the middle fossiliferous horizons corresponding to the -52 to -28 m stratigraphic interval (Bernor 1986). Apart from primary systematic studies by Pohlig (1886), Rodler (1888, 1889), Rodler & Weithofer (1890) and Mecquenem (1908, 1925), several later authors

revised particular bovid groups recovered at Maragheh (e.g., Heintz 1963; Gentry 1971; Solounias 1981; Bouvrain 1982, 1992, 1996; Bosscha-Erdbrink 1988; Watabe 1990). Even so, in most cases the species definitions, based mainly on specimens in the Paris collection, are too fragmentary and sometimes conflicting enough to provide a reliable synthesis of the Maragheh bovid association.

In order to have a more accurate and up-to-date taxonomy, a revision of the entire Maragheh bovid assemblage is provided here. Two basic sources of evidence have been used: the Maragheh collection in the Muséum national d'Histoire naturelle, Paris and the Maragheh MMTT-Howard sample in the Laboratory of Evolutionary Biology, Washington, DC. The MNHN.F Maragheh collection was briefly communicated by Mecquenem (1908, 1925). Thanks to the great efforts of the MNHN.F staff, this collection has recently been curated allowing proper arrangement and storage. The International Lake Rezaieyeh Expedition (1974-1976) led by Bernard Campbell (Bernor 1978; Campbell *et al.* 1980) successfully pursued a stratigraphically controlled collection from the Maragheh Basin, part of which is temporary stored in HUW. Selected specimens from the Naturhistorisches Museum, Vienna, the Natural History Museum, London and the Kyoto University Expedition are also discussed. The present work concentrates on the systematic identification and comparison of the Maragheh Bovidae and their stratigraphic and biogeographic distribution.

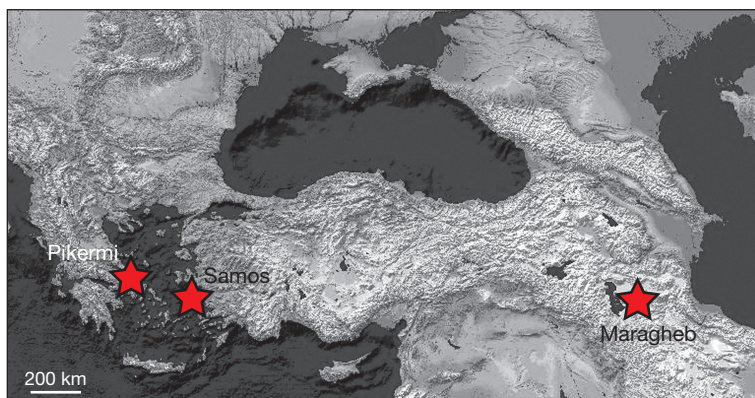


Fig. 1. — Geographic location of Maragheh, Samos and Pikermi, Iran.

METHODOLOGY

Tooth nomenclature is according to Heintz (1970). All measurements are in millimeters. Upper-case letters are for the maxillary teeth and lower-case letters for the mandibular teeth. In the absence of cranial material, size fit, occlusal matching criteria and dental morphological compatibility with well-known species from other sites (especially from Samos, Pikermi and Axios Valley sites) are followed for testing correspondence between upper and lower dentitions incorporated into the same Maragheh taxon. For the sake of economy, the bulk of descriptions follow a general inventory of the main morphological characters of each species based on all available Maragheh specimens instead of a description of each specimen separately, unless this was necessary. Finally, descriptions and comparisons are unevenly weighted in several cases, as attention was particularly paid on what was missing from existing Maragheh literature.

ABBREVIATIONS

Museums and institutions

AMNH	American Museum of Natural History, New York;
HUW	Howard University, Laboratory of Evolutionary Biology, Washington, DC;
MGPUA	Museum of Geology & Paleontology, Athens University;
MNHN	Muséum national d'Histoire naturelle, Paris;

NHML	Natural History Museum, London;
NHMW	Naturhistorisches Museum, Vienna.

Collections and expeditions

KUE	Kyoto University Expedition;
LRE	Lake Rezaieyh Expedition;
MMTT	fossils from Maragheh localities of LRE deposited either in Tehran or in Washington, DC;
MNHN.F	MNHN, collection of Palaeontology.

Descriptions and measurements

APD _{hc7}	anteroposterior diameter at 7 cm above the horn-core base and along the main axis;
APD _{hcb}	anteroposterior diameter at the horn-core base along the main axis;
CI	horn-core compression index ($TD_{hcb} \times 100 / APD_{hcb}$);
dex	right;
H _{hc}	height of the horn-core measured at the posterior surface as a chord from the base to the tip;
H _{oc}	height of the occiput from the top of the foramen magnum to the top of the occipital protuberance;
L	length;
L _{ahc-ocp}	length from the anterior of horn-cores to the occipital protuberance along the midline;
L _{b-ch}	length from basion to anterior most point of choanae;
L _{b-P2}	length from basion to the anterior of P2 along the midline;
L _{fp-ocp}	length from the frontoparietal suture to the occipital protuberance;
L _{fr}	length of frontals along the midline;

TABLE 1. — List of Bovidae Gray, 1821 recorded at Maragheh (Iran) according to several authors. Abbreviations: **R & W**, Rodler & Weithofer 1890; **de M.**, de Mecquenem 1925; **L**, lower; **M**, middle; **U**, upper Maragheh.

Taxa	R & W	de M.	Bernor 1986	Watabe 1990	Bernor et al. 1996		
					L	M	U
<i>Gazella</i> sp.			+	+			
<i>Gazella deperdita</i>	+		+		+	+	+
<i>Gazella capricornis</i>	+	+			+	+	+
<i>Gazella brevicornis</i>		+					
<i>Gazella gaudryi</i>		+					
" <i>Gazella</i> " <i>rodleri</i>			+			+	
<i>Palaeoryx pallasii</i>	+	+					
<i>Protoryx carolinae</i>		+					
<i>Pachytragus crassicornis</i>			+				+
<i>Pachytragus laticeps</i>			+			+	
<i>Miotragocerus monacensis</i>				+		+	
<i>Tragoportax amalthea</i>	+	+	+		+		
<i>Tragoportax rugosifrons</i>		+	+			+	
<i>Samokeros minotaurus</i>						?	
<i>Protragelaphus skouzei</i>	+	+	+			+	
<i>Prostrepsiceros houtumschindleri</i>	+	+	+	+	+	+	
<i>Prostrepsiceros rotundicornis</i>	+	+	+	+		+	
<i>Oioceros rothii</i>		+	+	+		+	
<i>Oioceros atropatenes</i>	+	+	+	+		(+)	
<i>Oioceros boulei</i>		+	+	+		(+)	
<i>Urmiatherium polaki</i>		+	+			+	
Antilope indet. (large size)		+					
Antilope indet. (small size)		+					

- L_{hc} length of the horn-core along the anterior surface;
- Lm lower molar row length;
- LM upper molar row length;
- L_{nas} length of nasals along the midline;
- Lp lower premolar row length;
- LP upper premolar row length;
- Lpm length p2-m3;
- LPM length P2-M3;
- M/m upper/lower molars;
- MNI minimum number of individuals;
- P/p upper/lower premolars;
- sin left;
- TD_{hc7} transverse diameter at 7 cm above the horn-core base and perpendicularly to APD_{hc7};
- TD_{hcb} transverse diameter at the horn-core base perpendicularly to APD_{hcb};
- W width;
- W_{atb} width of the basioccipital at the anterior tuberosities;

- W_{bc} maximum width of the braincase;
- W_{bcon} bi-condylar width;
- W_{bhc} width of the skull behind the horn-cores;
- W_{bmas} bi-mastoid width;
- W_{or} width of the skull at the orbits;
- W_{ptb} width of the basioccipital at the posterior tuberosities;
- W_{shc} width of the skull at the lateral surfaces of the horn-cores;
- W_{so} distance of the supraorbital pits at their uppermost edge.

SYSTEMATIC PALEONTOLOGY

Order ARTIODACTYLA Owen, 1848
 Family BOVIDAE Gray, 1821

Genus *Gazella* Blainville, 1816

TYPE SPECIES. — *Gazella dorcas* (Linnaeus, 1758).

Gazella capricornis (Wagner, 1848)
 (Fig. 3)

Antilope capricornis Wagner, 1848: 368: pl. 4, fig. 6.

Gazella deperdita – Rodler & Weithofer 1890:14. — Mecquenem 1925: 30, pl. 3, figs 2, 5, 8. — Bernor 1978: 78; 1986: table 1. — Solounias 1981: table 4. — Bernor et al. 1996: table 10.2.

TYPE LOCALITY. — Pikermi, Greece (late Miocene).

MATERIAL EXAMINED. — MNHN.F: Frontlet MAR1031 (Mecquenem 1925: pl. III, fig. 2 as *G. deperdita*), MAR1033; part of skull MAR1034 (old number 8044; Mecquenem 1925: pl. III, fig. 1 as *G. gaudryi*); occipital part of skull MAR1062; right horn-core, MAR1097, 1114, 1392, 1393; left horn-core MAR1032, 1090, 1095, 1098, 1099, 1101, 1111, 1112, 3172; part of horn-core 1088, 1089, 1105, 1116; P2-M3, MAR1028 (Mecquenem 1925: pl. III, fig. 5 as *G. deperdita*); lower tooth row with p2-m3, MAR1027 (Mecquenem 1925: pl. III, fig. 8 as *G. deperdita*), MAR1843. — HUW: skull MMTT13/2583 (MCW59).

DESCRIPTION AND REMARKS

Accounting for the number of the Maragheh *Gazella* species and their taxonomic status remain debatable due to the puzzling alpha taxonomy in late Miocene representatives. Rodler (1885) recognized the oc-

currence of *G. deperdita* (Gervais, 1847) within the Maragheh fauna while Pohlig (1886) reported *G. brevicornis* (Roth & Wagner, 1854) at Maragheh. Later on, Rodler & Weithofer (1890) recognized both of these taxa as occurring at Maragheh and introduced a new taxon, *G. capricornis*, a name that, however, was pre-occupied by Wagner (1848) for the Pikerimian gazelle. Mecquenem (1925) described *G. brevicornis*, “*G. capricornis*” Rodler & Weithofer, 1890 and *G. gaudryi* Schlosser, 1904 (valid name *G. pilgrimi* Bohlin, 1935) from Maragheh. Pilgrim & Hopwood (1928) put in synonymy *G. brevicornis* with *G. capricornis* and proposed the new species name *G. rodleri* for the Maragheh “*G. capricornis*”. Bernor (1978) and Bernor *et al.* (1996) referred to a single gazelle species, *G. deperdita/capricornis* implying either impossibility of distinction or synonymy between these two species. Watabe (1990) refrained from making species identifications for KUE gazelle specimens. Bouvrain (1996) noted that “plusieurs espèces de gazelles sont présentes dans le matériel de Maragha” and attributed the smaller horn-core specimens in the Paris collection to *Gazella cf. gracile* (Korotkevich, 1976). Apart from “*Gazella rodleri* that will be discussed later, the sample currently under study from Maragheh includes 36 cranial and isolated horn-core specimens. Two basic horn-core morphs are indeed present within the Paris sample but their dimensions show a continuous range that prohibits (Fig. 2; Table 2) a sharp distinction between them based on horn-cores alone. Nevertheless, two almost complete skulls in HUW (MMTT13/2583 and MCW80-next section) allow a better taxonomical resolution.

MMTT13/2583 (Fig. 3; Table 3) is slightly deformed and lacks the anterior portion of the maxilla and premaxilla. MAR1034 (Mecquenem 1925: pl. III, fig. 1; Table 3) is badly damaged but still retains most of the cranial roof and maxillae and the proximal part of the horn-cores. MAR1062 preserves only the occipital region but it could belong to the same individual as MAR1034. The braincase is fairly long and widens slightly anteriorly; its top is gently convex in a lateral profile, set at a steep angle to the occipital surface (*c.* 120°), and gently bent on the face (*c.* 145°). The midfrontal suture is slightly constricted between the horn-cores. The

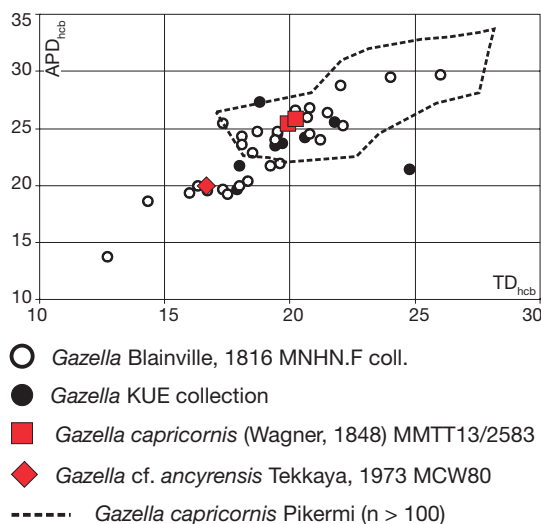


FIG. 2. — Bivariate plots of basal horn-core dimensions in *Gazella* Blainville, 1816 from Maragheh (transverse diameter [TD] against anteroposterior diameter [APD]). KUE data from Watabe (1991).

temporal lines are visible only in their anterior part, directly behind the orbits. The dorsal orbital rims are moderately wide. The orbit is large and round with its anterior margin above the back lobe of M2. The postcornual fossae are usually large, oval-shaped and deep. The supraorbital foramina are placed in small triangular depressions close to the base of the pedicles. The infraorbital foramina open above P3. The lacrimal fossa is large, round, moderately deep with well-marked ventral rim and close to the orbit. The ethmoidal fissure is short and narrow. The nasals are shorter than the frontals, weakly domed in lateral profile, without lateral flanges, wider posteriorly than anteriorly, with bilobed fronto-nasal suture, and broadly pointed anteriorly. The premaxillae are in contact with the nasals. The occipital is semicircular shaped and faces partly laterally. The external occipital crest is weak. The mastoid is narrow and faces mostly posteriorly. The foramen magnum is approximately square-shaped and wider than high. The occipital condyles are rather small. The basioccipital is moderately long with strong, ridge-like posterior tuberosities perpendicular to the sagittal plane and small to moderate anterior tuberosities well-localized and developed mostly ventrally. A thin crest runs the length of the

TABLE 2. — Horn-core measurements (in mm) of *Gazella* Blainville, 1816 species from Maragheh. For abbreviations see text.

Collection no.		TD _{hcb}	APD _{hcb}	TD _{hc7}	APD _{hc7}	L _{hc} /H _{hc}
<i>Gazella capricornis</i> (Wagner, 1848)						
MNHN.F						
MAR1031	dex	26.00	29.70	18.20	20.70	135/110
	sin	22.00	28.80	16.00	18.00	
MAR1033	dex	20.70	26.00	14.80	17.90	105/89.5
	sin	20.20	26.60	14.60	17.60	
MAR1034	dex	19.50	24.80			
	sin	18.70	24.80			
MAR1393	dex	20.80	24.50			
MAR1392	dex	20.80	26.80	14.30	16.60	
MAR1114	dex	17.30	25.50			
MAR1112	sin	19.40	24.00			
MAR1098	sin	21.50	26.40			115/92
MAR3172	sin	19.20	21.70			77/72
MAR1090	sin	19.60	22.00	11.50	13.00	90/76
MAR1095	sin	21.20	24.00	13.20	13.70	
MAR1032	sin	18.10	24.30	10.30	13.10	90/76
MAR1101	sin	24.00	29.50	15.80	17.60	110/86
MAR1097	dex	22.10	25.30	12.90	16.60	
MAR1111	sin	18.50	22.90			
MAR1099	sin	18.10	23.60			
HUW						
MMTT13/2583	dex	19.70	25.50	14.90	16.90	120/95
	sin	20.10	25.90	15.20	16.80	
<i>Gazella cf. ancylensis</i> Tekkaya, 1973						
MNHN.F						
MAR1094	sin	16.70	19.60	7.20	7.20	90/84
MAR1096	sin	18.00	20.00			
MAR1091	sin	17.50	19.30			
MAR1092	dex	18.30	20.40			
MAR1113	dex	16.00	19.40			
MAR1088		14.30	18.60			c. 70/-
MAR1116		12.70	13.80			c. 50/-
MAR1117	dex	17.30	19.70			70/64
	sin	16.30	20.00			
HUW						
MCW80		16.70	19.80			

basioccipital bone. The auditory bulla is large and bulbous. The external auditory meatus is large and almost round. The palatine foramina open at the level of the anterior lobe of M3. The choanae are “V”-shaped and open at the posterior limit of M3 and slightly anteriorly to the lateral indentations. The pedicles are rather short. The horn-cores are moderately long (maximum 135 mm) inserted above the orbits and set well apart at their bases. They are fairly curved (index L_{hc}/H_{hc} [Kostopoulos 2005]: 1.06-1.23, $n = 9$) and weakly inclined back-

wards, showing moderate mediolateral compression throughout their length (mean compression index, CI = 81% at the base, $n = 29$; mean CI at 7 cm above the base = 87%, $n = 12$) (Table 2). The horn-core divergence is usually of the “V”-type (at about 45°), although in a few specimens this angle may be wider (MAR1037). The parallel horn-cores seen on the specimen MAR1033 are obviously due to distortion of the frontals, whereas MAR1031 does not differ enough from the basic morphotype to be excluded (*contra* to Bouvrain 1996). The longer

axis of the horn-core base trends anteroposteriorly, forming an acute angle with the sagittal plane. Longitudinal furrows run along the antero-medial and posterior faces of the horn-cores.

The skull morphology (long opisthocranium, weak slope of the cranial roof on the face, wide dorsal orbital rims, flat and wide fronto-nasal region, short and domed nasals, small occipital condyles, rectangular basioccipital, deep and large postcornual fossae, moderately long, weakly tilted, fairly curved backwards and moderately compressed mediolaterally horn-cores) are clearly different from those of *G. pilgrimi* from Axios valley (MNHN.F.Slq809) and Samos and very similar to those of *G. capricornis* from Pikermi (NHML M11440, MNHN.F.PIK2001, MGPUA PA1355/91). Comparison of the horn-core proportions between the Pikermi and the Maragheh samples does not show important size differences (Fig. 2), whereas the horn-cores of *G. deperdita* from Mont Luberon (France) appear more compressed mediolaterally (mean CI = 75% at the base, n = 31; mean CI = 74% at 7 cm above the base, n = 31).

The length of the upper molar row ranges from 33.7 mm (MAR1034) to 34.4 mm (MAR1028) (Table 4). As in *G. capricornis* and *G. deperdita* and unlike *G. pilgrimi* the paracone rib of the Maragheh P4 is vertically placed and the parastyle of the upper molars is strong. Only a couple of lower toothrows can be securely attributed to this species (Table 5). The lower premolar row represents 58.8–61.8% of the molars (Fig. 4). The parastylid of the lower molars is well-developed, the p3 is simple with well-developed paraconid and the p4 has a strong paraconid and a subtriangular metaconid, which leaves the posterior valley open until an advanced stage of wear, in contrast to *G. deperdita* (Heintz 1971).

Gazella cf. ancylensis Tekkaya, 1973
(Fig. 5)

Gazella ancylensis Tekkaya, 1973: 118, pl. 1, figs 1, 2; pl. 2, fig. 1.

Gazella gaudryi – Mecquenem 1925: 30, pl. 3, figs 1, 4.

Gazella cf. gracile – Bouvrain 1996: 113.

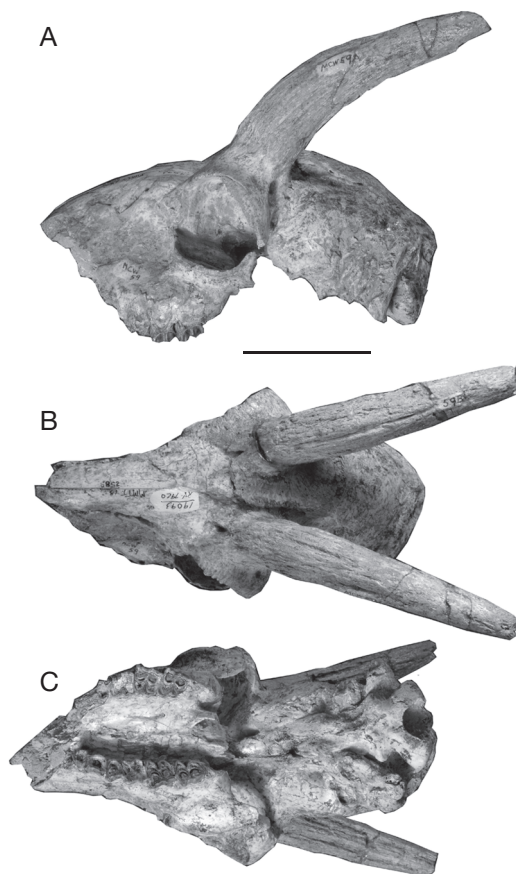


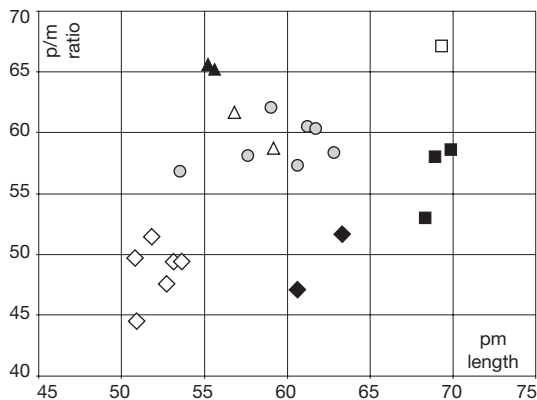
FIG. 3. — *Gazella capricornis* (Wagner, 1848) cranium MM13/2583 from Maragheh in lateral (A), dorsal (B) and ventral (C) views. Scale bar: 5 cm.

TYPE LOCALITY. — Middle Sinap, Turkey (late Miocene).

MATERIAL EXAMINED. — MNHN.F: frontlet MAR1117; right horn-core, MAR1092, 1113; left horn-core, MAR1091, 1094, 1096; isolated horn-cores, MAR1088, 1116. — HUW: skull (cranium and mandible) MCW80.

DESCRIPTION AND REMARKS

MCW80 is from the MMTT13 locality; it lacks the anterior part of the muzzle and the basioccipital whereas the horn-cores are broken just above their contact with the pedicles (Fig. 5; Table 3). The braincase is rather short and bulbous with anteriorly widened lateral sides. The cranial roof curves significantly down posteriorly and moder-



- ▲ *Gazella cf. ancyrensis* Tekkaya, 1973
- △ *Gazella capricornis* (Wagner, 1848)
- ◇ *Oioceros atropatenes* (Rodler & Weithofer, 1890)
- *Oioceros rothii* (Wagner, 1857)
- ◆ *Prostrepsiceros cf. vinayaki* (Pilgrim, 1939)
- *Prostrepsiceros houtumschindleri* (Rodler & Weithofer, 1890)
- *Prostrepsiceros fraasi* (Andree, 1926)

FIG. 4. — Bivariate scatter plots of lower tooththrow dimensions (tooththrow length [pm length] against premaxilar/molar ratio [p/m ratio]) in several bovids from Maragheh.

ately bent on the face (125°). The frontoparietal suture is quite complicated and “T”-shaped. The temporal lines are smooth but visible and converge to the rear forming a low hump in the intraparietal

region. The midfrontal suture is simple and not raised like a crest. The dorsal orbital rims project moderately and the orbits are large and oval-shaped. The anterior margin of the orbit is placed above the anterior lobe of M3. The ethmoidal fissure is long and narrow extended anteriorly above P4-M1 limit and equally bordered by the lacrimal, maxilla, nasal and frontal bones. The premaxillae are in contact with the nasals. The infraorbital foramina open above P3. The lacrimal fossa is large and shallow. The supraorbital foramina are small, sunken into oval-shaped pits that are placed on the base of the pedicles. The postcornual fossae are rather large and shallow. The nasals are longer than the frontals with weak lateral flanges at their anterior part and long fronto-nasal suture of inverse “V” outline. The choanae are “U”-shaped and open at the posterior limit of M3, slightly behind the lateral indentations. The horn-cores are inserted above the back half of the orbital roof, widely apart from each other and strongly inclined backwards. Their basal dimensions are similar to those of the second gazelle morphotype in MNHN.F (Fig. 2, Table 2), which is characterized by rather short (maximum length 90 mm) and slender horn-cores with round cross-section (mean CI = 86% at the base, n = 9; and 100% at 7 cm above the base, n = 1) and weak posterior curvature.

The teeth are moderately hypsodont with high and sharp labial cusps. The upper molars have well-developed styles and ribs and lack central is-

TABLE 3. — Comparison of *Gazella* Blainville, 1816 skull measurements (in mm) from Maragheh, Pikermi and Axios valley. For abbreviations see text.

	<i>G. capricornis</i> (Wagner, 1848)			<i>Gazella cf. ancyrensis</i>	<i>Gazella pilgrimi</i>
	MNHN.F. MAR1034	HUW MMTT13/2583	MNHN.F. PIK2001	Tekkaya, 1973 HUW MCW80	Bohlin, 1935 MNHN.F.SIq809
L _{fr}	(58)	60.00	65.00	45.70	48.80
L _{nas}		55.40	61.60	59.30	
LP		22.00		23.20	
LM	33.70	28.8	30.50	31.70	30.00
W _{or}		83.00	81.30	82+	(71)
W _{bc}	55.00	50.60	56.50	54.70	51.10
W _{so}	32.70	32.50	34.00	36.20	33.90
W _{shc}	66.60	62.80	71.40	50.30	59.50
W _{bmas}		(52)			
W _{bcon}		32.60			
W _{ptb}		25.00			

lets or basal pillars. The upper premolars represent *c.* 72% of the molar row (Table 4). The P2 and P3 are trapezoidal shaped, weakly molarized lingually and have the paracone in mesial position. The i1 is much wider than the i2 and i3. The lower premolar row is rather long compared to the molars (*c.* 65%; Fig. 4, Table 5). The hypoconid of p3 and p4 is narrow, angular and protrudes labially. The paraconid is well-separated from the parastyloid in both the p3 and p4, the anterior valley remains widely open, and the entoconid is fused quickly with the entostyloid. The metaconid of the p3 is simple and distally directed, whereas on the p4 it is distally placed and triangular-shaped in occlusal view. The m1 bears a small basal pillar that is reduced to a knob on m2. The parastyloid is weakly developed and more salient on the m3 than on the m1-m2.

Apart from the differences on the horn-core pattern, the described species is distinguished from *Gazella capricornis* from Maragheh in having *c.* 30% shorter and 10% wider opisthocranium curved down posteriorly, longer nasals compared to the skull size, “U”-shaped choanae behind the lateral indentations, longer ethmoidal fissure, stronger temporal lines, shorter molar row and highly browsing mesowear teeth pattern. Small *Gazella*-like horn-core specimens are frequent in several early Turolian mammal sites of Anatolia but the usual absence of corresponding skulls make their taxonomic status uncertain. Bouvrain (1996) provisionally ascribed those Maragheh specimens to *Gazella gracile*, a species originally described from Berislava (Ukraine) as a small subspecies of *G. schlosseri* Pavlow, 1913. Although the Maragheh horn-cores have similar size with those from Berislava, their morphology differs significantly in the absence of both the characteristic basal swelling and the faintly sigmoid anterior profile, the less deep longitudinal furrows and the longer pedicles. On the contrary, the horn-core proportions of the small specimens from Maragheh match those from Garkin, Kemiklipe D (Turkey; Bouvrain 1994) and lower fossil levels of Samos (Kostopoulos 2009a), suggesting the presence of a distinct small-sized *Gazella* species. Based on a single horn-core and some dental and postcranial remains, Tekkaya (1973) described from Vallesian levels of Middle Sinap (Turkey) a

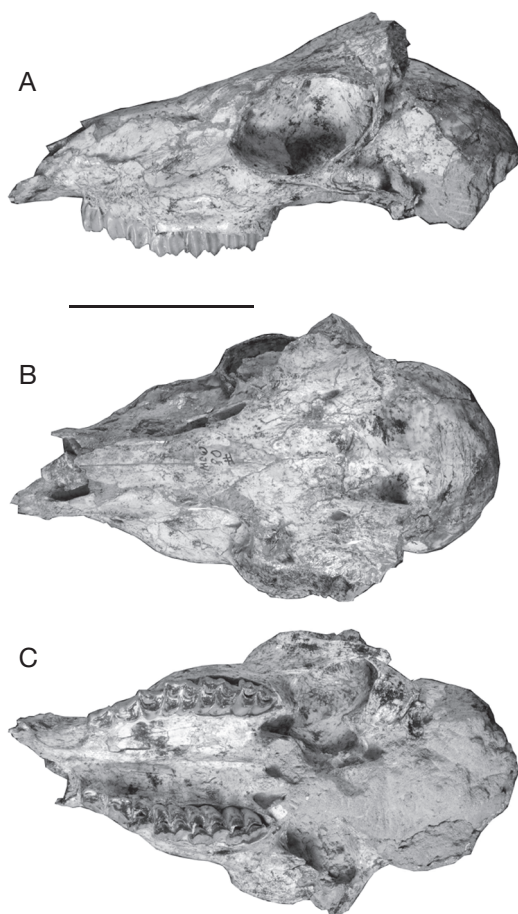


FIG. 5. — *Gazella cf. ancyrensis* Tekkaya, 1973 cranium (MCW80) from Maragheh in lateral (A), dorsal (B) and ventral (C) views. Scale bar: 5 cm.

new gazelle, *G. ancyrensis* with small, straight and weakly compressed mediolaterally horn-cores, having some strong longitudinal furrows on the anterior and posterolateral sides. Unfortunately, new material from Middle Sinap did not provide additional information (Gentry 2003). By their size, insertion and overall shape, the Maragheh horn-cores are more like those of *G. ancyrensis*, even though they show a more accentuated posterior curvature and stronger longitudinal furrows, characters that may, however, vary significantly within a gazelle species. The features of the teeth allocated by Tekkaya (1973) to *G. ancyrensis* also fit those of the Maragheh gazelle,

TABLE 4. — Upper tooth row measurements (in mm) of several Maragheh bovids. For abbreviations see text.

	LP	LM	LPM
<i>Gazella capricornis</i> (Wagner, 1848)			
MNHN.F.MAR1034		33.70	
MNHN.F.MAR1028		34.40	
MMTT13/2583	22.00	28.76	50.00
<i>Gazella cf. ancyrensis</i> Tekkaya, 1973			
MCW80	23.20	31.70	53.00
MCWb	22.40	31.40	52.30
<i>Oioceros atropatensis</i> (Rodler & Weithofer, 1890)			
MNHN.F.MAR1121	18.30	26.80	44.70
MNHN.F.MAR3141	17.70	28.70	46.80
MNHN.F.MAR3146	21.00	31.70	52.05
MNHN.F.MAR1849	20.80		
MNHN.F.MAR1847	20.30		
MNHN.F.MAR1020	19.70	30.70	51.00
MMTT13/1357		31.50	
MMTT13/1206	19.30	31.20	50.30
MMTT13/1205	19.90	31.20	49.70
MMTT13/1248	19.60	32.00	50.70
MMTT13/1361	21.60	32.40	52.10
<i>Prostrepsiceros houtumschindleri</i> (Rodler & Weithofer, 1890)			
MNHN.F.MAR1464	27.22	40.50	66.30
MNHN.F.MAR1312		43.80	
MNHN.F.MAR3173	26.40	41.00	66.750
MNHN.F.MAR3235	24.00	38.70	62.20
MNHN.F.MAR1834	22.60	39.80	62.60
MNHN.F.MAR3237		40.00	
<i>Prostrepsiceros fraasi</i> (Andree, 1926)			
MNHN.F.MAR2127		41.00	
MNHN.F.MAR2111	24.00		
MNHN.F.MAR1961		40.30	
MNHN.F.MAR3236		44.70	
<i>Protragelaphus skouzesi</i> Dames, 1883			
MNHN.F.MAR1397	31.60	49.00	79.50
MNHN.F.MAR1307		47.90	
MNHN.F.MAR3228	31.60	45.90	76.90
MMTT7/2294	31.40	44.10	74.80

albeit the latter shows somewhat longer premolar row comparatively to the molars; nevertheless, both samples are very poor for safe conclusions. We suggest therefore referring the small gazelle from Maragheh to as *Gazella cf. ancyrensis*.

Genus *Demecquenemia* n. gen.

TYPE SPECIES. — *Demecquenemia rodleri* (Pilgrim & Hopwood, 1928) n. comb.

ETYMOLOGY. — Dedicated to R. de Mecquenem, one of the Maragheh pioneers.

AGE. — Late Miocene, Turolian

DIAGNOSIS. — As for the single known species.

TAXONOMIC OVERVIEW

Rodler & Weithofer (1890) described a frontlet from Maragheh (NHMW A4898) as a new species, *Gazella capricornis*, to which Mecquenem (1925) assigned later several specimens from the same area, now in MNHN.F. Pilgrim & Hopwood (1928) were the first authors to point out that "*Gazella capricornis*" from Maragheh is a different species from *Gazella capricornis* from Pikerimi, and proposed referring the Maragheh bovid to a new species, *Gazella rodleri*. Pilgrim (1939) suggested affiliations of *G. rodleri* with *Oioceros* Gailard, 1902, an idea rejected by Gentry (1970) but adopted by Solounias (1981). Korotkevich (1976) ascribed to this species a rich sample from Belka (Ukraine) and she assigned it to a new subgenus *Procopra* (*Vetaprocopra*) *rodleri*, the type species of which is *Antilope capricornis* Wagner, 1848. Bernor (1978) refers to the species as *Gazella rodleri* but Bouvrain (1996) explicitly excluded it from *Gazella*. Gentry & Heizman (1996) challenged once again its generic attribution and provisionally allocated it to *Hispanodorcas* Thomas, Morales & Heintz, 1982.

Demecquenemia rodleri

(Pilgrim & Hopwood, 1928) n. comb.

Gazella rodleri Pilgrim & Hopwood, 1928: 16. — Bernor 1978: 82.

Gazella capricornis Rodler & Weithofer, 1890: 15, pl. 5, fig. 1; pl. 6, fig. 1. — Mecquenem 1925: 30, pl. 3, fig. 3. Non *Gazella capricornis* (Wagner, 1848).

Oioceros rodleri – Pilgrim 1939: 45. — Solounias 1981: table 4.

Procopra (*Vetaprocopra*) *rodleri* – Korotkevich 1976: 184.

?*Hispanodorcas rodleri* – Gentry & Heizmann 1996: 383.



FIG. 6. — *Demecquenemia rodleri* (Pilgrim & Hopwood, 1928) n. comb. frontlet (MNHN.F.MAR1030) from Maragheh in caudal (A), lateral (B) and frontal (C) views. Scale bar: 5 cm.

HOLOTYPE (by monotypy). — Frontlet NHMW A4898 (Table 6; Rodler & Weithofer 1890: pl. 5, fig. 1; pl. 6, fig. 1).

TYPE LOCALITY. — Maragheh, Iran (late Miocene).

MATERIAL EXAMINED. — MNHN.F: Frontlet MAR1030, 1022, 1023, 2098+2099, 3140, 1110, 1118; right horn-cores MAR1100, 1103, 1104, 1107; left horn-cores MAR1093, 1106, 1108, 1394, 1398; part of horn-core MAR1102. — NHML: frontlets A34, C23.

AGE. — Late Miocene, Turolian.

DIAGNOSIS. — Small sized bovid with fairly thick and not very long horn-cores of weak homonymous torsion; horn-cores moderately curved backwards in side view, set close together at the base and increasingly divergent towards their tips; deep postcornual fossae; wide orbital rims; absence of postorbital lamina; thickened hollowed frontals between the horn-cores.

OTHER OCCURENCES. — Belka, Nova Emetovka 2 (Ukraine), ?Taraklia (Moldova).

DESCRIPTION AND REMARKS

Apart from the type frontlet in Vienna illustrated by Rodler & Weithofer (1890: pl. V, fig. 1 and pl. VI, fig. 1), *Demecquenemia rodleri* n. comb. is represented in the Paris collection from Maragheh by 12 individuals at least (MNI according to the horn-core elements; Table 6). The species is characterized by

wide dorsal orbital rims, small and oval-shaped supraorbital foramina without surrounding depressions, complicated fronto-parietal suture, depressed frontals behind the horn-cores, slightly pinched midfrontal suture, presence of a parietal hump well behind the fronto-parietal suture, large elliptical and deep post-cornual fossae placed posterolaterally, short pedicles posteriorly but moderately high anteriorly. The frontal region between the horn-cores is thickened and hollowed (MNHN.F.MAR1023, 1030, 1118), with several small sinuses marginally extending into the pedicles. The horn-cores are proximally converged, short (<110 mm) with weak homonymous torsion (Fig. 6A, C), weak posterior curvature (Fig. 6B), increased divergence toward the tips (Fig. 6C), well-marked posterior grooves (Fig. 6A) and occasional presence of an anterior furrow. The basal cross-section of the horn-cores is elliptical with rather flat lateral and convex medial sides (*contra* to Rodler & Weithofer 1890: pl. V, fig. 1); the mediolateral compression ranges from 67 to 81% at the base (mean CI = 72%; n = 21) and weakly decreases towards the horn tips (55-85% at 7 cm above the base, mean CI = 67.5%; n = 9) (Table 6). The same morphological features have been also seen in two additional frontlets of the “Savage collection” in London, also from Maragheh (NHML A34 and C23; Table 6). Unfortunately no

TABLE 5. — Lower tooth row measurements (in mm) of several Maragheh bovids. For abbreviations see text.

	Lp	Lm	Lpm		Lp	Lm	Lpm
<i>Gazella capricornis</i> (Wagner, 1848)				<i>O. rothii</i> (continuation)			
MNHN.F.MAR1027	22.00	35.60	56.70	MNHN.F.MAR1892		37.70	
MNHN.F.MAR1843	22.00	37.40	59.10	MNHN.F.MAR1907		38.40	
<i>Gazella cf. ancyrensis</i>				MMTT37/2170	21.50	37.00	57.60
MCW80 sin	21.90	33.45	55.30	MMTT31/2257	21.90	38.20	60.60
MCW80 dex	21.85	33.50	55.40	<i>Prostrepsiceros houtumschindleri</i>			
<i>Oioceros atropatenes</i> (Rodler & Weithofer, 1890)				(Rodler & Weithofer, 1890)			
MNHN.F.MAR1029	17.08	35.90	52.70	MNHN.F.MAR1472			
MNHN.F.MAR1860	17.25	34.70	50.80	dex	25.80	44.00	69.85
MNHN.F.MAR3149	17.50	34.00	51.80	MNHN.F.MAR1472			
MNHN.F.MAR1841	17.70	35.90	53.65	sin	25.30	43.60	68.90
MNHN.F.MAR1021	17.55	35.60	53.20	MNHN.F.MAR1066	23.90	45.10	68.30
MNHN.F.MAR2739		30.70	c. 46.7	MNHN.F.MAR3222	23.30		
MNHN.F.MAR1164		35.00		MNHN.F.MAR3224	25.65		
MNHN.F.MAR1856		36.10		MNHN.F.MAR3225	25.10		
MNHN.F.MAR1026		32.15		MNHN.F.MAR3226		45.80	
MMTT13/1300	15.40	34.60	50.90	MNHN.F.MAR1983		43.00	
MMTT13/1396		35.40		MNHN.F.MAR3216		46.00	
MMTT13/1372	17.20			MNHN.F.MAR1968		42.50	
MMTT13/1293	15.70			MNHN.F.MAR3217		44.20	
MMTT7/2435		32.30		<i>Prostrepsiceros cf. vinayaki</i> (Pilgrim, 1939)			
<i>Oioceros rothii</i> (Wagner, 1857)				MNHN.F.MAR1391	21.70	42.00	63.30
MNHN.F.MAR1846	19.50	34.30	53.50	MNHN.F.MAR3145	19.40	41.20	60.60
MNHN.F.MAR1829	23.60	39.10	61.70	<i>Prostrepsiceros fraasi</i> (Andree, 1926)			
MNHN.F.MAR1905	23.30	38.50	61.20	MNHN.F.MAR3179	27.80	41.40	69.30
MNHN.F.MAR1828	23.30	39.90	62.80	MNHN.F.MAR3219		44.20	
MNHN.F.MAR1903	22.60	36.40	59.00	MNHN.F.MAR1895		39.60	
MNHN.F.MAR1890		39.00		<i>Protragelaphus skouzesi</i> Dames, 1883			
MNHN.F.MAR1891		38.00		MNHN.F.MAR1827		50.60	
MNHN.F.MAR1902		39.90					

dental material from Maragheh can be attributed to this species at present.

Korotkevich (1976) assigned to the same species a large sample from Belka, Nova Emetovka 2 and other Ukrainian sites referred to as *Procapra (Vetaprocapra) rodleri*. Although the Belka sample in Kiev is not accessible because of storage problems, examination of a single skull in exhibition (Korotkevich 1976: pl. X, figs 1, 2) as well as of some isolated frontlets from other Ukrainian late Miocene sites confirms that the Maragheh and the Black Sea species are identical. Korotkevich (1976) preferred assigning the species to *Procapra* Hodgson, 1846 instead of *Gazella* based largely on the absence of horns in females. Nevertheless, a comparison of Korotkevich's illustrations (1976: pl. VII-XII) with living *Procapra gutturosa* (Pallas, 1777), does not provide convincing evidence

of co-generic affinity; the absence of horns in females is additionally a character commonly seen in several Late Miocene bovid lineages.

Obviously, the combination of skull and horn-core features (homonymous and markedly divergent horn-cores; strongly thickened and hollowed frontals without postorbital lamina; wide orbital rims) remove the Maragheh species from *Gazella* as Pilgrim (1939) and Bouvrain (1996) previously stated. Even though some living gazelles might occasionally show a tendency to horn torsion mostly in their tips, this character does not usually extend to the horn-cores in recent or fossil *Gazella* species and if it does it is heteronymous (e.g., Pilgrim 1939; Bouvrain & Bonis 1988; pers. obs.). In comparison with the similar-sized *Gazella desperdita* from Mont Lubéron (France), the horn-cores of *Demecquenemia rodleri* n. comb. are larger,

especially at the base (Fig. 7), and more compressed mediolaterally. Obviously the species should be also excluded from *Oioceros*, which shows much stronger horn-core torsion associated by well-developed keels and furrows and weaker medio-lateral compression.

Apart from the shared homonymous horn-core torsion, there are very few similarities linking the Late Miocene *Hispanodorcas* from Spain and Greece (Thomas *et al.* 1982; Bouvrain & Bonis 1988) with the Maragheh and Belka species. Unlike them, *Hispanodorcas* shows more intense homonymous horn twisting, shorter pedicles anteriorly, laterally placed and smaller postcornual fossae, direct opening of the supraorbital foramina into the orbits, absence of frontal sinuses, and horn-cores rather gracile and less inclined backwards, set wider apart on the frontals and with a rather characteristic lateral furrow. Furthermore, the opisthocranial morphology of *D. rodleri* n. comb. from Belka is quite different from that of the late Miocene *Hispanodorcas orientalis* Bouvrain & Bonis, 1988 from Greece, the braincase of which is shallower and less curved downwards posteriorly, the condyles are directed more posteriorly and the basioccipital has larger anterior tuberosities and a well-developed median longitudinal groove. Since the Maragheh antelope cannot be affiliated either to *Gazella*, *Oioceros*, *Hispanodorcas* or to any other known late Miocene genus, we suggest to refer it to a new genus, *Demecquenemia* n. gen., but a wider review including the bulk of the Black Sea samples is certainly needed. The phylogenetic relationships of *Demecquenemia* n. gen. with recent bovid tribes are questionable but the thickened hollowed frontals and the homonymous torsion of the horn-cores might indicate a caprine rather than an antilopine.

Genus *Oioceros* Gaillard, 1902

TYPE SPECIES. — *Oioceros rothii* (Wagner, 1857).

Oioceros atropatenes (Rodler & Weithofer, 1890)

Antidorcas? atropatenes Rodler & Weithofer, 1890: 15, pl. 4, fig. 8; pl. 6, fig. 3-5.

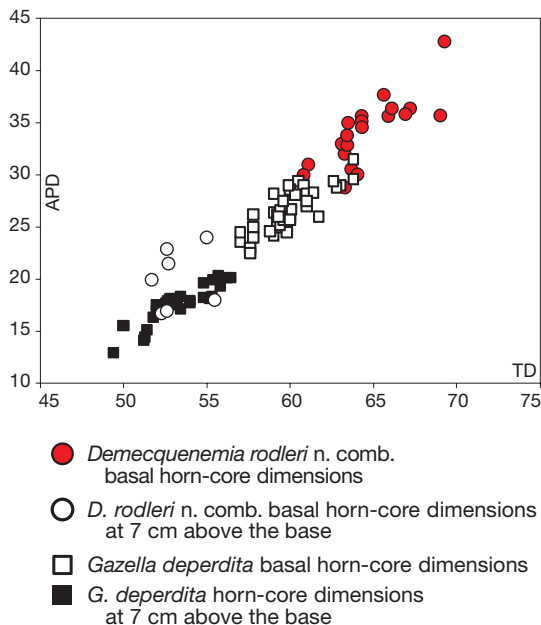


FIG. 7. — Bivariate plots of horn-core dimensions (transverse diameter [TD] against anteroposterior diameter [APD]) in *Demecquenemia rodleri* (Pilgrim & Hopwood, 1928) n. comb. from Maragheh compared to *Gazella deperdita* (Gervais, 1847) from Mont Lubéron, France. Dimensions in mm.

Oioceros atropatenes – Gaillard 1902: 93. — Heintz 1963: 110.

Oioceros boulei Mecquenem, 1925: 41, text-figs 10, 11.

LECTOTYPE (designated by Bouvrain & Bonis 1985). — Right horn-core (Rodler & Weithofer 1890: pl. 6, fig. 5).

TYPE LOCALITY. — Maragheh, Iran (late Miocene).

MATERIAL EXAMINED. — MNHN.F: Part of skull, MAR1121 (Mecquenem 1925: pl. VII, fig. 8 as *Oioceros boulei*), MAR1327; frontlet, MAR1326 (Mecquenem 1925: pl. VIII, fig. 2 as *Oioceros boulei*), 2741, 2727, 2756; isolated right horn-cores, MAR1826 (Mecquenem 1925: pl. VII, fig. 3), 2757, 2747, 2705, 2753, 2701, 2744, 2783d, 2690, 2688, 2709, 2723, 2716, 2713, 2743, 2706, 2683, 2680, 2685, 2686, 2742, 2682, 2718, 2687, 2698, 2711; isolated left horn-cores MAR2752, 2751, 2758, 2750, 2681, 2699, 2707, 2693, 2748, 2717, 2684, 2692, 2695, 2746, 2719, 2708, 2702, 2754, 2720, 2697, 2712, 2721, 2714, 2749, 2704, 2691, 2696; palate, MAR3141; P2-M3, MAR3146 (old label: MMTT13/1501), MAR1020; P2-P4, MAR1849, 1847; p4-m3sin, MAR2739 (Mecquenem 1925: pl. VII, fig. 6 as *Oioceros boulei*); mandible MAR1021+1029 (Mecquenem

TABLE 6. — Cranial and horn-core measurements (in mm) of *Demecquenemia rodleri* (Pilgrim & Hopwood, 1928) n. comb. from Maragheh. For abbreviations see text.

	TD _{hcb}	APD _{hcb}	TD _{hc7}	APD _{hc7}	L/H	W _{shc}	W _{bhc}	W _{so}	W _{or}
MNHN.F									
MAR1030 dex	21.90	30.30	12.50	17.00	105/84	62.00	55.00		82.00
sin	21.60	30.90	12.90	18.10	105/84	62.00	55.00		82.00
MAR3140 sin	23.50	35.00	12.70	21.50	105/80	64.70	c. 50	32.50	
dex	24.30	34.60			105/80	64.70	c. 50	32.50	
MAR1023 sin	25.90	35.70				71.40		38.40	
dex	26.00	36.10				71.40		38.40	
MAR1118 sin	25.70	37.70			c. 110/-	65.60			
dex	27.00	36.00	15.00	24.00	c. 110/-	65.60			
MAR1103 dex	19.40	28.90	12.20	16.80	c. 95/-				
MAR1022 sin	23.10	32.80				65.00	54.20		
MAR1394 sin	19.60	28.00			85/-				
MAR1107 dex	19.70	28.90							
MAR1108 sin	22.70	31.00							
MAR1100 dex	23.30	32.00	15.40	18.10					
MAR1093 sin	23.30	28.80							
MAR1102	23.40	33.80	12.60	22.90					
MAR1110 sin	23.40	32.70	11.70	20.00					
MAR1106 sin	23.70	30.60	12.50	17.90	110/90				
MAR2099 sin	24.30	35.10							
MAR1104 dex	24.30	35.40							
MAR1398 sin	29.00	35.70							
NHML									
A34	24.00	30.00							
C23 dex	20.80	30.00							
sin	21.10	31.00							
NHMW									
A4898 dex	27.10	36.16							
sin	29.25	42.80							

1925: pl. III, fig. 7, 7a as *G. gaudryi*); p2-m3, MAR1841, 1856, 1860, 1164, 1026, 3149. — NHML: 5 isolated unnumbered horn-cores in the Savage collection. — HUW: isolated horn-cores, MMTT13/1214, 13/nn; P2-M3, MMTT13/1248, 13/1206, 13/1205, 13/1357, 13/1361; p2-m3, MMTT7/2435, 31/1873, 13/1300, 13/1396, 13/1372, 13/1293.

REMARKS

Spiral-horned antelopes of either clock- or anticlockwise torsion are well-documented in the Maragheh collection both in number of specimens and taxa but species level taxonomy is in many cases confusing and certainly still open to discussion. Besides *Oioceros rothii* (Wagner, 1857) and *O. atropatenes* (Rodler & Weithofer, 1890), Mecquenem (1925) introduced one more species *O. boulei*, while later Pilgrim (1934) suggested referring the *O. rothii* skull illustrated by Mec-

quenem (1925: pl. VII, fig.7) to as a new taxon *O. mecquenemi*.

Oioceros atropatenes is the most abundant species of the Maragheh bovid assemblage, represented in the MNHN.F collection by no less than 32 individuals (MNI based upon horn-cores; Tables 7 & 8). Heintz (1963) addressed most of the taxonomic questions concerning the systematics of the species and gave a detailed description of the MNHN.F sample that, however, includes several additional unpublished specimens (Fig. 8; Table 8).

The cranial specimen MAR1121 is badly damaged behind the orbits (Mecquenem 1925: figs 10, 11; Table 7). The nasals are elongated comparatively to the frontals ($L_{fr} = 39.0$ mm, $L_{nas} = 48.5$ mm); the lacrimal fossa is deep and round; the orbit is large and round with its anterior margin placed above the M2. The cranium MAR1327 assigned

TABLE 7. — Cranial and horn-core measurements (in mm) of *Oioceros* Gaillard, 1902 species from Maragheh. For abbreviations see text.

	W _{so}	W _{shc}	W _{bhc}	W _{or}	L _{hc}	right hc		left hc	
						TD _{hcb}	APD _{hcb}	TD _{hcb}	APD _{hcb}
<i>Oioceros atropatenes</i> (Rodler & Weithofer, 1890)									
MNHN.F.									
MAR1326	30.05	49.60		(64.5)		16.60	18.02	17.20	17.20
MAR2741	31.30	50.80		74.00		17.50	20.00	17.40	20.00
MAR2727	(30)	52.90	45.10			19.70	22.00	19.20	21.50
MAR2756	(34)		46.60			19.30	19.60		
MAR1327	31.20	49.90	47.20	77.70		18.10	21.10	17.70	22.20
MAR1121	31.70	58.20	(46)	c. 82		20.20	22.10	20.10	21.60
<i>Oioceros rothii</i> (Wagner, 1857)									
MNHN.F.									
MAR1320	43.70	66.40	55.00	88.20	135	20.10	28.10	22.40	28.80
MAR1120	36.80	62.40	57.10	(94)		20.05	26.90	21.5	27.07
MAR1119	(40)	64.80				22.00	28.70	21.70	29.40
MAR2728		65.40	54.10			18.10	27.20	19.50	
MAR1806	(40)	65.30			c. 150	22.40	29.00		

to *O. boulei* ($W_{bmas} = 49.3$ mm, $W_{bcon} = 30.8$ mm, $W_{ptb} = 18.3$ mm, $L_{fp-ocp} = c. 30.5$ mm; Fig. 8; Table 7) lacks the entire face and is partly damaged ventrally. Although the basal diameters of the *O. atropatenes* horn-cores (Table 8) show a continuous distribution with slightly positive allometry of APD *vs* TD ($a = 1.09$; Fig. 9), Heintz (1963: 112) recognized two size-categories interpreted as representing sexual dimorphism. Female horn-cores are about 13–15% smaller in basal dimension, longer and less tightly twisted than male horn-cores. The great axis of the horn-core base forms a 45° angle with the sagittal plane. The horn-core compression is weak (CI: 77.8–100.8% in males, $n = 39$; 75.7–107.7% in females, $n = 28$) and usually anteroposterior (in 98% of the males and in 86% of the females). The postcornual fossa varies from rather small and shallow (63%) to large and shallow or occasionally deep. About a fourth of the specimens bear an additional fossa just above the postcornual one. In 16% of the studied cases the horn-core longitudinal axis declines from a straight line indicating a weak degree of close spiralling independently of sex, whereas in 20% of the sample the characteristic lateral furrow is barely recognized or absent. In a few specimens the horn core seems to extend onto the anterior face of the pedicle forming a

“V” projection and in those cases an incipient anterior keel is present.

Apart from the upper tooththrow of the specimen MAR1121 described by Heintz (1963) (Fig. 10A) we refer the palate MAR3141 (Fig. 10B) and two right P2–M3 (MAR3146, MAR1020), as well as two premolar rows, MAR1349 (Fig. 10C–E) and MAR1847 to *O. atropatenes* (Table 4). This hypodigm shares all the morphological features defined by Heintz (1963) but with a somewhat wider size and morphological variation. The upper premolar row represents 61–68% of the molar row length (Table 4). The upper molars have no basal pillars or central islets; their posterior lobe is square-shaped; the labial ribs are weak; the mesostyle is thin but well-developed and the parastyle is rather strong and mesially directed (Fig. 10A, B). The P2 and P3 are asymmetrical with weak lingual bilobation and strong, mesially placed paracone (Fig. 10A). The P4 is more symmetrical with strong parastyle moderately developed metastyle and weak metacone.

Heintz (1963: 111) referred to *O. atropatenes* the mandibular fragment with p4–m3, MAR2739 figured by Mecquenem (1925: pl. VII, figs 6, 6a) and two more specimens with m2–m3. Nevertheless, several additional lower tooththrows in Paris and Washington compare closely in size to the

TABLE 8. — Horn-core measurements (in mm) of *Oioceros atropatenes* (Rodler & Weithofer, 1890) from Maragheh. For abbreviations see text.

Coll. no.		L _{hc}	TD _{hcb}	APD _{hcb}	Coll. no.		L _{hc}	TD _{hcb}	APD _{hcb}
NHML S1	dex		16.9	16.5	MNHN.F.				
NHML S2	sin	108.5	15.7	18.7	MAR2708	sin		17.6	18.5
NHML S3	sin	119.0	15.3	18.2	MAR2709	dex		16.9	18.6
NHML S4	sin		20.2	21	MAR2711	dex		15.3	17.7
NHML S5	sin		15	17	MAR2712	sin		15.9	17.9
MNHN.F.					MAR2713	dex		20	21.9
MAR1826	dex	120.0	17	19.2	MAR2714	sin	80.0	19.2	20.4
MAR2680	dex		17.7	20.6	MAR2716	dex		18.5	19.6
MAR2681	sin		18.7	22	MAR2717	sin	60.0	17.7	18.7
MAR2682	dex		16.3	18.3	MAR2718	dex		15	16.8
MAR2683	dex		17.9	23	MAR2719	sin		16.8	20.7
MAR2684	sin	75.0	16.6	20	MAR2720	sin		17.6	20.7
MAR2685	dex		20.5	21.1	MAR2721	sin		18.1	20.4
MAR2686	dex		17.4	20.4	MAR2723	dex		19.2	19.03
MAR2687	dex		15.6	17.5	MAR2742	dex		19	21
MAR2688	dex		16.3	18	MAR2743	dex	86.0	14	17
MAR2690	dex	80.0	20.5	21.3	MAR2744	dex		16	19.5
MAR2691	sin		16.1	19.6	MAR2746	sin			16.7
MAR2692	sin		18.5	18.7	MAR2747	dex	90.0	17.2	20.6
MAR2693	sin		14.2	15.4	MAR2748	sin		14	18.5
MAR2695	sin		16.4	17.7	MAR2749	sin	85.0	17.9	19.6
MAR2696	sin		16.8	17.9	MAR2750	sin	115.0	15.6	15.8
MAR2697	sin	65.0	14.5	16.4	MAR2751	sin	105.0	17.3	19.4
MAR2698	dex		15.7	15.7	MAR2752	sin	90.0	16.76	19
MAR2699	sin		15.8	17.8	MAR2753	dex		17.8	19.4
MAR2701	dex		16.7	20.03	MAR2754	sin		15	17.9
MAR2702	sin		16.4	18.8	MAR2757	dex	100.0	16.3	17.3
MAR2704	sin		16.6	18	MAR2758	sin		16.3	20.4
MAR2705	dex		18.3	17.65	MAR2783	dex		15.86	19.9
MAR2706	dex		16.8	15.6	MMTT nn		95.0		
MAR2707	sin		19.4	19.6	MMTT13-1214		85.0	14	15.4

hypodigm of *O. atropatenes* (Table 5). The lower premolar row is much reduced representing 44.5–51.5% of the molars (Fig. 4). The lower molars have no basal pillars but a weak goat fold is present on m1 and m2 (Fig. 10C, D). The parastylid is strong especially on the m3 and the metastylid directs distally. The talonid of the m3 is bi-cuspid. The p3 has a narrow, pinched hypoconid, very weak paraconid that fuses quickly with the parastylid, and distally directed, short metaconid closing the posterior valley in advanced stage of wear. The p4 is quite similar to the p3 but the paraconid is occasionally stronger and the metaconid is elongated and curves distally (Fig. 10A); in half of the specimens the posterior valley appears closed from the first stages of wear.

The species is so far known only from Maragheh but Dmitrieva (2007) recently ascribed to it several samples from Mongolia. Nevertheless, the overall size of the Mongolian horn-core specimens (i.e. longer and rather larger than *O. atropatenes*) and their morphology (i.e. more mediolaterally compressed compared to *O. atropatenes*, more strongly twisted, clearly lyrated and distally divergent with flattened antero-lateral basal surface) led us to reject Dmitrieva's interpretation; we refer these horn-cores to *Oioceros rothii*. Furthermore, the description of *O. atropatenes* given by the same author does not conform with our current observations on the Maragheh sample, while the provided generic diagnosis of *Oioceros* neglects recent advances on the type species (i.e. Roussiakis 2003) allowing misleading conclusions.

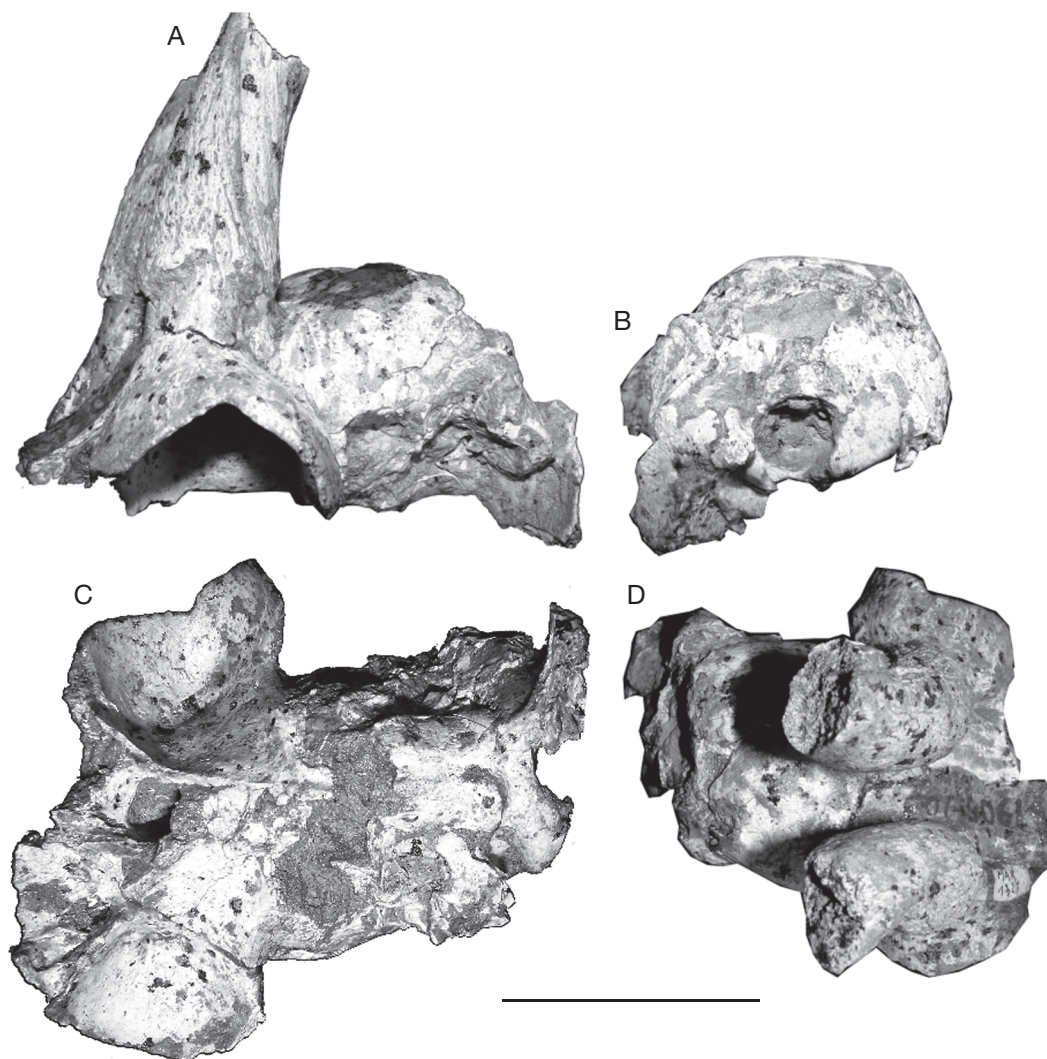


FIG. 8. — *Oioceros atropatenes* (Rodler & Weithofer, 1890) cranium (MNHN.F.MAR1327) from Maragheh in lateral (A), occipital (B), ventral (C) and dorsal (D) views. Scale bar: 5 cm

Oioceros rothii (Wagner, 1857)

Antilope rothii Wagner, 1857: 154, pl. 6, fig. 20.

Oioceros rothii – Gaillard 1902: 93.

Oioceros? *mecquenemi* Pilgrim, 1934: 3.

TYPE LOCALITY. — Pikermi, Greece (late Miocene).

MATERIAL EXAMINED. — MNHN.F: Part of skull MAR2726 (Mecquenem 1925: pl. VI, fig. 4; pl. VII, fig. 7); opisthocranium, MAR1057; frontlet MAR1320 (Mecquenem 1925: pl. VII, fig. 4), 2728, 1119, 1120, 1806+1808; right horn-core, MAR1810 ($L_{hc} = 140$ mm, $TD_{hcb} = 18.1$ mm, $APD_{hcb} = 27.9$ mm); left horn-core, MAR1809 ($L_{hc} = 135$ mm, $APD_{hcb} = 25.7$ mm); lower tooththrows, MAR1828, 1829 (Mecquenem 1925: pl. VII, fig. 5 as *Helicophora rotundicornis*), 1890-1892, 1902, 1903, 1905 (labeled as *Prostrespiceros rotundicornis*), 1907, 1846. — HUW: mandible, MMTT37/2170; left p2-m3, MMTT31/2257

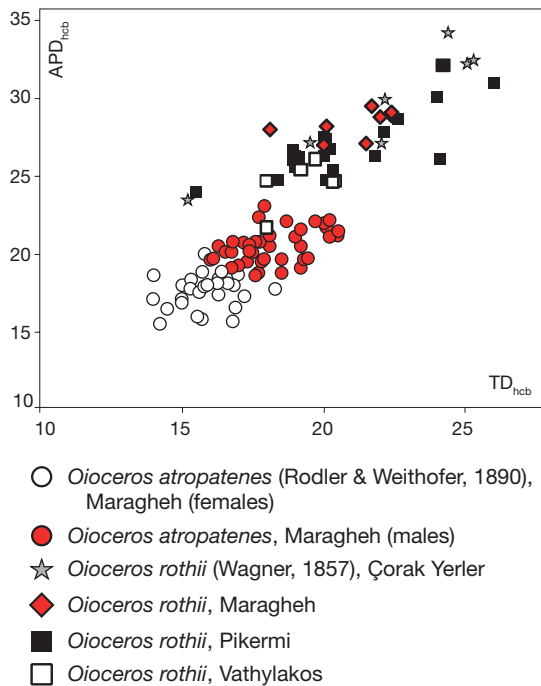


FIG. 9. — Bivariate plots of basal horn-core dimensions (in mm) in *Oioceros* Gaillard, 1902 (transverse diameter [TD] against anteroposterior diameter [APD]). Data for Çorak Yerler, Turkey from Köhler (1987).

DESCRIPTION AND REMARKS

Much less well-known, the second *Oioceros* species from Maragheh is represented by finely preserved frontlets and some tooth rows (Tables 4, 5, 7). Compared to the smaller *Oioceros atropatenes*, the orbits project more laterally, the postcornual fossae are rather large and shallow, the supraorbital foramina are smaller, the temporal lines are less developed, and the horn-cores are more uprightly inserted, more mediolaterally compressed, more strongly twisted (1+ coil), slightly curved backwards at the middle of their height and clearly divergent at their distal part (Fig. 11E, F; Table 7). Whereas in *O. atropatenes* the longitudinal furrows descend above the postcornual fossa at the posterolateral edge of the horn-core base, in *O. rothii* they originate more anteriorly on the lateral surface forming a wider zone that reaches the anterior side of the horn-core (Fig. 11E, F). This zone is extremely porous in the lower half of

the horn-core. There is one predominant lateral furrow, instead of usually two in *O. atropatenes*; this furrow forms the characteristic wrapping of the horn-core, exceptionally evident in the proximal half. A second narrow and shallow furrow appears on the upper half of the anterior surface due to the horn's twisting. Morphological comparison between Maragheh, Axios Valley (Arambourg & Piveteau 1929) and Pikermi (Gaudry 1865; Roussiakis 2003) horn-core samples (Figs 9; 11) does not show important differences; the set of the Maragheh horn-core characters is consistent with those of specimens from Pikermi described by Roussiakis (2003). The Axios Valley horn-cores have much less developed porous zone, weaker distal divergence and weaker backward curvature than the Maragheh specimens and they are also smaller on the average but not enough to be excluded from the species (*contra* to Bernor [1978] who referred them to *O. atropatenes*). The Pikermi sample shows a greater size variation with the larger specimens (PIK2249) to be even larger than those from Maragheh (MAR1320) and the smaller ones to fit the size of the Axios Valley morph (Fig. 9).

The cranium MAR2726 ($W_{bc} = 63.2$ mm, $W_{shc} = c. 74$ mm, $W_{bcon} = 47.7$ mm, $W_{bmas} = 66.3$ mm, $LM = c. 35$ mm, $W_{ptb} = 31.7$ mm, $H_{oc} = 25.9$ mm) is badly preserved, the horn-cores are broken at their contact with the pedicles, and a part of the parietal is missing (Mecquenem 1925: pl. VII, fig. 7). MAR1057 retains only the occipital region. The cranial vault is globular and the top of the braincase curves down posteriorly. The face is high and the nasals are weakly domed in lateral profile. The anterior rim of the orbit is placed above the M2-M3 limit. The midfrontal suture is open and complicated. The occiput is semicircular shaped and faces postero-laterally, whereas the mastoid faces mostly posteriorly. The occipital condyles are keeled and they do not deflect significantly from the occipital level. The foramen magnum is large. The nuchal crest is weak. The basioccipital faces partly laterally, it is trapezoidal with ridge-like posterior tuberosities perpendicular to the sagittal plane and long, ridge-like anterior tuberosities trending

anteroposteriorly. The foramina ovale open at the level of the anterior tuberosities of the basioccipital and face mainly laterally. The cranium MAR2726 is slightly larger than the single known skull of *Oioceros rothii* from the type locality of Pikermi (PG95/1502a; Roussiakis 2003) but it shares with it the high face, the domed nasals, the long and curved down posteriorly opisthocranium, as well as, the higher bi-laterally faced occiput and the longer basioccipital, characters that distinguish them from *O. atropatenes*.

In his discussion of the dental morphology of *Oioceros rothii* from Pikermi, Roussiakis (2003) excluded MAR3145 from this species (*contra* to Mecquenem 1925: pl. VI, fig. 2) and included in it the mandible MAR1828 (type of *Antidorcas ?gaudryi* Mecquenem, 1908; Mecquenem 1925: pl. VII, figs 5-5a); we agree with this attribution (Tables 4, 5). Both the upper and lower dental morphologies of Maragheh *O. rothii* are very similar to those from Pikermi (Roussiakis 2003) except perhaps for the stronger and more frequent basal pillars that appear in all upper molars of MAR2726 and in several m1 and m2 but less often on m3. Furthermore, the paraconid is still present in half of the preserved p4 and in a few p3 from Maragheh. The lower premolars represent 57-62% of the molar row length (Fig. 4; Table 5).

Genus *Nisidorcas* Bouvrain, 1979

TYPE SPECIES. — *Nisidorcas planicornis* (Pilgrim, 1939).

Nisidorcas sp. (Fig. 12)

Antilope indet. — Mecquenem 1925: pl. 8, fig. 1.

Nisidorcas planicornis — Köhler 1987: 199.

MATERIAL EXAMINED. — MNHN.F: Frontlet MAR1323 (Mecquenem 1925: pl. VIII, fig. 1 as *Antilope* indet.; $W_{shc} = 84.0$ mm, $W_{bhc} = 58.0$ mm, $W_{so} = 38.2$ mm, $L_{hc} = c. 150$ mm, $TD_{hcb} = 26.2$ mm, $APD_{hcb} = 32.3$ mm); distal part of horn-core, MAR1807; proximal part of horn-core, MAR1813 ($TD_{hcb} = 20.4$ mm, $APD_{hcb} = 26.1$ mm).

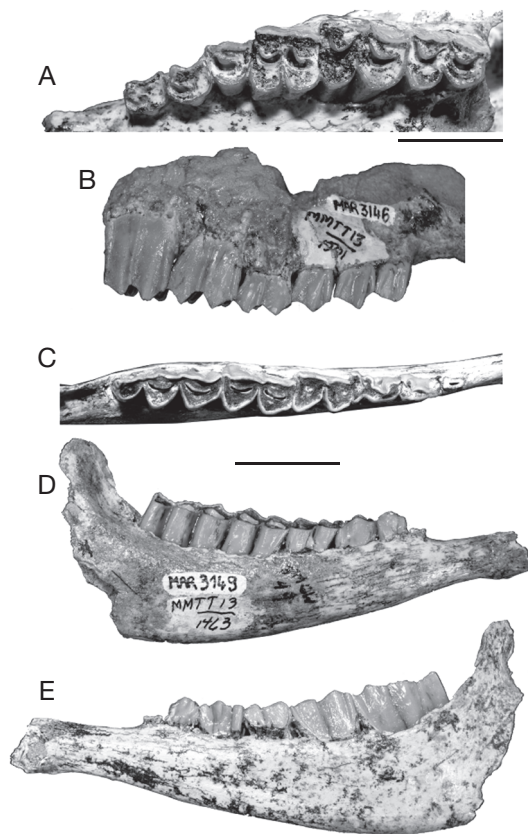


FIG. 10. — *Oioceros atropatenes* (Rodler & Weithofer, 1890) dentitions from Maragheh: **A**, P2-M3 sin (MNNHP MAR1121) in occlusal view; **B**, P2-M3 dex (MNHN.F.MAR3146) in labial view; **C-E**, right mandibular ramus (MNHN.F.MAR3149) in occlusal (**C**), labial (**D**) and lingual (**E**) views. Scale bars: 2 cm.

REMARKS

Nisidorcas occurs in the early to early middle Turolian faunas of Eastern Mediterranean, mainly Greece and Turkey as well as in Perim Island, India (Bouvrain 1979; Kostopoulos 2006). Recent data allow a much better understanding of the species and its morphological and metrical variability (Geraads & Güleç 1999; Kostopoulos & Koufos 1999; Bouvrain 2001; Kostopoulos 2006). Köhler (1987) based on MAR1323 (Fig. 12), was the first to mention similarities of Mecquenem's small *Antilope* indet. with *Nisidorcas*. The three available specimens from Maragheh have heteronymously twisted and straight horn-cores that are moderately divergent

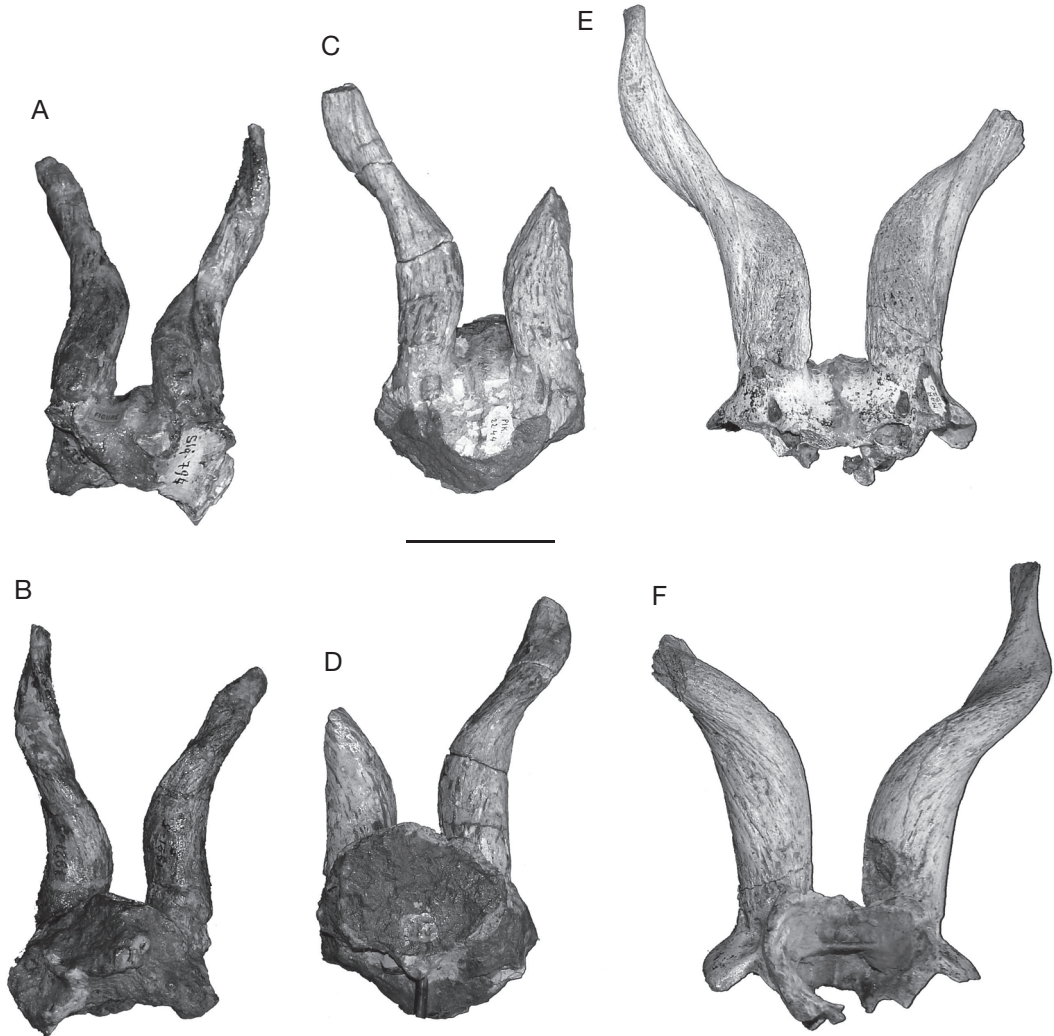


FIG. 11. — Comparison of *Oioceros rothii* (Wagner, 1857) horn-cores from: **A, B**, Axios Valley (MNHN.F.SIq794); **C, D**, Pikermi (MNHN.F.PIK2244); **E, F**, Maragheh (MNHN.F.MAR1320); **A, C, E**, frontal views; **B, D, F**, caudal views. Scale bar: 5 cm.

and bent strongly backwards (Fig. 12 and Mecquenem 1925: pl. VIII, fig. 1). Their greater basal axis is strongly oblique comparatively to the sagittal plan indicating a rather anteroposterior proximal compression. A moderate to strong posterior keel descends postero-laterally and trends straightwards to the apex (Fig. 12B, C); it is further underlined by the strong grooving of the posterior horn-core surface. In the antero-basal part of the horn-core a blunt constriction that ascends helically upwards

replaces what would be an anterior keel. The post-cornual fossa is wide and shallow.

In contrast to Geraads & Güleç (1999) we believe that *Antilospira incarinatus* Tekkaya, 1969 is not worthy of distinction at the species level; the Turkish material re-described by Köhler (1987) falls well within the morphological variability of *N. planicornis* (see Kostopoulos 2006). The morphological and metrical characters of the Maragheh species also resemble those of Greek *Nisidorcas*

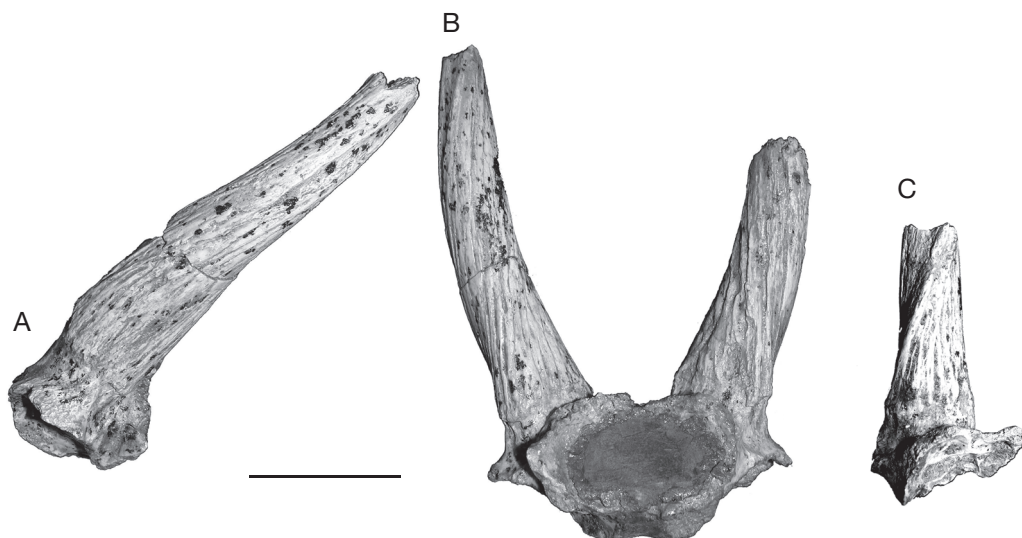


FIG. 12. — *Nisidorcas* sp. from Maragheh: frontlet (MNHN.F.MAR1323) in lateral (A) and caudal (B) views; basal horn-core (MNHN.F.MAR1813) in posterior view (C). Scale bar: 5 cm.

planicornis summarized by Kostopoulos (2006). Nevertheless, the Maragheh horn-cores show more lyriform divergence and stronger longitudinal grooving of their posterior surface than usually seen in *N. planicornis* but the sample is limited for certain conclusion.

Genus *Prostrepsiceros* Major, 1891

TYPE SPECIES. — *Prostrepsiceros houtumschindleri* (Rodler & Weithofer, 1890).

Prostrepsiceros houtumschindleri (Rodler & Weithofer, 1890) (Fig. 13E-H)

Tragelaphus? houtum-schindleri Rodler & Weithofer, 1890: 768, pl. 6, fig. 2.

Tragelaphus houtum schindleri – Mecquenem 1925: 37.

Prostrepsiceros houtumschindleri – Gentry 1971: 263 *partim*.

HOLOTYPE. — Frontlet NHMW 1886-XXVIII.6 (Rodler & Weithofer 1890: pl. 6, fig. 2).

TYPE LOCALITY. — Maragheh, Iran (late Miocene).

MATERIAL EXAMINED. — MNHN.F: Part of cranium MAR1464 (Mecquenem 1925: pl. V, fig. 5), 1324, 1312, 1308, 3212 (Mecquenem 1925: pl. VI, fig. 7); opisthocranium, MAR1061; frontlet, MAR1309, 1831, 1315, 3211, 3213, 3214, 1314; isolated horn-cores, 1819, 1319, 1001, 1816, 1000, 1820, 1818, 1018, 1317, 1815, 1814, 1473; upper tooththrows, MAR3173, 3235, 1834; P4-M2, MAR1943, 3237; M3, MAR3238; lower tooththrows, MAR1472 (Mecquenem 1925: pl. V, fig. 7), 1066 (Mecquenem 1925: pl. VI, fig. 5); p2-m1, MAR3222; p2-m2, MAR3224; p3-m3, MAR3226, 1983, 3216, 1968; p3-m2, MAR3220; p4-m3, MAR3217; p2-p4, MAR3225. — NHMW: holotype, frontlet NHMW 1886XXVIII.6.

DESCRIPTION AND REMARKS

Both Mecquenem's (1925: 37) and Gentry's (1971) reports on the Maragheh sample of *P. houtumschindleri* do not acknowledge its importance as the second most abundant bovid at the site. The species is represented by six crania, seven frontlets, a dozen isolated horn-cores and numerous tooththrows (Tables 4, 5, 9, 10), listing as a whole more than 20 individuals in the MNHN.F collection. Gentry's (1971) descriptions of this species incorporate characters observed on Samos samples that we do not consider conspecific. Bouvrain & Thomas (1992)

TABLE 9. — Cranial measurements (in mm) of *Prostrepsiceros houtumschindleri* (Rodler & Weithofer, 1890) and *Prostrepsiceros fraasi* (Andree, 1926) from Maragheh. For abbreviations see text.

	W _{so}	W _{shc}	L _{fr}	L _{fp-ocp}	W _{or}	W _{bc}	W _{bmas}	W _{bcon}	W _{ptb}	W _{atb}	L _{nas}	H _{oc}
<i>Prostrepsiceros houtumschindleri</i> (Rodler & Weithofer, 1890)												
MNHN.F.												
MAR1464	40.3	98.0	68.0		c. 125						75.4	
MAR1324		87+		44.5		62.0	69.0	46.4	23.7	16.9		27.2
MAR1312	c. 37	91.3	65.2		99+						68.2	
MAR1308	35.2	89.5	(58)			61.3				12.5		31.0
MAR1316	(37)		68.0	36		58.7						
MAR1309	38.8	86.4		(46.5)								
MAR1061							67.1	42.0	c. 24	14.0		26.0
MAR1831	c. 36	92.5										
MAR1315	36.8	93.1	c. 65									
MAR3211	38.0	97.0	c. 64									
MAR3212	41.7	99.5	66.0	52.6								
MAR3213	37.6	92.3										
MAR3214												
MAR1314	37.6	89.5										
MAR1024	34.5	92.7										
MAR1313	42.9	98.1										
<i>Prostrepsiceros fraasi</i> (Andree, 1926)												
MAR1310		(92)	(63)	64.7	(100)	60.0	68.4	(42)	25.8	14.6		29.6
MAR1060							73.9	44.4	24.3	16.2		32.0
MAR1306	35.2	89.7			102.0							
MAR1322	35.0	94.2										
MAR1318	37.0	90.1										
MAR1010	(42)											

proposed a detailed emended diagnosis of *P. houtumschindleri* that is largely followed here.

The braincase (MNHN.F.MAR1308, 1324, 1061) is rather wide, short and low (Fig. 13F; Table 9), strongly angled on the face. Its lateral sides run parallel to each other and the dorsal surface is rather flat. The temporal lines are very weak to absent and when visible they converge quickly to the rear. The parieto-temporal suture forms in its posterior end a weak constriction. A deep depression is present just in front of the external auditory meatus, which is small with great diameter trending anteroventrally to posterodorsally. The nuchal crest is well-developed and the occiput semi-oval-shaped. The external occipital crest is blunt and the relevant protuberance is not developed. The occiput faces postero-dorsally and the mastoid mostly laterally (Fig. 13F). The occipital condyles protrude almost vertically from the occipital plane. The basioccipital is narrow and long with strong ridge-like posterior tuberosities and strong, elongated anterior tuber-

osities trending antero-posteriorly, close together and parallel to each other. A strong crest runs along the mid-basioccipital line between the posterior tuberosities. The foramen ovale is small and faces rather laterally. The auditory bullae are long, not very swollen and their posterior edge fuses with the paroccipital process. The choanae open slightly in front of the lateral indentations of the palate, just at the level of the middle of M3 (Fig. 13H). The orbits are large and round to obliquely ovate with a possible antero-ventral indentation. They do not project significantly on the lateral sides and their anterior rim is placed above the M2-M3 limit (Fig. 13E). The lacrimal fossa is rather shallow without well-defined borders. A thin, long ethmoidal fissure exists. The facial tuberosities are clear and placed above M1-M2 limit. The infra-orbital foramina are small, placed slightly above the P3. The premaxillae have a short contact with the nasals, which are long and have weak anterior and posterior lateral flanges (Fig. 13G). The frontals

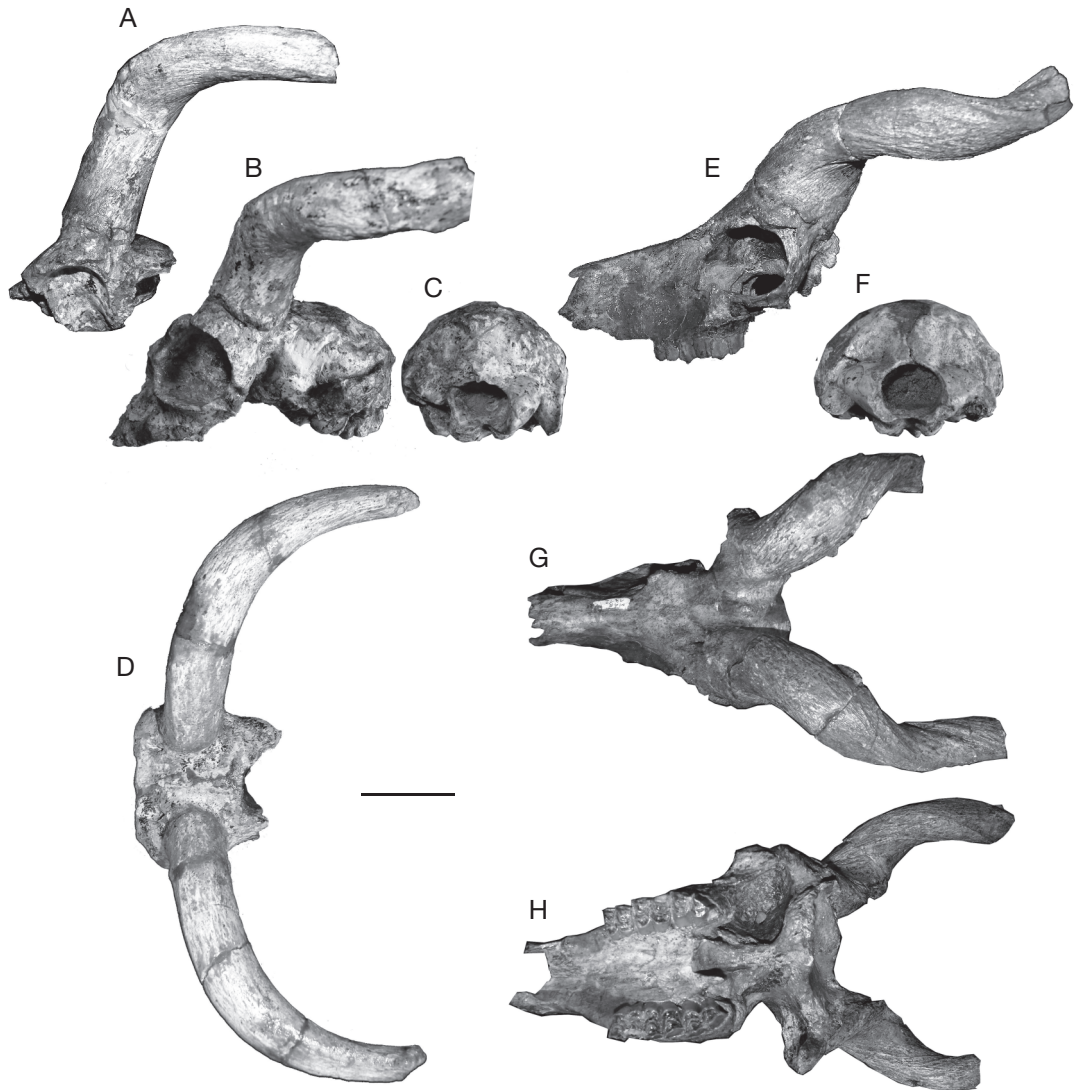


FIG. 13. — Comparison between *Prostrepsiceros fraasi* (Andree, 1926) (A-D) and *Prostrepsiceros houtumschindleri* (Rodler & Weithofer, 1890) (E-H) from Maragheh: A, frontlet (MNHN.F.MAR1010) in lateral view; B, C, cranium (MNHN.F.MAR1310) in lateral (B) and occipital (C) views; D, frontlet (MNHN.F.MAR1306) in dorsal view; E, G, H, cranium (MNHN.F.MAR1312) in lateral (E), dorsal (G) and ventral (H) views; F, MNHN.F.MAR1061 in occipital view. Scale bar: 5 cm.

between the horn-cores are weakly elevated with a pinched midfrontal suture. The frontoparietal suture is rather complicated and almost perpendicular to the midfrontal one. The supraorbital foramina are sunken into a large and deep depression, the posterior edge of which is placed above the middle of the orbit, i.e. relatively far from the horn-core base

(19.5-26.6 mm). The pedicle is very short to absent posteriorly and short anteriorly. A characteristic shallow notch appears anteriorly on the crown of the corneal process.

The horn-cores are inserted on the posterior half of the dorsal orbital rim, being moderately to strongly inclined backwards in their proximal

TABLE 10. — Horn-core measurements (in mm) of *Prostrepsiceros houtumschindleri* (Rodler & Weithofer, 1890) from Maragheh. For abbreviations see text but H_{hc} is taken here along the anterior surface.

Collection no.	TD _{hcb}	APD _{hcb}	TD _{hc7}	APD _{hc7}	L _{hc} /H _{hc}
MNHN.F.					
MAR1309 dex	27.10	42.00	29.00	21.00	200/175
sin	27.60	40.00			200/175
MAR1831 dex			34.50	24.30	260/200+
sin	33.20	43.10			260/200+
MAR1315 dex	32.00	44.80			210/190
sin	34.80	44.80	33.60	22.70	210/190
MAR3211 dex	28.80	45.90			
sin	31.40	42.10			
MAR3212 dex	31.40	41.60			
sin	31.60	45.20			
MAR3213 sin	29.40	42.40	29.30	22.70	220/200
MAR1314 sin	28.20	40.60	28.20	21.70	200/180
MAR1024	33.00	46.70	33.00	23.70	
MAR1313 dex	30.70	32.00			
sin	32.00	44.90			
MAR1006 sin	32.00	42.50			
MAR1464 dex	29.00	43.60	30.20	21.50	
sin	30.50	44.60			
MAR1324 dex	29.30	45.60	32.30	25.00	250/220
MAR1312 dex	33.40	41.50			
sin	34.60	45.60	27.10	21.30	
MAR1308 sin	32.30	44.80	29.20	22.00	200/180
MAR1316 sin	36.50	44.50	31.50	23.40	280/230
MAR1819 dex	30.00	42.00			
MAR3214 sin	30.30	37.70			
MAR1319	28.10	45.30	32.90	22.60	
MAR1001	36.20	49.30	30.00	24.00	
MAR1816	31.30	41.20			
MAR1000	32.40	42.80			
MAR1820	33.00	46.30	30.70	21.40	
MAR1818	25.00	38.60			
NHMW 1886-XXVIII.6 (holotype)	29.30	42.80			

part. They are rather widely spaced at the base; the internal distance between the horn-cores ranges from 22 to 26—rarely to 28 mm. The horn-cores are long, mediolaterally compressed (Table 10), moderately twisted and closely spiralled (1 ½ coils); their maximum uncoiled length probably extended 250–300 mm (Fig. 13E, G, H). The greatest axis of the horn-core base forms a 40–50° angle with the sagittal plane. Seven centimeters above the base, the same axis trends perpendicular to the sagittal plane, whereas 3 cm after, it becomes almost parallel to the same plane. The mean horn-core compression index is 72% at the base (CI = 62–82%; n = 30) and 135.5% at 7 cm above the base (CI = 125–148%; n = 13) (Fig. 14). Proximally, the medial surface of the horn-cores is less convex

than the lateral one. The posterior keel is always strong, descending postero-laterally above the round to oval and shallow postcornual fossa and associated with a longitudinal furrow along its anterior rim. In most of the studied specimens this furrow disappears towards the horn's apex. In some of the specimens a set of deep longitudinal furrows descends on the antero-medial edge of the horn-core base, whereas in some others this feature is replaced by a blunt swelling. In several specimens a deep furrow of anteromedial origin is still present in the distal part of the horn-cores. In lateral view the horn-cores curve backwards some centimetres above the base and then run parallel to the horizontal plane (Fig. 13E, G), whereas they re-curve upwards in their distal part. In frontal

view the horn-cores diverge moderately in their proximal part and then after they run almost parallel to each other.

The teeth are fairly hypsodont. The premolars represent 56.8-67.2% of the upper and 52.9-58.6% of the lower molar row length (Fig. 4; Tables 4, 5). The main dental characters of the upper toothrow are the strong paracone rib of the upper premolars and molars that is placed strongly obliquely in P2, P3, M1 and M2, the strong parastyle of P4 and M1-M3, the strong mesostyle and the absence of basal pillars on the upper molars, and the posteriorly protruding metastyle of M3. In the lower dentition, the entoconid of p2 is distinct, the metaconid of the p3 and p4 is elongated and directs strongly distally even though the posterior valley remains as a narrow fissure, the paraconid of the p3 and p4 is strong and vertically placed and their hypoconid protrudes buccally, the lower molars occasionally have basal pillars and they usually have a strong goat fold, and the third lobe of the m3 is single-cuspid and semicircular-shaped.

The homogeneity of the hypodigm's morphology, as currently understood, as well as the metric dimensions of *P. houtumschindleri* from Maragheh confirms the species-concept of Bouvrain (1982) and Bouvrain & Thomas (1992) and contradicts earlier observations by Gentry (1971) adopted later by Solounias (1981) and more recently by Bibi (2008), according to which *P. zitteli* Schlosser, 1904 from Samos is synonymised with *P. houtumschindleri*. Bernor (1978) referred to *P. houtumschindleri* several dentitions and horn-cores collected from the Maragheh sites MMTT1A, 1B, 7, 13, 37 and MMTT43 during the LRE. This material is currently housed in Iran and therefore it was not accessible to the first author but the brief descriptions provided by Bernor (1978: 85) allow suggesting that his original horn-core sample includes specimens with quite distinct morphology that probably correspond to different *Prostrepsiceros* species. Some additional cranial specimens of *P. houtumschindleri* from Site III of KUE, stored in Kyoto were described later by Watabe (1990: pl. III, figs 3, 4). A morphometrical comparison with relevant Maragheh species is given in the following sections.

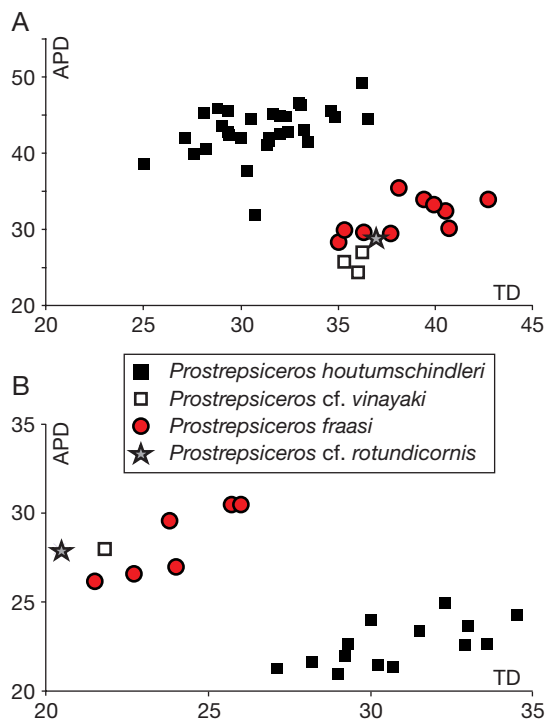


FIG. 14. — Bivariate plots of horn-core dimensions (transverse diameter [TD] against anteroposterior diameter [APD]) in *Prostrepsiceros* Major, 1891 from Maragheh: **A**, basal dimensions; **B**, dimensions at 7 cm above the base. Dimensions in mm.

Prostrepsiceros cf. *vinayaki* (Pilgrim, 1939)
(Fig. 15)

Gazellinae? gen. indet. (aff. *Helicotragus*) *vinayaki* Pilgrim, 1939: 42, pl. 1, fig. 10.

Prostrepsiceros houtumschindleri – Gentry 1971: 263 *partim*.

TYPE LOCALITY. — Nila-Dhok Pathan, Siwaliks, India (late Miocene).

MATERIAL EXAMINED. — MNHN.F: basal part of horn-core MAR1005, 1003; p2-m3, MAR3145 sin (Mecquenem 1925: pl. VI, fig. 2 as *Oioceros rothii*), MAR1391 dex. — NHMW: right horn-core A4900.

DESCRIPTION AND REMARKS

This poorly known spiral-horned antelope, never previously reported from Maragheh is represented in the MNHN.F collection by a couple of basal horn-core fragments with frontals, labelled as Antilopinae

TABLE 11. — Comparison of horn-core measurements (in mm) of *Prostrepsiceros* cf. *vinayaki* (Pilgrim, 1939) from Maragheh with those of the holotype specimen (cast NHML M42957) from Siwaliks and *Pr.* aff. *vinayaki* from Baynunah Fm, Abu Dabi (AUH441; Gentry 1999). For abbreviations see text.

	MNHN.F. MAR1003		MNHN.F. MAR1005		<i>Pr. vinayaki</i>	
			NHMW A4900	M42957	AUH441	
APD _{hcb}	36.00	35.30	36.20	26.50	29.60	
TD _{hcb}	24.30	25.80	27.10	19.50	20.90	
APD _{hc7}	28.00	28.70				
TD _{hc7}	20.40	19.90				

indet. One more, nearly complete horn-core in Vienna, so far attributed to *P. houtumschindleri* (Gentry 1971) is further referred to *Prostrepsiceros* cf. *vinayaki* herein. Two mandibular rami in MNHN.F, one of them (MAR3145) previously ascribed to *Oioceros* by Mecquenem (1925: pl. VI, fig. 2) are assigned here to *P. cf. vinayaki* as well (Table 5).

The horn-cores are extremely compressed with strong anterior keel, which in the distal part may be associated or replaced by a relatively deep furrow with irregular rims (MAR1003; NHMW A4900) (Fig. 15; Table 11). The insertion of the horn-cores on the frontals is very oblique with the great basal axis of the horn-core almost perpendicular to the sagittal plane (Fig. 15B, E). The cross-section is elongated elliptical with the anterior keel in medial position. There is no posterior keel and the strongly convex posterior surface of the horn-core bears some strong longitudinal furrows. From the base to the top, the horn-core curves slightly posterolaterally forming an open spiralling of less than one complete coil. The median face of the horn-cores is weakly convex and the lateral one strongly convex. The supraorbital foramina open into an elongated depression. The pedicles are short and the frontoparietal suture passes just behind them.

Although the general appearance of the described horn-cores is similar to that of *Prostrepsiceros houtumschindleri* from the same area, the orientation of the horn-core basal axis (Fig. 14A) and the development of a strong anterior keel prevent referral to the same species. These horn-cores appear also to

be 14–17% smaller in basal dimensions than those of *P. houtumschindleri*. Their morphology strongly resembles that of *Prostrepsiceros vinayaki* (Pilgrim, 1939) and *Sivoreas eremita* Pilgrim, 1939, both originally known from Siwaliks, Pakistan. Following Made & Hussain (1994), *P. vinayaki* differs from *S. eremita* in the more openly spiralled and weaker torsioned horn-cores, flaring strongly out, the less developed posterior keel, and the larger supraorbital pits. Hence, the Maragheh antelope matches better the Indo-Pakistani *P. vinayaki*, which appears, however, to be about 35% smaller in horn-core basal dimensions (Table 11).

The dental morphology of the two available lower tooththrows tentatively referred to this species is very similar to that of *P. houtumschindleri* but about 10% smaller and with rather shorter premolar row (47.0–51.6% of the molars instead of 53.0–58.0% in *P. houtumschindleri*) (Table 5). Furthermore, basal pillars occur only on m1, the goat fold is less marked than in *P. houtumschindleri* and the distinction between the paraconid and the parastylid on the p3 and p4 is less clear.

Prostrepsiceros fraasi (Andree, 1926) (Fig. 13A–D)

Helicoceros fraasi Andree, 1926: 163, pl. 11, fig. 4; pl. 15, fig. 1.

Helicophora rotundicornis – Mecquenem 1925: 39.

Prostrepsiceros rotundicornis – Gentry 1971: 265 *partim*.

TYPE LOCALITY. — Samos, Greece (late Miocene).

MATERIAL EXAMINED. — MNHN.F: A partial cranium, MAR1310; opisthocranium, MAR1060, 1059 juvenile; frontlet, MAR1010, 1306 (Mecquenem 1925: pl. VII, fig. 1 as *Helicophora rotundicornis*), 1322, 1318; isolated horn-cores, MAR1002, 2094, 1817, 1833; P2-M1, MAR2111; P3-M3, MAR2127; P4-M2, MAR1961, 1934; P4-M3, MAR3236; p2-m3, MAR3179; p3-m3, MAR3219; p4-m3, MAR1895.

DESCRIPTION AND REMARKS

This is probably one of the most confusing bovid taxa in the Maragheh assemblage, referred either to *Prostrepsiceros rotundicornis* (Weithofer, 1888) (i.e. Rodler & Weithofer 1890; Gentry 1971; Solou-



FIG. 15. — *Prostrepsiceros* cf. *vinayaki* (Pilgrim, 1939) from Maragheh: **A-C**, left horn-core (MNHN.F.MAR1005) in dorsal (**A**), frontal (**B**) and lateral (**C**) views; **D, E**, left horn-core (MNHN.F.MAR1003) in caudal (**D**) and frontal (**E**) views. Scale bars: 5 cm.

nias 1981; Watabe 1990) or to *P. fraasi* (i.e. Andree 1926; Bouvrain 1982; Bouvrain & Thomas 1992). Mecquenem (1908) originally described this spiral horned antelope as a new species *Antidorcas? gaudryi* but he later (Mecquenem 1925) changed his mind referring it to *Pr. rotundicornis*. Apart from the frontlet illustrated by Mecquenem (1925: pl. VII, fig. 1) the species is documented in the Maragheh collection of Paris by several additional cranial and dental specimens representing at least 8 individuals (Fig. 13A-D; Tables 4, 5, 12). More material has been published by Watabe (1990: 25, pl. III, figs 1, 2), whereas part of the *P. houtumschindleri* sample discussed by Bernor (1978) might belong to this species as well.

In distinction from *P. houtumschindleri*, the greatest axis of the horn-core base forms a 50-70° angle with the sagittal plane, whereas at 7 cm above the base the same axis is trending medio-posteriorly to antero-laterally forming a 30° angle with the sagittal plane. The mean horn-core compression index is 122% at the base (CI: 107.3-134.7; n = 9) and 84% at 7 cm above the base (CI: 77.8-88.9; n = 7) (Fig. 14, Table 12). The horn-cores are more uprightly inserted on the frontals than in *P. houtumschindleri* (Fig. 13A, B vs E), their divergence is much stronger even from the base (Fig. 13D vs G), the spiralling is widely open and the twisting less intense. None of the nine studied Paris specimens

TABLE 12. — Horn-core measurements (in mm) of *Prostrepsiceros fraasi* (Andree, 1926) from Maragheh. For abbreviations see text but H_{hc} is taken here along the anterior surface.

Coll. no. MNHN.F.	TD_{hcb}	APD_{hcb}	TD_{hc7}	APD_{hc7}	L_{hc}/H_{hc}
MAR1010 sin	40.50	32.50	25.70	30.50	
MAR1310 sin	42.70	34.00	24.00	27.00	
MAR1306 dex	35.00	28.40	22.70	26.60	
MAR1306 sin	35.30	30.00	21.50	26.20	230/180
MAR1322 dex	39.40	34.00	26.00	30.50	
MAR1322 sin	38.10	35.50			
MAR1318 dex	40.70	30.20			
MAR1318 sin	37.70	29.50	23.80	29.60	
MAR1002 dex	36.30	29.70			
MAR2094	40.00		25.30	29.70	
MAR1833	39.90	33.30			
MAR1817	35.80				

has either a posterior keel or grooving, whereas all bear a very weak anterior keel descending antero-medially to medially. In contrast to *P. houtumschindleri* the supraorbital depressions are placed close to the horn-core base (11.5–15.0 mm), the braincase is higher and more globular but of the same length, the occiput is higher (Fig. 13C vs F), the external occipital crest is ridge-like, the occipital condyles protrude downwards, the basi-occipital is comparatively longer, the paroccipital processes project more ventrally, and the lacrimal fossa is rather deeper.

In comparison with *P. houtumschindleri*, the tooththrows ascribed to this species (Fig. 4; Tables 4, 5) exhibit less developed and more centrally placed paracone on P3 and P4, strong metastyle on P4 (absent in *P. houtumschindleri*), anteroposteriorly developed metaconid on p4 and narrower lower molars with weaker entostylid.

The cranial and horn-core features of the Maragheh species are much closer to those of *P. fraasi* from Samos than to *P. rotundicornis* from Pikermi, which is characterized by shorter opisthocranium, shorter and more robust horn-cores that are less uprightly inserted on the frontals, more closely spiralled, taper faster upwards, and show more developed accessory features (keels, grooves). The single known skull of *P. fraasi* from Samos shows some features that are probably more advanced than

the Maragheh morph (i.e. stronger cranio-facial angle, slightly shorter opisthocranium, stronger temporal lines, strong-crest-like midfrontal and fronto-parietal sutures, absence of postcornual grooves and keel traces) but those characters are not worth species distinction and may represent time or local variation.

Prostrepsiceros cf. *rotundicornis* (Weithofer, 1888)
(Fig. 16)

Helicoceras rotundicorne Weithofer, 1888: 288, pl. 18, figs 1–4.

TYPE LOCALITY. — Pikermi, Greece (late Miocene).

MATERIAL EXAMINED. — MNHN.F: right horn-core, MAR1832.

REMARKS

A single isolated horn-core in MNHN.F (Fig. 16A, B) differs from the *P. fraasi* sample in its closer spiralling, tighter twisting, faster tapering, presence of a weak posterior keel associated with a furrow in the proximal part and some anterior grooving. The specimen lacks any indication of its insertion on the frontals and thus the orientation of its basal cross-section relatively to the sagittal plane is unknown. The horn-core proportions are 37.0×28.6 mm at the base and 21.8×28.0 mm at 7 cm above the base. These metrics imply less compressed horn-cores than in *P. cf. vinayaki* from Maragheh, which also differs in the stronger anterior keel. The specimen falls by its size within the lower values of *P. houtumschindleri* range but it is distinguished from it by the much weaker expressed posterior keel, the presence of anterior furrows and the less strong posterior curvature in side view. Most of MAR1832 characters compare very closely with those of *P. rotundicornis* from Pikermi (Fig. 16C) and Chomateri (Roussiakis 2009), and is the most likely referral.

Genus *Protragelaphus* Dames, 1883

TYPE SPECIES. — *Protragelaphus skouzesi* Dames, 1883.

Protragelaphus skouzesi Dames, 1883
(Fig. 17)

Protragelaphus skouzesi Dames, 1883: 97.

TYPE LOCALITY. — Pikermi, Greece (late Miocene).

MATERIAL EXAMINED. — MNHN.F: part of skull MAR1397 (Mecquenem 1925: pl. V, fig. 2, pl. VI, fig. 6), 1307; horn-core of juvenile individual MAR1830; palate MAR3228; mandible MAR1827 (Mecquenem 1925: pl. VI, fig. 1). — NHMW: part of frontal with left horn-core, A4898; frontlet without register number. — HUW: P2-M3 sin, MMTT7/2294; p2-p3 dex, MMTT13/1519.

DESCRIPTION AND REMARKS

Maragheh material ascribed to this species has been briefly communicated by Rodler & Weithofer (1890) and Mecquenem (1925). *Protragelaphus skouzesi* has been well defined by Gentry (1971) and Bouvrain (1978, 1992), who have also discussed the most important morphological features of the two Maragheh skulls stored in MNHN.F. A summary of the basic morphology is given here (Fig. 17; Tables 4, 5, 13):

The opisthocranium is short comparatively to the face (Fig. 17A, B). In dorsal view, the braincase has parallel lateral sides. The temporal lines are weak and converge to the rear. The nuchal crest is moderately developed. The occiput is rather low and wide (Table 13). The occipital bone is pentagonal-shaped and faces posteriorly. The mastoids are exposed mostly laterally. The basioccipital has strong, ridge-like posterior tuberosities and ridge-like anterior tuberosities that are elongated posteriorly. The foramina ovale open anterior to the anterior tuberosities. The auditory bulla is small. The main axis of the dorsal part of the paroccipital processes is obliquely oriented compared to the sagittal plane. The “V”-shaped choanae open distal to the M3, just behind the lateral indentations of the palate. The dorsal orbital rims do not project significantly. The anterior rim of the orbit is placed above the M3 (Fig. 17A, B). The lacrymal fossa is deep and elongated (MNHN.F.MAR1307). The infraorbital foramina are small and open above the P2-P3 limit. The nasals are long (Table 13) and most probably they have lateral flanges anteriorly. The frontal



FIG. 16. — *Prostrepsiceros* cf. *rotundicornis* (Weithofer, 1888) right horn-core (MNHN.F.MAR1832) from Maragheh in frontal (A) and caudal (B) views compared with *Prostrepsiceros rotundicornis* left horn-core (NHML M11438) from Pikermi in lateral view (C). Scale bar: 5 cm.

area is wide and in lateral view it forms an open angle with the parietal. The frontals between the horn-cores are elevated and convex. The midfrontal and fronto-parietal sutures are complicated and form together a “Y”. The supraorbital foramina are small, round and not sunken into depressions. The postcornual fossae are large and shallow. The horn-cores are placed posterior to the orbit, uniformly divergent from the base to the tip (Fig. 17A, B, D). They are robust at the base with greatest basal axis trending antero-posteriorly (Table 13). The posterior keel is strong as in *P. houtumschindleri* and it is usually associated with a furrow in the basal part (Fig. 17C, D). The torsion is loose and the spiraling very close, so that the overall pattern is that of twisting along a straight axis but less tightly than in *Palaeoreas* Gaudry, 1861. The horn-cores describe 1½ coil. There is no anterior keel but a porous zone is present anteriorly, close to the base.

The P2 and P3 are bilobed lingually with protocone distinct from hypocone. The P4 is less molarized and bears a posterior spur in the central fossette. The molar enamel is wrinkled and the styles are strong, especially the parastyle and the mesostyle. A hypoconal spur is present in some M2 and M3. The

TABLE 13. — Cranial and horn-core measurements (in mm) of *Protragelaphus skouzesi* Dames, 1883 from Maragheh, Pikermi and Samos. For abbreviations see text.

	Maragheh				Pikermi		Samos			
	MNHN.F. MAR1397	MNHN.F. MAR1307	MNHN.F. MAR1830 juvenile	NHMW A4898	Cast M10840	BMNH M4068	NHMS 13279			
W_{shc}	114.9	112.2								
W_{bc}	71.5	68.0			67.0	67.0				
W_{or}		(138)			113.0	112.8	(133)			
L_{fr}	92.6	89.8								
L_{fp-ocp}		134.3								
W_{so}		46.5			38.8		(46.3)			
L_{nas}	>85	–								
W_{bmas}		82.8			80.0					
W_{bcon}		52.5			52.0					
W_{ptb}		28.6			31.0					
W_{atb}		19.5			23.6	22.0				
H_{oc}		31.0			28+					
LM	49.0	47.9				45.5				
L_{hc}	260+	265	c. 220		>200		(224)			
	dex	sin	dex	sin	dex	sin				
TD_{hcb}	38.9	39.9	36.9	37.4	34.6	39.2	36.0	36.0	42.5	35.0
APD_{hcb}	55.2	57.2	49.5	51.3	44.6	45.7	40.3	38.2	44.0	47.0
TD_{hc7}	32.1	31.6	29.8	27.8						
APD_{hc7}	44.5	44.4	36.4	34.0						

M1 bears a small basal pillar. The p3 and p4 have independent and strong paraconid. The metaconid of the p4 extends strongly forwards. The lower molars lack a goat fold, the m1 has a small basal pillar and the third lobe of m3 consists of a single cuspid.

Protragelaphus skouzesi remains a rather rare late Miocene bovid species known from Greece (Pikermi, Samos, Halmyropotamos; Roussiakis 2009) and Maragheh. Geraads & Güleç (1999) described a few more isolated horn-cores from some Turkish localities, whereas more recently Roussiakis (2009) described some more frontlets from the locality Chomateri (Greece). Evidently the Samos frontlet (and probably the Manisa horn-core; Geraads & Güleç 1999: fig. 2d, e) presents significantly tighter horn-core torsion than the Pikermi, Chomateri and Maragheh specimens, whereas the Pikermi and Chomateri horn-cores appear to be less mediolaterally compressed (CI = 78.5–96.5%, n = 14; Roussiakis 2009 and pers. data) than those from Maragheh (CI = 70–74.5%, n = 4) and Samos (CI = 74.5%, n = 2). Nevertheless, these differences can be accommodated within intraspecific variability (Table 13).

Genus *Palaeoreas* Gaudry, 1861

TYPE SPECIES. — *Palaeoreas lindermayeri* (Wagner, 1848).

cf. *Palaeoreas* sp. (Fig. 18)

MATERIAL EXAMINED. — HUW: P2-M3sin, MMTT7/2159 (LP = 25.0 mm, LM = 38.4 mm, LPM = 62.2 mm); p2-m3dex, MMTT7/2338 (LP = 23.5 mm, Lm = 41.6 mm, Lpm = 65.5 mm); p4-m3dex, MMTT7/1912 (Lm = 43.3 mm).

REMARKS

A medium sized antelope from MMTT7 is documented in the HUW collection by a few tooththrows (Fig. 18), previously referred to as *Prostrepsiceros* (Bernor 1978). The premolars represent 65% of the upper and 56.5% of the lower molar row. In distinction from the similar-sized *Prostrepsiceros*, the teeth are more brachyodont with bulbous styles and ribs and the tooth enamel is thin rippled. The upper premolars are simple with the

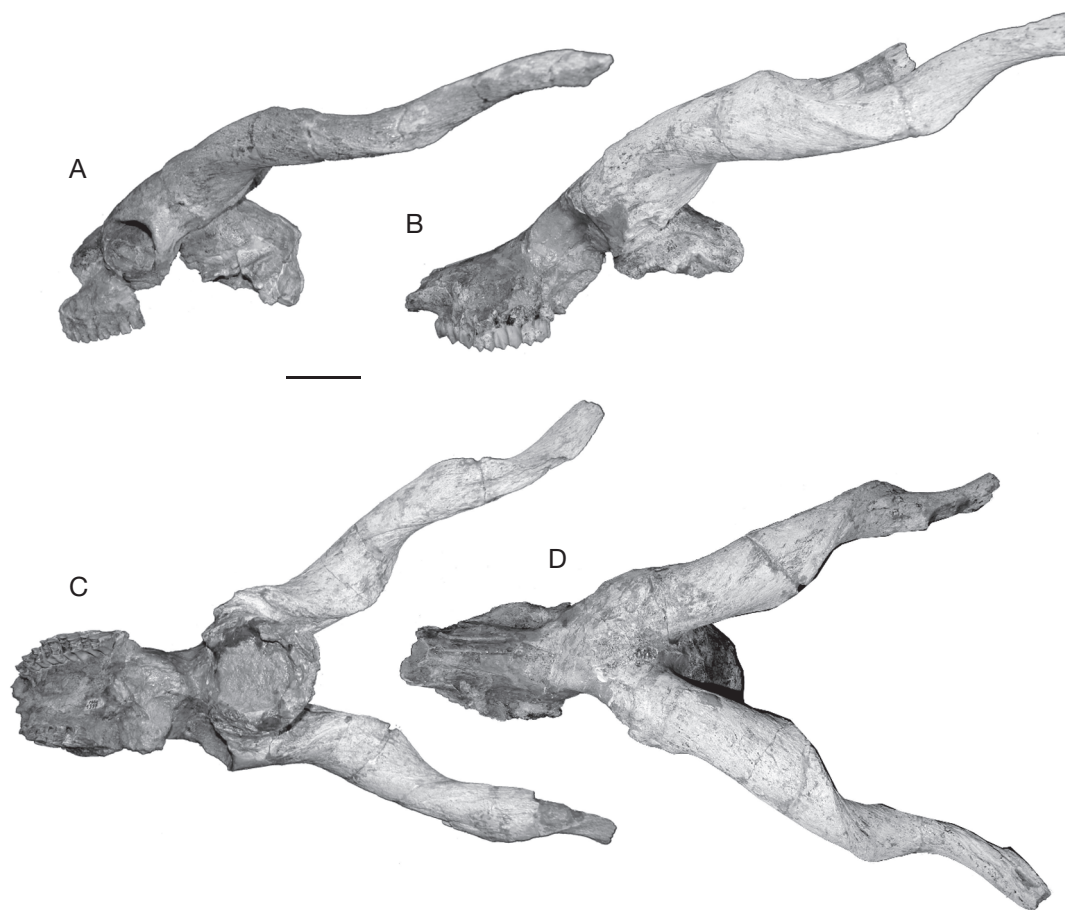


FIG. 17. — *Protragelaphus skouzesi* Dames, 1883 crania from Maragheh: **A**, MNHN.F.MAR1307 in lateral view; **B-D**, MNHN.F.MAR1397 in lateral (**B**), ventral (**C**) and dorsal (**D**) views. Scale bar: 5 cm.

P2 as long as the P3 but narrower (Fig. 18E). The upper molars bear a central islet (double on M2) and the metastyle of M3 directs distally (Fig. 18E). The hypoconid of the p3 and p4 is well-distinguished from the protoconid by a deep labial groove (Fig. 18A, C). The anterior valley of the p4 is open and the metaconid is weakly developed anteroposteriorly and fused in later stages of wear with the entoconid. All lower molars of MMTT7/2338 bear a rather strong basal pillar and a weak goat fold, characters that appear, however, to be variable: in MMTT7/1912 a weak basal pillar is present only on m1 whereas the goat fold of m3 is significantly strong. The main

dental characters of these specimens and their proportions match pretty well those of *Palaeoreas lindermayeri* (Wagner, 1848) from Greece and Bulgaria (Gaudry 1865; Gentry 1971; Geraads *et al.* 2003) from which they differ in the development of accessory features (goat folds, basal pillars, etc.) but the material is certainly insufficient for an accurate identification.

Genus *Skoufotragus* Kostopoulos, 2009

TYPE SPECIES. — *Skoufotragus schlosseri* (Andree, 1926).

TABLE 14. — Cranial and horn-core measurements (in mm) of *Skoufotragus laticeps* (Andree, 1926) from Maragheh, Pikermi and Samos. For abbreviations see text.

	MNHN.F				NHML	
	MAR3206		MAR1321		MAR2092	M3878
W _{shc}	108.20		100.00			
W _{bhc}			76.90			
W _{or}						132.00
W _{bc}						73.80
W _{so}	40.60		39.30			
L _{fr}	94.7					
W _{ptb}						38.10
W _{atb}						24.50
LPM	(94)					
LP	(38)					
LM	59.00					
L _{hc} /H _{hc}						c. 320/c. 270
	<u>dex</u>	<u>sin</u>	<u>dex</u>	<u>sin</u>	<u>dex</u>	<u>sin</u>
TD _{hcb}	36.30	37.75	37.80	42.00	(36)	46.00
APD _{hcb}	57.10	57.30	57.80	62.30	65.20	72.70
TD _{hc7}	26.0	27.10	28.20	29.40		
APD _{hc7}	43.90	41.90	48.30	48.10		

Skoufotragus laticeps (Andree, 1926)
(Fig. 19)

Protoryx carolinae var. *laticeps* Andree, 1926: 153, pl. 12, figs 5, 9.

Protoryx longiceps Pilgrim & Hopwood, 1928: 34.

Protoryx carolinae – Mecquenem 1925: 33. — Bosscha-Erdbrink 1988: 130-137.

Pachytragus laticeps – Gentry 1971: 244. — Solounias 1981: 199. — Bernor *et al.* 1996: table 10.2.

TYPE LOCALITY. — Samos, Greece (late Miocene).

MATERIAL EXAMINED. — MNHN.F: Part of cranium, MAR3206 (Mecquenem 1925: pl. V, fig. 3 as *Protoryx carolinae*); frontlet, MAR1321 (Mecquenem 1925: pl. V, fig. 4 as *Pr. carolinae*); part of right horn-core, MAR2092+2122; left P2-P4, MAR1079 (Mecquenem 1925: pl. IV, fig. 5 as *Pr. carolinae*); right P2-P4, MAR2991 (LP = 37.8 mm); left M2-M3, MAR3002; right p3-m3, MAR1063 (Mecquenem 1925: pl. IV, fig. 4 as *Pr. carolinae*; Lm = 63.9 mm); left p4-m3, MAR2972 (Lm = 61.1 mm); right m1-m3part, 2985+3005. — NHML: part of cranium M3878 (Pilgrim & Hopwood 1928: pl. III, figs 2, 2a labelled as M3841). — HUW: p2-m1dex, MMTT13/1397 (Lp = 39.6 mm); m2-m3sin, MMTT13/2504; MMTT7/1987; m3sin.

DESCRIPTION AND REMARKS

Large antelopes are mainly represented in the Maragheh fauna by the so-called protoryxoid bovids. Two partial crania and a mandible from Maragheh identified by Mecquenem (1925: pl. IV, fig. 4; pl. V, figs 3, 4) as *Protoryx carolinae* Major, 1891 were later attributed to a new species *Protoryx longiceps* Pilgrim & Hopwood, 1928 together with the Maragheh cranium NHML M3878 (Fig. 19). After revising the systematics of this bovid group, Gentry (1971: 245) ascribed the Maragheh sample to *Pachytragus laticeps* Schlosser, 1904. Descriptions and illustrations of both the London cranium and the Paris cranial sample are already given by Mecquenem (1925), Pilgrim & Hopwood (1928) and Gentry (1971) (see also Fig. 19, Table 14). In summary, the braincase is narrow and long (Fig. 19B, C) with the cranial roof facing partly laterally, the occipital condyles are rather small, the basioccipital is long with very strong posterior and strong, well-localized anterior tuberosities, the dorsal orbital rims project weakly laterally, the fronto-parietal and midfrontal sutures are open, the supraorbital foramina are small, oval and not sunken into depressions, there are no postcornual fossae, the fronto-nasal suture ends to a single point, the

frontals are moderately elevated and hollowed, the anterior rim of the orbit is placed behind M3, the ethmoidal fissure is long and narrow, the lacrimal fossa is long, rather shallow and without sharp limits, and the infraorbital foramen opens above P3-P4 limit. The horn-cores are inserted above the orbits, gently and uniformly curved backwards, with increasing upward divergence, flat medial surface and elliptical cross-section that may become semicircular to spindle-shaped towards the tips (Fig. 19A, B).

The MNHN.F Maragheh sample includes some additional tooththrow specimens attributable to this species; a few tooththrows in HUW should be also referred here. The upper dentition of this species is characterized by bilobed P2 with an anteriorly placed paracone rib and a weak parastyle. The P3 has a strong parastyle, a thin but strong metastyle and a strong, sharp paracone rib. The P4 shows a weakly developed hypocone, a strong parastyle and a blunt paracone rib. The protocone of the M1 protrudes strongly lingually. The upper molars show a central islet, thin and weak mesostyle and strong parastyle and metastyle, the latter one being directed distally on M3. In the lower tooththrow, the p3 and p4 are simple with strong hypoconid, a paraconid well separated from the parastylid (less so on p4), an entoconid quickly merged with the entostylid and a distally placed metaconid that directs backwards on p3, where it is associated by an anterior lingual flange instead of being curved to the front on p4, closing the anterior valley in the lower half of the crown. The lower molars have a strong parastylid, no goat folds, moderate lingual ribs, a basal pillar is usually present on the m1 and less often on the m2, and the third lob of the m3 is semicircular.

Bosscha-Erdbrink (1988) described an important sample of crania and tooththrows recovered in 1973 from the localities Guzuguneh, K1 and K2 of Maragheh; disagreeing with Gentry's (1971) view, he referred them to *Protoryx carolinae*. Bernor (1978) attributed a partial cranium with horn-cores and several tooththrows of the LRE to *Pachytragus crassicornis* Schlosser, 1904, adopting Gentry's (1971) systematic views. Solounias (1981) following only the species-level taxonomy

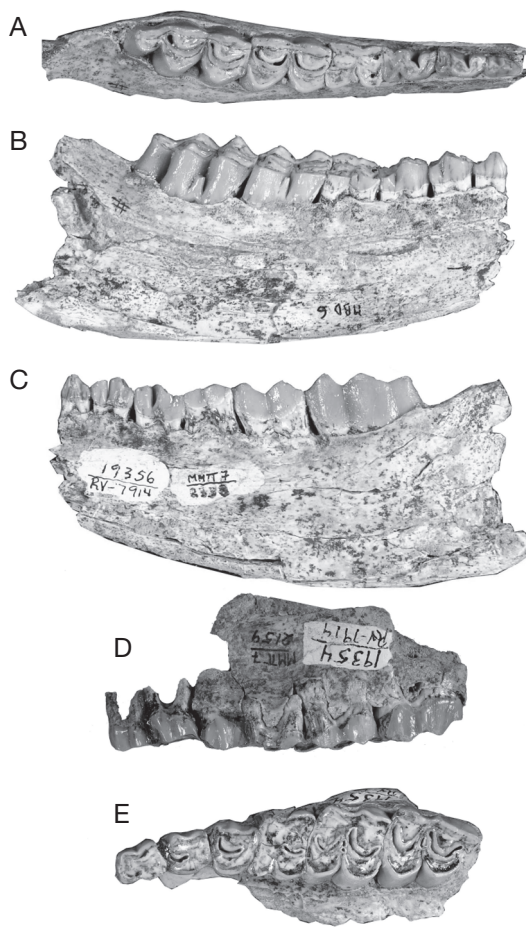


FIG. 18. — Cf. *Palaeoreas* sp. from Maragheh: **A-C**, right mandible (MMTT7/2338) in occlusal (**A**), labial (**B**) and lingual (**C**) views; **D, E**, left P2-M3 (MMTT7/2159) in labial (**D**) and occlusal (**E**) views. Scale bar: 5 cm.

proposed by Gentry (1971) recognized two species of *Protoryx* at Maragheh, while some years later (in Bernor *et al.* 1996) he accepted Gentry's (1971) distinction of genera. As a total, 12 more or less complete crania of the so-called "*Protoryx-Pachytragus* group" have been so far described from Maragheh, indicating that the relevant taxon (or taxa) was of rather great importance in the structure of the local ruminant community.

Given that the systematics of the "*Protoryx-Pachytragus* group" has been recently reviewed

TABLE 15. — Comparison of *Palaeoryx* Gaudry, 1861 dental characters from Maragheh and Pikerimi.

	Pikerimi	Maragheh
P2 parastyle	strong	stronger
P4 paracone	weaker than parastyle and more centrally placed than in P3	equal to parastyle and similar with P3
P4 metastyle	strong	stronger
Upper molars	moderate paracone rib	strong paracone rib and more quadrangular posterior lobe in lateral view
M2	without hypoconal spur	with weak hypoconal spur
p3	metaconid quickly fused with entoconid	metaconid staying more independent
p4	paraconid fused with metaconid and well-developed hypoconid	open second valley and less developed hypoconid
m3	rounded-squarish protoconid and hypoconid	angular protoconid-hypoconid

(Kostopoulos 2009a), there is no need to repeat all details. According to this viewpoint, *Protoryx* is generically distinct from *Pachytragus* (in accordance with Gentry [1971]), which in its turn is an invalid name replaced by a new one, *Skoufotragus*. *Skoufotragus*, originally known from Samos, Greece is represented by three species that succeed one another through time (Kostopoulos 2009a). Although the presence of a second *Skoufotragus* species at Maragheh (i.e. Bernor 1978; Bernor *et al.* 1996) cannot be excluded, the currently examined sample from Paris and London falls within the range of *Sk. laticeps* from Samos both morphologically and metrically; it is therefore referred to this species in agreement with Gentry (1971). Some of the specimens of the K2 site illustrated by Bosscha-Erdbrink (1988: pl. IV, V) look similar to *Sk. schlosseri* (Andree, 1926) (i.e. part of *Pachytragus crassicornis*; Kostopoulos 2009a) in their horn-core morphology but again their cranial aspect and basioccipital structure indicate closer affinities with *Sk. laticeps*.

Genus *Palaeoryx* Gaudry, 1861

TYPE SPECIES. — *Palaeoryx pallasi* (Wagner, 1857).

Palaeoryx sp.

Palaeoryx pallasi – Mecquenem 1925: 31.

MATERIAL EXAMINED. — MNHN.F: Palate, MAR1011 (Mecquenem 1925: pl. IV, fig. 2 as *P. pallasi*; $LP_{sin} = 62.1$ mm, $LM_{sin} = 82.6$ mm, $LPM_{sin} = 140.8$ mm); right mandibular ramus with p2-m3, MAR1012+1852 (Mecquenem 1925: pl. IV, fig. 3 as *P. pallasi*; $Lp = 54.0$ mm, $Lm = 84.6$ mm, $Lpm = 139.3$ mm); right mandibular ramus with m1-m3, MAR1068 ($Lm = 74.0$ mm very worn); left p2-p4, MAR3232 ($Lp = 55.4$ mm); left m2-m3, MAR3231.

REMARKS

Lydekker (1886) was the first to indicate the presence of *Palaeoryx* at Maragheh. Later, Rodler & Weithofer (1890) briefly described but did not illustrate an almost complete skull, referred to as *Palaeoryx pallasi* (Wagner, 1857). Mecquenem (1925) assigned to the same species a skull, two isolated horn-cores, a palate and a mandible. Arambourg & Piveteau (1929: footnote) and Geraads (1974) correctly stated that one of the horn-cores illustrated by Mecquenem (1925: fig. 9 left) belongs to a giraffid. Geraads (1974: 48, footnote) also believes that a Maragheh horn-core specimen (MAR658) previously referred by Mecquenem (1925: fig. 9 right) to *Palaeoryx* might in fact belong to a giraffid as well. Additionally, the cranium MAR1396 (Mecquenem 1925: pl. IV, fig. 1) demonstrates nothing in common with *Palaeoryx*, likely representing a boselaphine, which Bohlin (1936) and later Gentry (1971) ascribed to a large tragoportacine (but see discussion below). The latter author (Gentry 1971: 237) also suggested that there is no convincing evidence of *Palaeoryx* from Maragheh.

In contrast to this statement, some large tooththrows in MNHN.F (Mecquenem 1925: pl. IV, figs 2, 3) should be ascribed to *Palaeoryx* by their moderate hypsodonty, rugose enamel, long premolars compared to the molars, large upper premolars with bilobed P2 and P3, strong paracone rib and parastyle on the wide upper molars, knob-like upper and small lower basal pillars on the molars, and p4 with independent



FIG. 19. — *Skoufotragus laticeps* (Andree, 1926) cranium (NHML M3878) from Maragheh in frontal (A), lateral (B) and caudal (C) views. Scale bar: 5 cm.

metaconid. Although *Palaeoryx pallasii* was for many years the single known species of the genus from SE Europe and Eastern Mediterranean including several varieties, Kostopoulos (2005, 2009a) recognized that *Palaeoryx majori* Schlosser, 1904 is a valid species occurring in Samos, Halmyropotamos, Greece and Akkasdağı, Turkey. Dental comparison between Maragheh, Samos and Pikermi does not show striking morphological differences (Table 15) but toothrow linear measurements indicate that *P. majori* and *P. pallasii* are smaller than the Maragheh species (by about 15%). There is, however, an unpublished *Palaeoryx* palate from Pikermi in MNHN.F (PIK2447) labelled as “*Miotragocerus?*”, which is larger than the typical *P. pallasii* tooth rows and very similar both morphologically and metrically to the Maragheh palate. MAR1011 (Mecquenem 1925: pl. IV, fig. 2) differs from PIK2447 only in the slightly stronger development of the molar styles and the more developed paracone rib of P4, which forms a sharper angle with the parastyle. Unfortunately the absence of adequate material does not permit further comparison. It is,

however, worth noting that a *Palaeoryx* of comparable size is also known from Nova Emetovka 2, Ukraine (Krakhmalnaya 1996: 155). Examination of the two available crania (25-3312 and 25-1393) in Kiev suggests that the Nova Emetovka 2 form represents a distinct species from both *P. pallasii* and *P. majori* and very similar to the Maragheh form, from which it slightly differs in the P4 morphology.

Genus *Urmiatherium* Rodler, 1889

TYPE SPECIES. — *Urmiatherium polaki* Rodler, 1889.

Urmiatherium polaki Rodler, 1889 (Figs 20-22)

HOLOTYPE. — Part of skull (Rodler 1889: pls 1-4; cast NHML M4114).

TYPE LOCALITY. — Maragheh, Iran (late Miocene).

TABLE 16. — Cranial and horn-core measurements (in mm) of *Urmiatherium polaki* Rodler, 1889 from Maragheh. For abbreviations see text.

	NHML	MNHN.F.	
	M4114 cast	MAR3215	MAR1359
W_{bhc}		98.00	
W_{bc}	117.00	109.90	
W_{bmas}	134.50	130.70	
W_{bcon}	82.20	77.00	
W_{ptb}		38.90	
W_{atb}		45.30	
H_{oc}	67.50		
TD_{hcb}	42.00		
APD_{hcb}	97.00	>130	78.40

MATERIAL EXAMINED. — MNHN.F: cranium, MAR3215 (Mecquenem 1925: figs 12, 13; pl. VIII, fig. 9); partial frontals with the base of horn-core, MAR1359; atlas, axis and cervical vertebrae, MAR3090 (Mecquenem 1925: pl. VIII, figs 7, 8; pl. IX, fig. 1); left M3, MAR1055 (Mecquenem 1925: pl. VIII, fig. 4; L = 36.2 mm, W = 27.8 mm); right M2, MAR1054 (Mecquenem 1925: pl. VIII, fig. 3; L = 31.8 mm, W = 25.5 mm); left M1/2, MAR1056 (Mecquenem 1925: pl. VIII, fig. 5; L = 28.3 mm, W = 25.0 mm); D4-M1 (Mecquenem 1925: pl. VIII, fig. 6); p2-m3sin, MAR1035 (Mecquenem 1925: pl. V, fig. 8 as *Antilope* indet.); p4-m2sin, MAR2968; m2part-m3 dex, MAR2967; p2-m1sin, MAR2976; m3sin, MAR2027. — NHML: a cast (M4114) of the partially preserved holotype cranium described and figured by Rodler (1889: pls I-IV) and stored in Vienna. — HUW: metacarpal MMTT13/2462; proximal and distal part of metacarpal MMTT13/1256.

DESCRIPTION AND REMARKS

In 1888 A. Rodler announced the discovery of a supposedly sivatherine skull, collected by Dr J. E. Polak from Ilkhchi, SE from Maragheh. In this very brief first note, Rodler (1888) gave some morphological highlights and introduced a new generic name, *Urmiatherium*. One year later, Rodler (1889) described this cranium in detail as a new species *Urmiatherium polaki*. Mecquenem (1908, 1925) ascribed to the same species another partially preserved cranium (MAR3215; Fig. 20), several isolated upper molars (MAR1054-1056) and a few vertebrae (MAR3090; Fig. 20) stored in MNHN.F. Re-examination of the MNHN.F Maragheh collection allows, however, detecting some additional specimens that should be attrib-

uted to *U. polaki*. *Urmiatherium* is also the most likely referral for two metacarpals in the HUW collection.

The main dimensions of the two available skulls are given in Table 16, though their preservation status does not permit detailed measurements. Mecquenem (1925) suggested that the Paris cranium (Fig. 20) belongs to an individual ontogenically older than the holotype, possibly because of the shorter and unfused horn-cores of the latter specimen; this is probably correct, although absolute dimensions indicate that NHML M4114 is somewhat larger than MAR3215 (Table 16). MAR1359 is an additional skull fragment from Maragheh with unfused horn-cores. Since the face is missing from all known specimens, the cranial anatomy of *Urmiatherium polaki*, already given by Rodler (1889) and Mecquenem (1925), refers only to the braincase and horn-core morphology. Both crania are characterized by stout, short and wide braincase with extremely reduced parietal especially on the top of the cranial roof (Fig. 20). The enlarged occipital lies on the same level with the parietal and the back of the frontals, altogether facing dorso-caudally. The bulky and round occipital condyles lie on the same plane as the occipital surface and bear large supplementary facets for the atlas articulation. The strong paroccipital processes are placed more antero-ventrally than the condyles and are directed postero-ventrally; their internal faces also have large additional articular facets for the atlas. The mastoid is large and faces laterally. The nuchal crest is very strong and the fronto-parietal suture forms a rough and thick cord on that marks the posterior contact of the horn-cores with the frontals (Fig. 20). The external occipital crest is short but strong, surrounded by two localized muscular scars with rough limits (Mecquenem 1925: fig. 12). The temporal fossa is long and deep with salient borders (Fig. 20). The auditory meatus is round and rather large. The frontals are significantly elevated above the orbits and extensively hollowed with sinuses invading the horn-core base. The interfrontal suture forms a sharp crest in the holotype but it has been covered by the horn-cores in MAR3215. The orbits are rounded. The basioccipital is moderately

short, pentagonal in ventral view and very thick (Mecquenem 1925: pl. VIII, fig. 9); the left half of the basioccipital bone is slightly stronger than the right one in both skulls, indicating a clear asymmetry. The posterior tuberosities project strongly ventrally, forming together an accessory semicircular (or half-oval) facet for the articulation of the atlas. The anterior tuberosities look like elongated crests that surround the basioccipital towards the rear. A deep and narrow furrow runs between the anterior and the posterior tuberosities. The auditory bullae are small and their great axis is oblique to the sagittal plane. The foramen ovale is moderately large and faces laterally.

The base of the horn-cores covers most of the frontals extending from the anterior-most point above the orbits to the fronto-parietal suture (Fig. 20). The horn-cores are rather short and robust, with a strongly concave posterior face in MAR3215. Deep, wide longitudinal grooves are present on the posterior and lateral horn-core surfaces of MAR3215 and in the medial surface of the holotype. In lateral view, a deep longitudinal furrow (Mecquenem 1925: 43) distinguishes the anterior from the posterior part of the horn-core, which seem to follow different rates of development. In sub-mature ontogenetic stages (NHML M4114, MAR1359), the horn-cores are directed backwards, being weakly curved and having a spindle-shaped cross-section with great basal axes converging to the rear; at this stage, the anterior part of the horn-cores is probably low, forming an anteriorly extended buttress above the orbit. Further development (MAR3215) allows the horn-cores to expand their bases mostly medially and posteriorly resulting in their fusion along the sagittal plane and the incorporation of the fronto-parietal ridge into the horn-core base; at the same time, the supraorbital part of the horn-cores increases upwards forming step-like rugged plates that are attached to the posterior part. Bohlin (1935a, b; 1937) further discussed anatomical details of *Urmiatherium* horn-cores.

All upper molars are characterized by rather thick enamel and an almost square posterior lobe that is more buccally displaced in comparison with the anterior one. The anterior fossette shows a quite

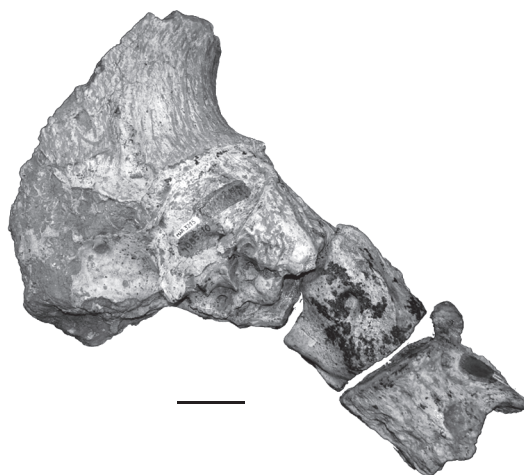


FIG. 20. — *Urmiatherium polaki* Rodler, 1889 cranium (MNHN.F.MAR3215) with attached cervical vertebrae from Maragheh in lateral view. Scale bar: 5 cm.

strong posterolingual projection. A large central islet is always present. The parastyle is very strong and is directed mesio-buccally. The mesostyle is strong with a deep, concave anterior flange. The metastyle is weaker than the other two styles and is directed distally. The paracone rib is well-developed. The cement is present.

The mandibular corpus is shallow (Fig. 21B, C). The lower premolar row is short, representing 47.7% of the molars (Table 17). The p2 (Fig. 21A) is simple with a weak parastylid, a distally directed metaconid and broad talonid. The paraconid and the parastylid of the p3 are fused into a single anterior stylid (Fig. 21A), even though a parastylid is still present in the less worn toothrow MAR2976. The strongly distally directed metaconid is long, covering the lingual wall of the talonid. The hypoconid is barely recognizable. The entostylid is short. The p4 is very similar to the p3 but with stronger anterostylid (paraconid+ parastylid) and more anteroposteriorly directed metaconid, both differences resulting in a less open anterior valley (Fig. 21A). The posterior part of the lingual wall of the p4 is continuous. The hypoconid is well-developed, protruding buccally. The first two molars bear a weak goat fold, a strong parastylid, a weak entostylid and a gently crenulated



FIG. 21. — *Urmiatherium polaki* Rodler, 1889 left mandible (MNHN.F.MAR1035) from Maragheh in occlusal (A), labial (B) and lingual (C) views. Scale bar: 5 cm.

lingual wall (Fig. 21A, C). There is no basal pillar (Fig. 21B). The m3 has a strong parastyloid, a well-developed entostyloid, and a moderately well developed metastyloid that is present in the upper half of the crown attached to the anterior lobe. A goat fold is absent from MAR2967 but it is present in MAR1035 and especially in MAR2027. The third lobe of m3 is buccally displaced, semi-circular shaped and with a rather strong posterior styloid (Fig. 21A, C).

Mecquenem (1925: 44-45) gave a basic morphological description of the cervical vertebrae of *Urmiatherium*, while Sickenberg (1933) and Bosscha-Erdbrink (1978) further discussed the neck anatomy of *Urmiatherium*. According to them, the tight atlanto-cranial joint including additional facets in the basicranium suggests a

low ability for anterior flexion of the skull while the atlas-axis articulation also indicates restricted lateral movements of the skull on the neck, features that are possibly related with ramming intraspecific behavior.

A complete metacarpal_{III+IV} (MMTT13/2462; Fig. 22) and parts of another metacarpal_{III+IV} (MMTT13/1256) in the MMTT-HUW collection cannot be associated with any other known bovid species from Maragheh and are consequently regarded as representing *Urmiatherium*. The metacarpal_{III+IV} is rather short (210 mm) and moderately robust (the robusticity index $DT_{diaphysis}/Length$ is 11.6; the index $DT_{distal}/Length$ is 20.7) with wider distal than proximal epiphysis ($DT_{proximal} = 39.5$ mm, $n = 1$; $DT_{distal} = 43.5-44.5$ mm, $n = 2$). The metacarpal diaphysis has

TABLE 17. — Lower tooth measurements (in mm) of *Urmiatherium polaki* Rodler, 1889 from Maragheh. For abbreviations see text.

	MNH.N.F. MAR1035	MNH.N.F. MAR2968	MNH.N.F. MAR2967	MNH.N.F. MAR2976	MNH.N.F. MAR2027
L _{pm}	123.90				
L _p	39.50	(39.9)	(39)		
L _m	82.70				
L _{p2}	10.50		10.30		
W _{p2}	6.70		7.10		
L _{p3}	13.40		14.30		
W _{p3}	8.80		9.30		
L _{p4}	16.30	16.30	15.20		
W _{p4}	10.50	11.20	10.80		
L _{m1}	19.20	19.20	17.20		
W _{m1}	14.30	15.00	14.80		
L _{m2}	26.20	22.80			
W _{m2}	16.00	15.30			
L _{m3}	37.95			35.50	35.10
W _{m3}	15.50			16.50	17.70

parallel sides and a flat palmar surface. The proximal anteromedial tuberosity is rather weak. The cranial longitudinal groove is reduced. The caudal notch of the proximal epiphysis is open, narrow and shallow. The proximal facet for the capitotrapezoideum is almost squarish. The distal condyles are asymmetric with parallel keels both in the caudal and cranial sides. The supra-articular tubercles of the distal epiphysis are weak and the incisura intertrochlearis is rather narrow.

The *Urmiatherium* lineage is central to a long discussion concerning tribal affiliations of a set of late Miocene bovid genera referred to as *Urmiatherium*-group (Gentry 1996). This group exhibits specialized horn-cores and peculiar occipital morphology including – or not – accessory articulations for the atlas (e.g., Bosscha-Erdbrink 1978; Bouvrain & Bonis 1984; Bouvrain 1994; Bouvrain *et al.* 1995; Gentry 1996; Gentry & Heizmann 1996; Gentry *et al.* 1999; Geraads *et al.* 2002; Chen & Zhang 2004; Geraads & Spassov 2008). Apart from *Urmiatherium*, potential members of this group are *Mesembriacerus* Bouvrain & Bonis, 1984 from the late Vallesian of Greece, *Criotherium* Major, 1891 from the early-early middle Turolian of W Anatolia and S Balkans, *Plesiaddax* Bohlin,



FIG. 22. — *Urmiatherium polaki* Rodler, 1889 metacarpal bone (MMTT13/2462) from Maragheh in cranial (A) and caudal (B) views. Scale bar: 5 cm.

1935, *Tsaidamotherium* Bohlin 1935, and a set of other late Miocene genera from China (Qiu *et al.* 2000; Zhang *et al.* 2000; Zhang 2003; Chen & Zhang 2004). *Urmiatherium* currently includes three species: *U. polaki* from Maragheh, *U. intermedium* Bohlin, 1935 from Shaanxi, China and *U. rugosifrons* (Sickenberg, 1932) from Samos, Greece (for synonymies see Gentry 1971; Solounias 1981; Bouvrain & Bonis 1984; Bouvrain *et al.* 1995; Gentry *et al.* 1999; Kostopoulos 2009a). The Chinese species is known from Locs 30, 43, 44, 49 and 108 of Shaanxi, as well as from Locs

115 and 116 of Kansu suggesting a late Miocene, middle-late Turolian-equivalent age (between 7.2 and 5.5 Ma; Li *et al.* 1984 and Zhang pers. comm. 2009). *Urmiatherium rugosifrons* occurs in Samos levels of late middle Turolian age, magneto-chronologically dated at 7.1 Ma (Kostopoulos *et al.* 2003). “*Parurmiatherium rugosifrons*” from Djebel Hamrin, Irak (Bouvrain *et al.* 1995) likely represents a primitive *Plesiaddax* rather than a small *Urmiatherium*, while the holotype cranium of *Plesiaddax simplex* Köhler, 1987 from Kayadibi, Turkey is undiagnostic at the genus level (see also Bouvrain *et al.* 1995; Geraads & Spassov 2008). Finally, the generic affiliations of *Plesiaddax inundatus* Bosscha-Erdbrink, 1978 from Garkin, Turkey remain open to discussion (i.e. Bouvrain *et al.* 1995; Geraads & Spassov 2008).

Since comparison on cranial anatomical details between *U. polaki* and other related species and genera are already given in Mecquenem (1925), Bohlin (1935a, b, 1937), Bosscha-Erdbrink (1978), Köhler (1987), and Bouvrain *et al.* (1995) there is no reason to repeat these previous assessments. The new material ascribed to *Urmiatherium polaki* from Maragheh suggests that this highly specialized large bovid was additionally characterized by a premolar tooth row that is short compared to the molar tooth row and, apparently, moderately elongate and rather stout and wide metapodials.

The upper molars of *U. polaki* described by Mecquenem (1925) are very similar but slightly larger than those of *U. intermedium* from China (Bohlin 1935a), whereas the lower molars of *U. intermedium* are slightly narrower than those of *U. polaki* described here. The lower toothrow of *U. polaki* (Lpm = 123.9 mm) is about 27% larger than that of *U. rugosifrons* from Samos (Lpm = 98 mm; Kostopoulos 2009a) and about 12% larger than that of *Plesiaddax depereti* Bohlin, 1935 from China (Lpm = 110-114 mm); it is fully comparable in size with the lower toothrow of *U. intermedium* from China (Lpm = 102.2-121.4 mm; Bohlin 1935a) and “*Plesiaddax inundatus*” from Garkin (Lpm = 112.5-133 mm). The reduction of the premolar row seen in *U. polaki* (47.7% of the molars) is analogous to that of *U. intermedium* (41.9-49.2%, n = 5, mean = 46.5%;

Bohlin 1935a) and *Plesiaddax depereti* from China (47.6-50.2%, n = 4, mean = 49%; Bohlin 1935a), and significantly more advanced than that of *U. rugosifrons* (56.1-58.5%, n = 2; Kostopoulos 2009a). “*Plesiaddax inundatus*” shows a greater range but on the average it has longer premolar row (45.3-63.9, n = 11, mean = 53.6; Bosscha-Erdbrink 1978). *Criotherium* from Samos and Turkey has slightly smaller lower dentition but with longer premolars than *U. polaki* (Bouvrain 1994 and pers. obs.).

Morphologically, *U. rugosifrons* differs from *U. polaki* in having longer and narrower p2, a p3 with distinct paraconid at first wear stages and more anteriorly oriented anterostylid, shorter and stronger labially protruding protoconid and hypoconid on the lower molars, no goat folds and round, not labially shifted talonid on m3. The mandibular corpus of *U. intermedium* is rather shallower than that of *U. polaki*, its p4 is more molarized with contact between the paraconid and the metaconid in 6 out of 8 illustrated specimens (Bohlin 1935a) and antero-posteriorly oriented metaconid in 5 out of 7 specimens. Its p3 has a subtriangular shaped metaconid, and the paraconid turns backwards in 7 out of 8 illustrated specimens. *Plesiaddax depereti* has longer diastema than *U. intermedium* and possibly *U. polaki* (Bohlin 1935a). It also differs from *U. polaki* in the less tightly fused lobes on the lower molars, the smaller talonid of m3, the much weaker parastylid and the better separated metaconid and entoconid on p4, the forwardly extended metaconid on p3 and the more transverse parastylid of the p3 and p4.

Thusfar, there are few postcranial elements that can be referred to *Urmiatherium*. Bohlin (1935a) himself refrained from attributing limb bones to the otherwise rich Chinese sample of *U. intermedium*. Nevertheless, Bohlin (1935a: text-fig. 134) records a rather short canon bone from Baode Loc. 116 that is quite similar to the metacarpals described above and it could be attributed either to *U. intermedium* or to *P. depereti*. Recently, Kostopoulos (2009a) ascribed to *Urmiatherium rugosifrons* some short and wide metacarpals from Samos, which show similarities in their proportions with the metacarpals from Maragheh MMTT 13. Köhler

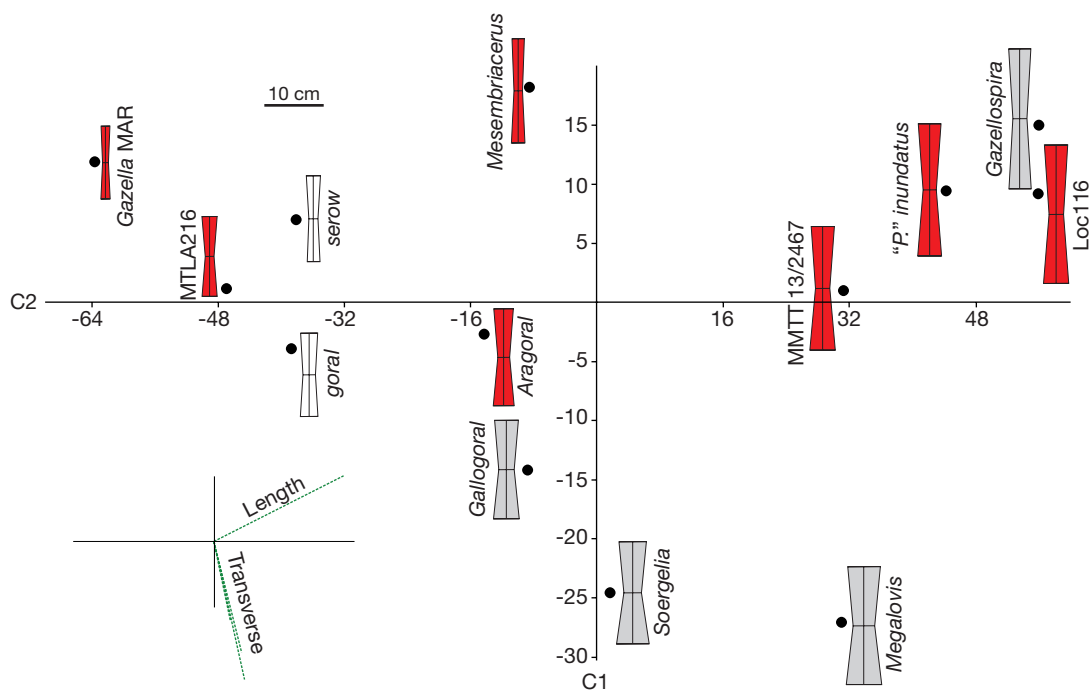


FIG. 23. — Principal Component Analysis of metacarpal measurements (Length, Transverse diameter at the proximal and distal epiphysis, and at the middle of the diaphysis) in several Miocene (marked in dark grey), Plio-Pleistocene (marked in grey) and living (marked in white) bovinds, with indication of the basic outline of the bone at the same scale. Abbreviations and collection numbers: **MLA216**, *Urmiatherium rugosifrons* (Sickenberg, 1932) from Samos, Greece (Kostopoulos 2009a); **Loc 116**, Baode Loc 116, *Urmiatherium* Rodler, 1889 or *Plesiaddax* Bohlin, 1935 from China (Bohlin 1935a); “**P.**” *inundatus*, questionable *Plesiaddax* from Garkin, Turkey (data from Köhler 1993); **MMTT13/2462**, *Urmiatherium polaki* Rodler, 1889 from Maragheh; **MAR**, Maragheh. For explanation see text.

(1993) also illustrated a couple of metacarpals from Garkin, which she referred to “*P.*” *inundatus*. Comparison of this set of metacarpals with those of several fossil and living antelopes shows that their proportions are intermediate between those of running antelopes and those of heavy Plio-Pleistocene rupicaprines and “ovibovines” (Fig. 23). The metacarpals of *Urmiatherium rugosifrons* are close to those of some small sized living Rupicaprini such as serows and gorals (Fig. 23) probably suggesting similar climbing locomotor adaptations on uneven ground (Scott 1979). *Urmiatherium polaki* metacarpals have exactly the same proportions but they are significantly larger. Their length places them close to the Pliocene spirral-horned antelopes but they show broader articular surfaces and shaft suggesting less cursorial adaptations.

Genus *Miotragocerus* Stromer, 1928

TYPE SPECIES. — *Miotragocerus monacensis* Stromer, 1928.

Miotragocerus cf. *maius* (Meladze, 1967) (Figs 24; 25)

Tragocerus (*Mirabilocerus*) *maius* Meladze, 1967: 98, pls 26, 27.

TYPE LOCALITY. — Bazaleti, Georgia (late Miocene).

MATERIAL EXAMINED. — MNHN.F: Frontlet, MAR1311 ($W_{shc} = 115.7$ mm, $W_{so} = 43.8$ mm, $TD_{hcb}dex = 40.3$ mm, $TD_{hcb}sin = 37.3$ mm, $APD_{hcb}dex = 65.0$ mm, $APD_{hcb}sin = 71.3$ mm); basioccipital, MAR3241 ($W_{oco} = 54.8$ mm, $W_{bmas} = c. 110$ mm, $W_{atb} = 40.2$ mm); left horn-core, MAR1073 ($TD_{hcb} = 37.4$ mm, $APD_{hcb} = 74.0$ mm);



FIG. 24. — *Miotragocerus* cf. *maius* (Meladze, 1967) from Maragheh: **A, B**, frontlet (MNHN.F.MAR1311) in frontal (**A**) and lateral (**B**) views and left horn-core (MNHN.F.MAR1073) in frontal (**C**) and medial (**D**) views. Scale bars: 5 cm.

part of horn-core MAR1078; right p2-m2, MAR1887 (Lp = 43.8 mm); right p4-m3, MAR1886 (Lm = 65.8 mm); left p2-p4, MAR2981 (Lp = 41.2 mm); left p2-p3, MAR3004.

DESCRIPTION AND REMARKS

Although geographically widespread and usually abundant in the fossil record, the late Miocene Eurasian boselaphines remain a complicated and hitherto imperfectly understood group. The Maragheh boselaphines have never been thoroughly studied. Based on a Maragheh horn-core and some dental remains, Rodler & Weithofer (1890) reported ?*Tragocerus amaltheus* (Roth & Wagner, 1854). A better sample has been described by Mecquenem (1925) as *Tragocerus amaltheus* var. *rugosifrons* Schlosser, 1904. Solounias (1981) referred some Maragheh specimens in Paris and New York to his new boselaphine-like genus and species *Samokeros minotaurus* and at the same time (Solounias 1981: fig. 31) he referred the cranium illustrated by Mecquenem (1925: pl. VI, fig. 3) to *Miotragocerus monacensis* Stromer, 1928. Bernor (1978) described numerous tooththrows of *Miotragocerus rugosifrons* and he later (Bernor 1986) reported that there are three *Miotragocerus* species in Maragheh, a small and primitive unnamed form, *Miotragocerus amalthea* (Roth & Wagner, 1854) from Kopran and a large, advanced and undescribed *Miotragocerus*, represented by specimens in MMTT 7 and MMTT 13 localities, as well as in the MNHN.F collection. Watabe (1990) attrib-

uted several additional cranial and dental remains in the KUE collection to *Miotragocerus monacensis*. Bernor *et al.* (1996) in their updated faunal list of Maragheh included *Miotragocerus monacensis*, *Tragoportax amalthea*, *Tragoportax rugosifrons* and probably *Samokeros minotaurus*. Spassov & Ger-aads (2004) recently confirm the presence of both *Miotragocerus* and *Tragoportax* in the MNHN.F Maragheh collection.

The Paris horn-cores (MNHN.F.MAR1311, 1073, 1078; Fig. 24) form a rather homogeneous sample in terms of preservation and morphology. They are short and robust with a strong anterior keel that descends antero-medially showing a weak homonymous torsion towards the tip (Fig. 24A, C). The keels extend onto the pedicles, defining a wide intercornual furrow on the frontals (Fig. 24A). Small horn-core steps can be occasionally seen along the anterior keel but 10–11 cm above the base, the keel disappears abruptly and a clear demarcation is shown (Fig. 24D). A variably developed groove runs along the rounded posterior face of the horn-core, which in lateral view is weakly concave in its proximal part. The medial face of the horn-cores is flat and the basal cross-section of the horn-cores is narrow pear-shaped. The horn-cores are strongly inclined backwards (Fig. 24B). The supraorbital foramina are placed close and lateral to the anterior extension of the anterior keels. A postcornual fossa is present. Large sinuses are present within the frontals and the base of the horn-cores. The

similar preservation suggest that occiput MAR3241 and the mandibles MAR1886 and MAR1887 may represent a single locality (or closely associated localities) occurrence for these specimens. The occiput is narrow and high, with laterally facing foramen ovale. The basioccipital lacks a medial groove but a rather strong crest runs between the anterior tuberosities. The horizontal ramus of the mandible is low and the premolar row is long compared to the molars (Fig. 25). The p3 and p4 are elongated (with $p3 < p4 > m1$; Fig. 25) and have a simple structure with elongated and distally directed metaconid and well-distinct paraconid. The lower molars bear moderate basal pillars and anterior folds. The overall horn-core and occipital morphology, and the long simple premolars suggest referral to a species of *Miotragocerus* (Spassov & Geraads 2004; Kostopoulos 2005) larger than *M. monacensis* and with shorter and more robust horn-cores than *M. valenciennesi* (Gaudry, 1861) (Kostopoulos 2005). The latter species also differs in the presence of weak heteronymous torsion on its horn-cores and the development of the p4 metaconid. Most of the Maragheh features approach *Miotragocerus maius* (Meladze, 1967) from Bezaleti, Georgia. This species was originally placed into *Mirabilocerus* Hadjiev, 1961 but most of its morphological characters (braincase shape, basioccipital structure, horn-core morphology) fall within the *Miotragocerus* concept provided by Spassov & Geraads (2004). The lower premolar rows MNHN.F.MAR2981 and 3004 labelled as Bovidae indet. might belong to the same taxon as well.

Miotragocerus sp.
(Fig. 26)

MATERIAL EXAMINED. — MNHN.F: Left p2-p4, MAR2975 ($L_p = 45.0$ mm). — NHML: cranium, M3838 ($L_{fp-ocp} = c. 67.0$ mm; $L_{fr} = c. 116.0$ mm; $W_{bc} = 67.0$ mm; $W_{ptb} = 21.7$ mm; $APD_{hcb} = 66.5$ mm; $TD_{hcb} = 32.0$ mm; $LP = 46.0$ mm; $LM = 58.8$ mm; $LPM = 103.5$ mm)

REMARKS

The lower premolar row MAR2975 is similar but not identical with MAR2981, 3004, suggesting

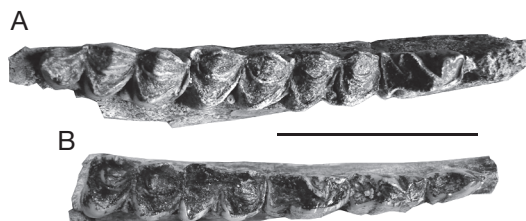


FIG. 25. — *Miotragocerus* cf. *maius* (Meladze, 1967) from Maragheh, right mandibular rami, in occlusal views: **A**, MNHN.F.MAR1886; **B**, MAR1887. Scale bar: 5 cm.

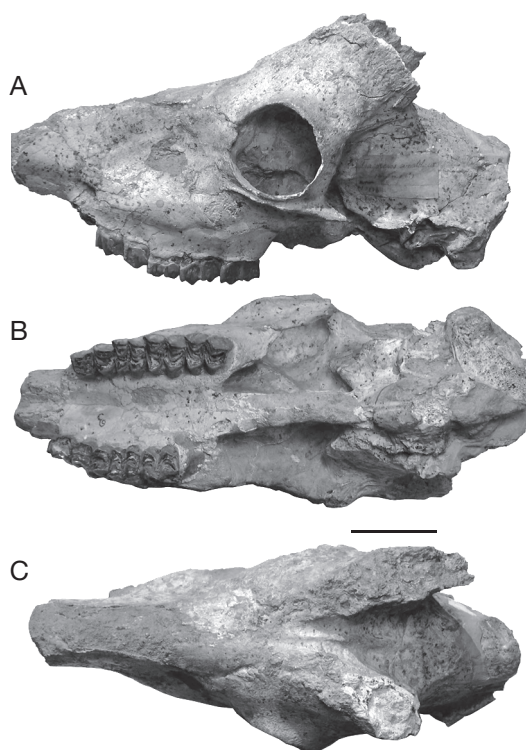


FIG. 26. — *Miotragocerus* sp. cranium (NHML M3838) from Maragheh in lateral (**A**), ventral (**B**) and dorsal (**C**) views. Scale bar: 5 cm.

the possible presence of a second *Miotragocerus* species in the MNHN.F collection. MAR2975 shows the long simple premolars of *Miotragocerus* but the premolars are slightly larger than those of the previously examined material, the p2 has a more developed anterior styloid, the metaconid

TABLE 18. — Comparison of cranial measurements (in mm) of *Tragoportax cf. amalthea* (Roth & Wagner, 1854) from Maragheh with *Tragoportax amalthea* from Pikermi. #, taken just behind the horn-cores; *, range of four Pikermi specimens in MNHN.F (MNHN.F.PIK2357, 2440, 2360 and 2345).

	<i>Tragoportax cf. amalthea</i> (Maragheh)				<i>T. amalthea</i> (Pikermi)	
	MNHN.F. MAR1395	MNHN.F. MAR3207	MNHN.F. MAR1058	MMTT13/1339	MNHN.F. PIK2286	MNHN.F. PIK2287
L _{b-ch}	107.60					
L _{b-P2}	227.00					
L _{ahc-ocp}	(164)	162.60			175.90	144.90
W _{bc}	91.00	85.90		85.60#	77.60	83.00
W _{bmas}	109.90	107.50			100.90	107.30
W _{bcon}	67.20	66.00	71.30		58.50	68.50
W _{ptb}	43.80	39.20	50.20		39.20	(36)
W _{atb}	27.60	25.80			28.30	
H _{oc}	51.40	51.20			50.70	(50.5)
TD _{hcb}	41.60	39.00		43.50	(35)	43.60
APD _{hcb}	(71)	82.00		36.00	89.00	75.60
LPM	112.70				103.30-108.60 (n = 4)*	
LP	49.20				45.00-47.80 (n = 4)*	
LM	66.50				58.30-64.00 (n = 4)*	

of the p4 is subtriangular and not trending distally and its hypoconid is narrower. By its size and morphology this specimen seems closer to *Miotragocerus vallenciennesi* from Pikermi. An additional almost complete cranium (M3838; Fig. 26) in the London collection shows a rather long and narrow opisthocranium weakly bent on the deep face (Fig. 26A, C) and with a fairly developed rugose area limited by rather weak crests (Fig. 26C), slightly elevated frontals and pinched midfrontal suture between the horn-cores, anterior rim of the orbit placed above M2-M3 limit, shallow lacrimal fossae, infraorbital foramina placed above P2, anterior tuberosities of the basioccipital facing mostly laterally, separated by a median crest, and rather large premolars comparatively to the molars (premolar to molar ratio = 78.2%; Fig. 26B). The horn-cores are badly damaged and crushed near their bases (Fig. 26A); they are inserted above the orbits, moderately inclined backwards and have a rounded posterior face; their basal dimensions appear smaller than those of *M. maius* and within the variation of *M. vallenciennesi*. Morphometrically, M3838 satisfactory matches Pikermi crania of *M. vallenciennesi* in London and Paris, indicating that a *Miotragocerus* species close to the Pikermian one may exist in some of the Maragheh fossil horizons.

Genus *Tragoportax* Pilgrim, 1937

TYPE SPECIES. — *Tragoportax salmontanus* Pilgrim, 1937.

Tragoportax cf. amalthea (Roth & Wagner, 1854) (Figs 27; 28)

Capra amalthea Roth & Wagner, 1854: 453: pl. 6, fig. 2.

Tragocerus amaltheus var. *rugosifrons* – Mecquenem 1925: 34.

Miotragocerus monacensis – Solounias 1981: table 4; text-fig. 31.

TYPE LOCALITY. — Pikermi, Greece (late Miocene).

MATERIAL EXAMINED. — MNHN.F: Male cranium, MAR1395 (Mecquenem 1925: pl. VI, fig. 3); partial male cranium, MAR3207; female cranium, MAR3208; part of occipital bone, MAR1058; left P3-M2, MAR1866, 1867; right M1-M3, MAR1868 (LM = 64.5 mm); mandible, MAR1009 (illustrated by Mecquenem 1925: pl. V, fig. 6 and VI, fig. 3 as part of the skull MAR1395 with old catalogue number 20950); right p3-m3, MAR1007, 1008; left p3-m3, MAR1069; right p3-m2, MAR1075; left p4-m3, MAR1067; right p2-m3, MAR1070; right p3-m3, MAR2970; right p2-m1, MAR1837; left p2-m1, MAR2969; right p2-p4, MAR1081; left p2-p4, MAR1087; right m1-m3, MAR1077; left m1-m3, MAR1835; left p3-m2, MAR1086. — HUW:

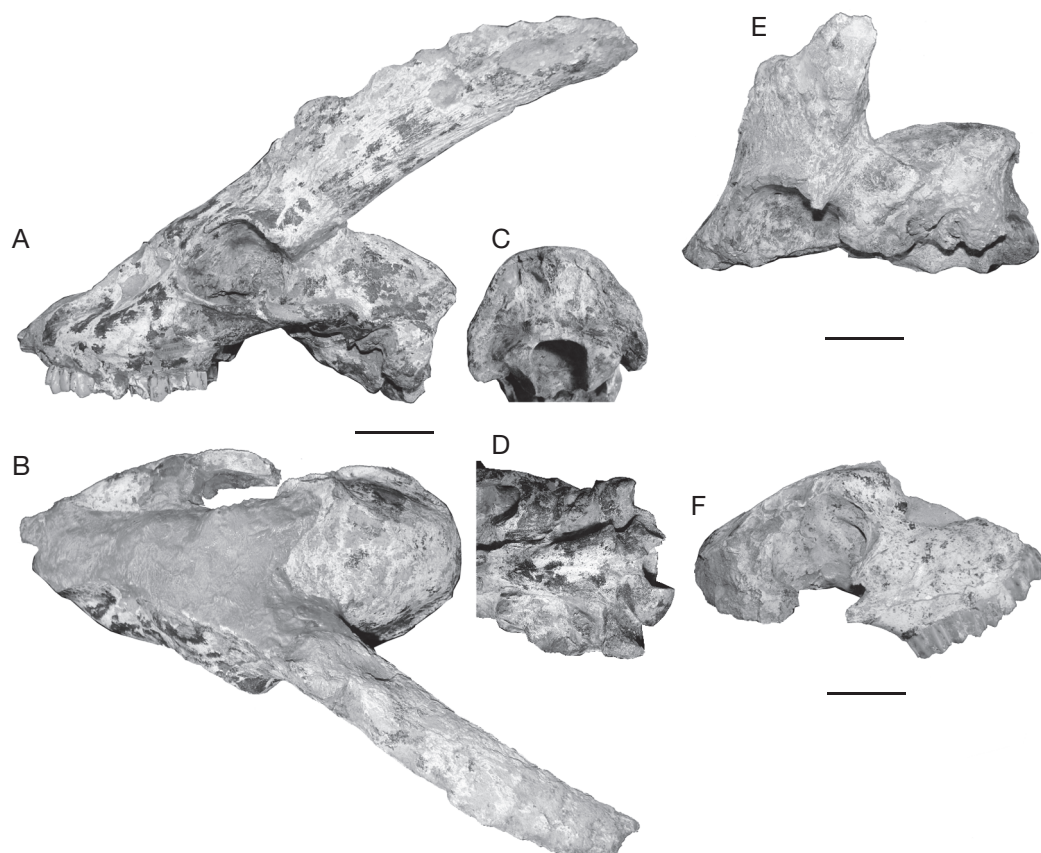


FIG. 27. — *Tragoportax* cf. *amalthea* (Roth & Wagner, 1854) from Maragheh: **A-D**, male cranium (MNHN.F.MAR1395) in lateral (**A**), dorsal (**B**), occipital (**C**) and basiooccipital (**D**) views; **E**, male cranium (MNHN.F.MAR3207); **F**, female cranium (MNHN.F.MAR3208) in lateral view. Scale bars: 5 cm.

frontlet MMTT13/1339; palate, MMTT13/1346 (LPM = 102.3 mm, LP = 45.0 mm, LM = 63.4 mm); left P2-P4, MMTT7/2160 (LP = 47.6 mm); right P2, MMTT13/1279; right p2-m3, MMTT7/2317; left p2-m1, MMTT7/1987 (19501/RV7914); right p4-m3, MMTT13/1334.

DESCRIPTION AND REMARKS

Solounias (1981: fig. 31) erroneously referred the cranium illustrated by Mecquenem (1925: pl. VI, fig. 3) to *Miotragocerus monacensis*. The basic morphological characters of the two available male crania (MNHN.F.MAR3207 and 1395; Fig. 27, Table 18) clearly point to a representative of *Tragoportax* (*sensu* Spassov & Geraads 2004): rather short, wide and low braincase with large occipital condyles trending

posteroventrally (Fig. 27A, C-E), strong external occipital protuberance, large square-shaped foramen magnum (Fig. 27C), large mastoids facing posterolaterally, occiput facing posteriorly (Fig. 27C, E), zygomatic arches running parallel to the braincase sides that slightly widen anteriorly (Fig. 27A, B), temporal crests far apart, large and ridge-like posterior tuberosities of the basioccipital perpendicular to the sagittal plane and separated by a wide, shallow furrow (Fig. 27D), small anterior tuberosities of the basioccipital with a longitudinal crest running in front of them along the medial axis of the basisphenoid (Fig. 27D), foramina ovalia facing ventrally, strong paroccipital processes curved medially, large fronto-parietal rugose area limited by strong crests

TABLE 19. — Lower tooth row measurements (in mm) of *Tragoportax* cf. *amalthea* (Roth & Wagner, 1854) from Maragheh. For abbreviations see text.

Coll. no.	Lpm	Lp	Lm
MNHN.F.			
MAR1009	113.40	47.10	65.70
MAR1070	113.30	46.60	68.10
MAR1837		46.30	
MAR1081		49.40	
MAR2969		44.90	
MAR1087		47.00	
MAR1067			67.60
MAR1007			66.50
MAR2970			69.40
MAR1008			68.50
MAR1069			66.80
MAR1077			72.00
MMTT7/2317	115.80	44.10	71.0
MMTT7/1987		47.30	
MMTT13/1334			71.20

(Fig. 27B), short but wide intercornual plateau, hollowed frontals and pedicles, supraorbital foramina small, not sunken into depressions and associated with narrow furrows to the front, moderately deep lacrimal fossa (Fig. 27A), choanae opening well behind the M3, anterior rim of the orbit above the front lobe of M3 (Fig. 27A), premolar row rather short compared to the molars (-74% in the upper and 68-72% in the lower toothrow), horn-cores moderately long with a weak heteronymous torsion, triangular basal cross-section and strong anterior keel without demarcations but with small to moderate irregularities along it (Fig. 27A, B). The overall skull morphology is very similar to that of *Tragoportax amalthea* from Pikerimi, Greece (Table 18) and *Tragoportax rugosifrons* from Hadjidimovo, Bulgaria (Spassov & Geraads 2004) and dimensionally closer to the latter form. It differs from both of them in the longer and more triangular shaped basioccipital without clear medial furrow and with a rather strong basisphenoid crest. Typical *Tragoportax rugosifrons* from Samos, Greece is more distinct in its longer untwisted horn-cores, parallel braincase sides, less posteriorly expanded rugose area, shorter basioccipital, shallower and probably larger lacrimal fossa and trapezoidal-shaped occiput.

The Maragheh dentitions appear slightly larger than that of *T. amalthea* from Pikerimi but within the range

of *T. rugosifrons* from Hadjidimovo and *T. rugosifrons* from Samos. Dental discrimination between these two species is rather hard because of their similar size and great morphological variability especially on accessory features (cingula, folds, pillars, etc.). The upper dentition of the skull MAR1395 differs from both typical *T. rugosifrons* and *T. amalthea* in its less asymmetrical P3, the protocone-hypocone lingual division of P4, the weak to absent basal pillars on the molars and the presence of a lingual cingulum on the posterior lobe of M1 and M2. The dental characters of the palate MMTT13/1346 (see below) are very similar to those of MAR1395, whereas the specimens MAR1867 and MMTT7/2160 appear closer to the *amalthea* or *rugosifrons* morphotypes. The lower dentition of both the MNHN.F and MMTT-HUW samples (Table 19; Mecquenem 1925: pl. V, fig. 6; pl. VI, fig. 3) shows well-developed basal pillars in all m1s (15 specimens), in most m2s and in 8 out of 10 m3s. Most m2s (8 out of 13 specimens) and a few m3s (2 out of 11 specimens) bear a basal lingual tubercle between the two lobes. A weak goat fold is rarely present on m3 (in 2 out of 11 specimens). The p3 is simple with elongated metaconid placed distally and directed posteriorly. All available p4s (n = 16) have an anteroposteriorly expanded metaconid of “T” or more often “Y” type with strongly developed anterior flange that comes into contact with the strong and posteriorly curved paraconid in early wear, closing quickly the anterior valley. This morphotype appears more advanced than that of *T. amalthea* from Pikerimi and *T. rugosifrons* from Hadjidimovo, Bulgaria and Axios valley, and similar to that of *T. rugosifrons* from Perivolaki, Greece (Spassov & Geraads 2004; Kostopoulos 2006).

Some more cranial specimens warrant further discussion. The cranium MAR3208 mentioned by Mecquenem (1925: 34; Fig. 27F) belongs to a female individual, since it lacks horn-cores. The frontals above the orbits are neither depressed nor rough. The dentition is about 10% smaller than that of MAR1395 but with very similar morphological features, even though the P4 is of the *T. amalthea* type. This cranium is fully compatible with those of hornless female skulls attributed to *T. rugosifrons* or related forms (see discussion in Kostopoulos 2006: 175 and alternative views in Spassov & Geraads 2004).



FIG. 28. — *Tragoportax* cf. *amalthea* (Roth & Wagner, 1854) from Maragheh: palate (MMTT13/1346) and frontlet (MMTT13/1339) of possibly the same young adult individual in lateral view. Scale bar: 5 cm.

The specimen MMTT13/1339 (casts MAR3204 in MNHN.F and AMNH101999 in AMNH; Fig. 28, Table 18) is a frontlet with partially preserved horn-cores. The supraorbital foramina are small, round, not sunken in pits and placed far from the horn bases. The area between them and the horn-cores is weakly swollen. There is no postcornual fossa. The midfrontal suture is complicated, slightly constricted between the horn-cores and open in front of them. The frontals between and behind the horn-cores are smooth without any rugosities. The frontals are in the same plane as the dorsal orbital rims. The horn-cores are thin (Table 18) and rather long (> 160 mm) placed above the back of the orbital roof, far apart each other at their base, moderately tilted and weakly curved backwards (Fig. 28). In frontal view they appear weakly divergent. They show a very weak heteronymous torsion and their great basal axis is almost perpendicular to the sagittal plane. They bear no keels and their basal cross-section is rather triangular with flat posterior and anterolateral faces; at their junction an incipient posterolateral dihedral is shown. The overall morphological characters of this specimen sug-

gest that it is a juvenile of *Tragoportax*. This frontlet excavated very close to the palate MMTT13/1346 (Fig. 28) and they may represent a single individual (Bernor pers. obs.). As already discussed, the dentition of MMTT13/1346 is very similar to that of MAR1395 supporting the assertion that this is a young adult individual of the same species, which is here referred to *Tragoportax* cf. *amalthea*.

Genus *Samokeros* Solounias, 1981

TYPE SPECIES. — *Samokeros minotaurus* Solounias, 1981.

Samokeros minotaurus Solounias, 1981 (Fig. 29)

Samokeros minotaurus Solounias, 1981: 127, text-figs 39, 40 *partim*.

Palaeoryx pallasi – Mécquenem 1925: pl. 4, fig. 1.

Tragoceros amaltheus – Mécquenem 1925: pl. 5, fig. 1.

TABLE 20. — Upper tooth measurements (in mm) of *Samokeros minotaurus* Solounias, 1981 from Maragheh. For abbreviations see text.

	MNHN.F.	MNHN.F.	MNHN.F.MAR3209	
	MAR1396	MAR3210	dex	sin
LPM	112.07	110+	113.14	113.13
LP		43.84	42.80	42.00
LM			71.00	72.15
LP2	13.40	13.53	13.50	13.18
WP2	13.68	13.40	14.50	14.04
LP3	15.50	16.58	15.50	14.96
WP3	16.18	16.40	15.50	15.25
LP4		16.26	15.14	15.23
WP4		18.60	17.80	18.14
LM1		22.15	19.94	20.00
WM1		23.84	22.30	21.68
LM2	(24.6)	27.67	26.50	26.73
WM2		24.60	24.16	24.14
LM3	27.66		27.70	28.24
WM3	25.74	23.26	25.00	24.50

TABLE 21. — Lower tooth measurements (in mm) of *Samokeros minotaurus* Solounias, 1981 from Maragheh. For abbreviations see text.

	MNHN.F.			
	MAR3229	MAR3230	MAR3233	MAR2979
Lpm	130.60			
Lp	52.17			52.17
Lm	78.90	78.30		
Lp2	14.40			14.66
Wp2	8.10			7.80
Lp3	18.50			18.53
Wp3	11.40			11.30
Lp4	19.16	21.00	19.11	19.18
Wp4	12.90	12.90	13.26	13.20
Lm1	20.50	19.78	21.30	
Wm1	15.10	16.00	15.86	
Lm2	25.30	25.50	25.40	
Wm2	16.00	16.90	16.40	
Lm3	34.50	35.20		
Wm3	16.70	16.38		

TYPE LOCALITY. — Samos, Greece (late Miocene).

MATERIAL EXAMINED. — Part of cranium with broken horn-cores, MAR1396 (Mecquenem 1925: pl. IV, fig. 1 as *P. pallasi*); palate, MAR3209 (Mecquenem 1925: pl. V, fig. 1 as *Tragocerus amaltheus*); P2-M3part, MAR3210 (labelled as *T. amalthea*); part of right mandibular ramus with p2-m3, MAR3229 (labelled as *P. pallasi*); part of right mandibular ramus with p4-m2, MAR3233 (labelled as *P. pallasi?*); part of left mandibular ramus with p4-m3, MAR3230 (labelled

as *P. pallasi?*); part of left mandibular ramus with p2-p4, MAR2979.

DESCRIPTION AND REMARKS

Solounias (1981: 127) erroneously referred the frontlet MAR1323 (Mecquenem 1925: pl. VII, fig. 1) to his new genus and species *Samokeros minotaurus*; as it has been already shown this specimen belongs to the small heteronymous spiral horned antelope *Nisidorcas*. Solounias (1981) also provisionally ascribed to *S. minotaurus* the Maragheh frontlet AMNH27817, as well as, the cranium MAR1396 originally referred by Mecquenem (1925) to *Palaeoryx pallasi* and discussed later by Bohlin (1936) and Gentry (1971) who thought it represents a large *Tragoptortax*.

The overall cranial structure of MAR1396 (Fig. 29A, B) is indeed very similar to that of *Tragoptortax* but wider at the orbital level and with wider and low, box-like braincase that is more strongly bent on the face. It also differs in the supraorbital foramina placed into shallow depressions, the presence of a narrow triangular ethmoidal fissure defined by the nasals, frontals and lacrimals (but probably not by the maxillae), the inverse “U”-shaped fronto-nasal suture, the large and rather bilobed facial part of the jugal, the long and shallow lacrimal fossa with an additional small and round internal depression above the M2, the posterior position of the rather large infraorbital foramina (above P3), the more anteriorly opening choanae and the posterior position of posterior palatine foramina at the level of M3, the non elevated frontals, the much less developed rugose area restricted on the frontals and not limited posteriorly by the characteristic *Tragoptortax* transverse bar, the presence of shallow frontal depressions behind the horn-cores, the elliptical basal cross-section of the horn-cores and the absence of keels on their preserved proximal part at least. Basic measurements of the cranium MAR1396 are (in mm): $W_{shc} = 136.5$, $W_{so} = 51.9$, $W_{bc} = 98.6$, $L_{fp-ocp} = 85.0$, $L_{fn-ocp} = 190.3$, $DT_{hcb} = 44.0$, $APD_{hcb} = 63.0$.

Dental morphology and dimensions of the MNHN.F sample also suggest important differences from other late Miocene boselaphines (Tables 20,

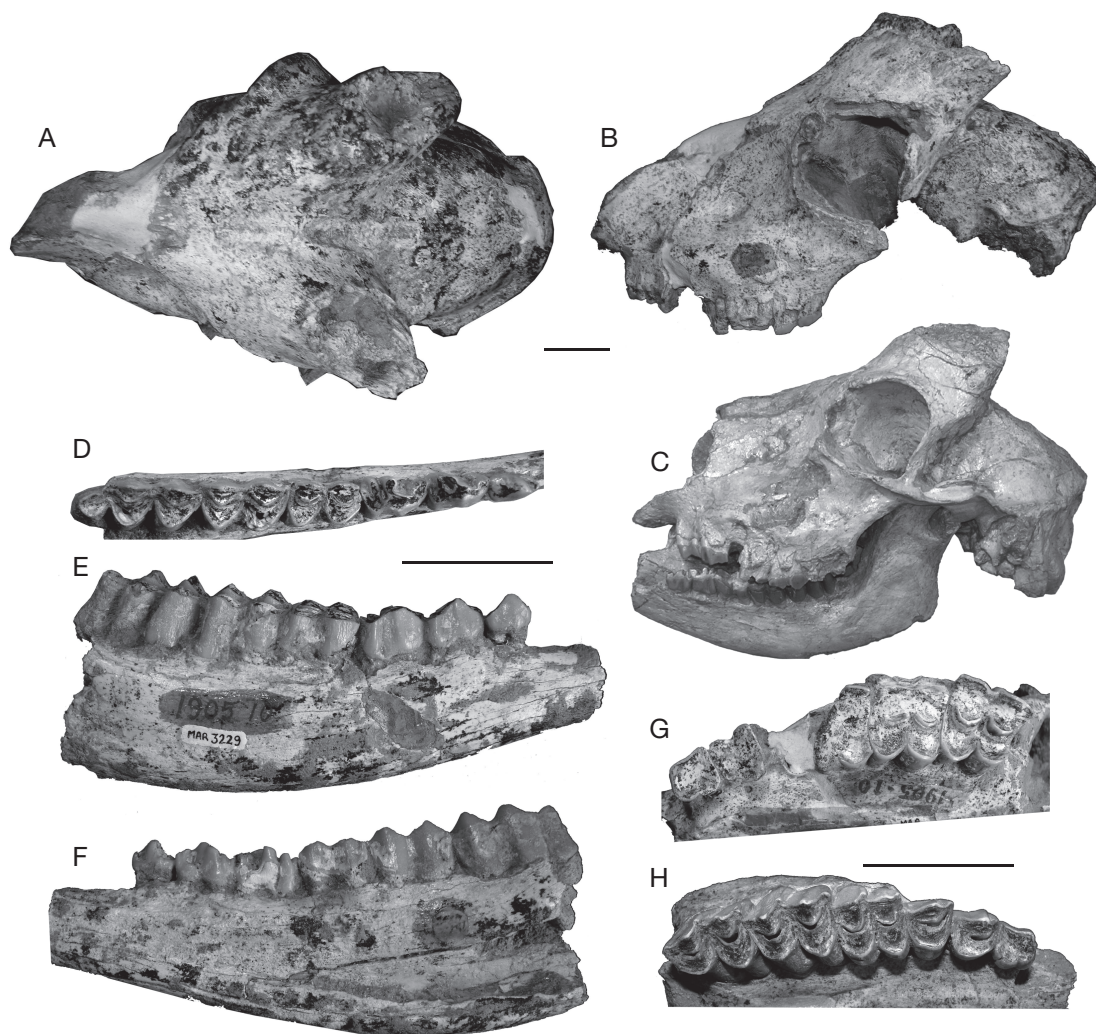


FIG. 29. — *Samokeros minotaurus* Solounias, 1981 from Maragheh and Samos: **A, B**, cranium (MNHN.F.MAR1396) from Maragheh in dorsal (**A**) and lateral (**B**) views; **C**, skull (AMNH23036) in lateral view; **D-F**, right mandibular ramus (MNHN.F.MAR3229) in occlusal (**D**), labial (**E**) and lingual (**F**) views; **G**, left toothrow of the cranium (MNHN.F.MAR1396) in occlusal view; **H**, right toothrow of the palate (MNHN.F.MAR3209) in occlusal view. Scale bars: 5 cm.

21). Thus, the premolar row is significantly shorter (58–60% of the upper and *c.* 66% of the lower molars instead of *c.* 74% and 68–72% respectively in Maragheh *Tragoportax*), the P2 is short, square-shaped and bilobed lingually (Fig. 29G, H), the basal pillars are less common on the upper molars that bear central islets instead (Fig. 29G, H), the cement is rather abundant on the lower molars, the protoconid of p4 is pinched and both the p3 and

the p4 are of primitive structure with widely open anterior valley and weak paraconid (Fig. 29D–F). The described dental material is of the size of *Palaeoryx* from the same locality, from which it differs in the much wider palate in front of P2, the much shorter P2, the narrower upper molars, the less developed paraconid of the p3 and p4, the thinner and longer metaconid of p3 and the weaker metastylid of the lower molars.

The general morphological characters of the cranium MAR1396 exhibit important differences with both *Tragoportax* and *Miotragocerus* from Maragheh and other Eurasian sites and indicate a taxon with more advanced characters. The opisthocranial morphology of MAR1396 and the basal shape of the horn-cores are fully compatible with those of PIM99, holotype of *Samokeros minotaurus*. Additionally, PIM99 bears robust horn-cores similar to those of the frontlet AMNH27817 from Maragheh. The cranium and dental morphology, of MAR1396 closely compare with those of the skull AMNH 23036 from Samos (Fig. 29C), which is referred to *Samokeros minotaurus* (Kostopoulos 2009a: 373). The p3 and p4 morphology of the latter specimen is also identical to that from Maragheh (MAR2979, 3229, 3230, 3233).

Bovidae indet.

MATERIAL EXAMINED. — HUW: left M3, MMTT1A/339 (L = 22.9 mm; $W_{\text{anterior lobe}}$ = 21.3 mm; $W_{\text{posterior lobe}}$ = 19.7 mm).

REMARKS

An upper left, possibly third molar from MMTT1A (Fig. 30) of Maragheh shows moderately wrinkled enamel, low crown, strong lingual cingulum that forms a low double basal pillar, a posteriorly placed and weak hypoconal fold (Fig. 30A), a moderately developed central islet, and well-developed styles and ribs (Fig. 30B) with the paracone converging with the parastyle towards the base of the crown. These morphological features distinguish MMTT1A/339 from similar-sized antelopes from Maragheh and point to an "ovibonine"-like bovid of medium size. The tooth is about 35% shorter and 25% narrower than the M3 of *Urmiatherium polaki* from Maragheh described by Mecquenem (1925), significantly wider (the width to length ratio is 0.93 in MMTT1A/339 versus 0.77 in MAR1055) and with much less square posterior lobe. MMTT1A/339 is about 15% smaller than the M3 of "*Plesiaddax*" from Garkin (Bosscha-Erdbrink 1978) and *U. intermedium* from China (Bohlin 1935a) and wider (the index W/L range from 0.70 to 0.90, n = 11 in Garkin and between

0.72 and 0.74 in the Chinese *Urmiatherium*). MMTT1A/339 is slightly smaller than the M3 of *Criotherium argalioides* Major, 1891 from Samos and Turkey, but differs in the less posteriorly expanded metastyle, the stronger mesostyle and the presence of lingual cingulum. The width to length ratio is also larger in MMTT1A/339 than in *Criotherium* (0.78-0.85 in M3, n = 10).

DISCUSSION

The present review of the Maragheh bovids have led us to recognize 18 species within the MNHN.F collection, some of which are also documented in the MMTT7, 13, 31 and 37 of the Lake Rezaieyeh Expedition in MMTT-HUW. The revised bovid data raise two main issues concerning: 1) the homogeneity of the Paris bovid sample and its bearing on the Middle Maragheh biostratigraphy; and 2) the position of the Maragheh fauna in the late Miocene Old World zoogeography.

Bernor (1986) and Bernor *et al.* (1980, 1996) recognized three successive fossiliferous intervals at Maragheh and based on radio-isotopic age determinations updated by Swisher (1996), Bernor *et al.* (1996) proposed an 8.9 to 8.2 Ma age for the Lower Maragheh interval (–150 to –52 m) or *Hipparion gettyi* Bernor, 1985 zone, an 8.2 to 8.0 Ma age for the Middle Maragheh interval (–52 to –20 m) or *H. prostylum* Gervais, 1849 zone and an 8.0 to 7.4 Ma age for the Upper Maragheh interval (–20 to +7 m) or *H. campbelli* Bernor, 1985 zone. Nevertheless, a current view of Maragheh biostratigraphy is that the lineage-based subdivision of the local sequence needs review to better demonstrate the evolution of *Hipparion* s.s. (Mirzae Ataabadi *et al.* in press; Bernor *et al.* unpubl. data). Although the Maragheh fauna ranges from nearly 9 Ma to about 7.4 Ma the bulk of the fossil material is from the middle and upper parts of the section, better defined by the locality MMTT1A at the bottom (–52 m) with an interpolated age of 8.16 Ma and by MMTT26 at the top (+7 m), dated at 7.68 Ma (Mirzae Ataabadi *et al.* in press). MMTT7 is placed in the uppermost part of the Middle Maragheh interval (–28 m; c. 8.0 Ma),

whereas MMTT13 (–18 m) is slightly younger, dated at around 7.6–7.7 Ma. MMTT37 or Ilkhchi is situated out of the central fossiliferous location and it is believed to be the youngest one in the Maragheh succession, *c.* 7.4 Ma old.

It is important to recognize that there is no precise stratigraphic data for the Paris sample that was collected by R. de Mecquenem at the beginning of the 20th century. The MNHN.F Maragheh collection is believed to come from the –52 to –28 m stratigraphic interval (Bernor 1986) likely referable to the Middle Maragheh (–52 m to –20 m; Bernor *et al.* 1996; Mirzae Ataabadi *et al.* in press). As a consequence, the Middle Maragheh bovid association is mainly based on taxonomic information from the MNHN.F collection, which remains the best source of reliable evidence at the species level. Nevertheless, the Maragheh bovid association in MNHN.F appears to be temporally heterogeneous. The combination of four *Prostrepsiceros* species together with four boselaphines, and numerous antelopes of apparent conflicting biochronological signal is problematic and is not replicated at any other Eurasian Late Miocene mammal locality with certain stratigraphic control. The presence of *Urmiatherium polaki* in MNHN.F is also puzzling as the species has been confidently recorded in sites ascribed to the Upper Maragheh interval (MMTT13, Ilkhchi). The same is probably also true for material here assigned to *Skoufotragus* that is known from the –28 m level (MMTT7) upwards. Obviously, the MNHN.F bovid association cannot be regarded as corresponding to a single mammal palaeoenvironment, and must have incorporated taxa from chronologically succeeding faunal assemblages, representing a lengthy stratigraphic interval.

There is not much to conclude at this point merely to explain what is known about the biostratigraphy of the Maragheh bovinds excluding the data from the Paris collection. The Lake Rezaieyeh Expedition and current studies at Maragheh have and will continue to provide precise stratigraphic information that will significantly improve our understanding of the biostratigraphy of the Maragheh fauna. Currently, there is unevenness in taxonomic evidence per fossiliferous horizon with some quarry samples concentrating our information

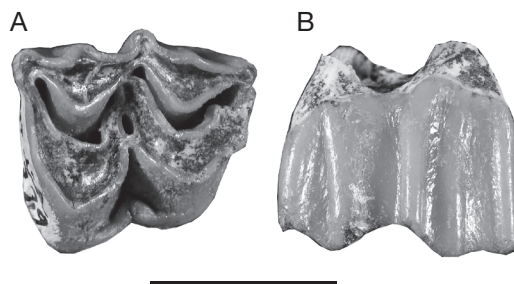


FIG. 30. — Bovidae indet., upper left molar (?M3) (MMTT1A/339) from Maragheh in occlusal (A) and labial (B) views. Scale bar: 2 cm.

about the fauna while intervening intervals have poorer faunal representation. Lower Maragheh bovinds, below the –52 m level (Bernor 1986), are poorly sampled. Bernor (1986) and Bernor *et al.* (1996) recorded *Prostrepsiceros houtumschindleri*, *Gazella deperditalcapricornis* and *Oioceros atropatenes* but reconsideration of the original material (*i.e.* Bernor 1978), on which these identifications are based indicates that it is too fragmentary to accurately allow species recognition in some cases. Bernor (1978) also recorded *Miotragocerus* sp. from MMTT41 (–115 m) of Lower Maragheh but he mentioned later (Bernor 1986) that “there are two *Miotragocerus* species known from Maragheh, a smaller more primitive form, *Miotragocerus amalthea* collected by Rodler [...] from Kopran (–150 to –115 m interval) and a larger, more advanced form [...] collected by the Lake Rezaieyeh Expedition from MMTT7 [...] and MMTT13 [...] as well as Mecquenem [...]”. Since the first author (DSK) has not seen the Kopran material referred to *T. amalthea* he cannot judge the taxonomic validity of this assignment. However, taking into account that MMTT7 and MMTT13 material, later ascribed to *T. rugosifrons* (Bernor *et al.* 1996), is in fact very similar to *Tragoportax amalthea*, we suspect that the “smaller and more primitive” Kopran form might in fact represent a *Miotragocerus* s.s. instead of a *Tragoportax*.

Middle and Upper Maragheh bovinds are much more abundant and better defined at species level but again their biostratigraphic distribution is less clear. The available data do not allow recognizing which *Prostrepsiceros* species co-exist in each Maragheh fos-

sil interval. Horn-cores attributed to *Prostrepsiceros* are recorded from the base of the Maragheh section (MMTT43) up to its top (MMTT37; Bernor 1978, 1986) but in several cases the material is too fragmentary for secure species identifications, while tooth row samples have been misidentified even at the genus level. An unpublished frontlet of *Prostrepsiceros houtumschindleri* from MMTT7 stored in Tehran (Z. Orak pers. comm. 2009) confirms the presence of this species in the upper part of the Middle Maragheh interval. The co-occurrence of both *Pr. houtumschindleri* and *Pr. fraasi* in Site III of the the KUE (Watabe 1990), which is roughly correlated with MMTT1 to MMTT6 of the Middle Maragheh (Mirzae Ataabadi pers. comm. 2009) confirms that these two species co-occur during the -52 to -30 m interval at least. Still, it seems impossible even to suppose which, if any one of these species extends into either older or younger levels, whereas the biostratigraphy of the other two species (*Pr. cf. rotundicornis* and *Pr. cf. vinayaki*) remains obscure.

Apart from the MNHN.F collection, specimens certainly attributed to *Protragelaphus skouzesi* are known from MMTT5, 7 and 13, suggesting that the species distribution covers the entire Middle and the lower part of the Upper Maragheh interval. Furthermore, *P. skouzesi* specimens in NHMW are labeled as from Kopran implying that the species was already present in lower horizons. Possible *Palaeoreas* is known at the moment by dental remains only from MMTT7.

Oioceros atropatenes is recorded in the entire Maragheh section, even though its occurrence in the Lower Maragheh is presently based on a single horn-core fragment from locality MMTT9 (Bernor 1978, 1986). The oldest certain recorded stratigraphic occurrence of *O. rothii* in Maragheh is in locality MMTT1B (Bernor 1978, 1986), indicating that the concurrent presence of two *Oioceros* species might characterize the levels above the -32 m and not the entire Middle Maragheh interval. The presence of *O. rothii* in Site III of the KUE does not really allow resolving the issue as it corresponds to a rather wide stratigraphic interval.

The single securely recorded stratigraphic evidence of *Demecquenemia rodleri* n. comb. in Ma-

ragheh is from locality MMTT1A at the base of the Middle Maragheh interval (Bernor 1978). The type specimen of the species in NHMW has no precise stratigraphic provenance. The high representation of *D. rodleri* n. comb. in the MNHN.F collection (where it is about a third as common as the most abundant bovid *O. atropatenes*) contrasts with its absence from the Site III of the KUE or from the rich localities MMTT7 and MMTT13 of the LRE and therefore calls its eventual biostratigraphic extension above the MMTT1A level in question.

Gazella is known at Maragheh from the -115 m level upwards (Bernor 1978, 1986; Bernor *et al.* 1996). Both revised species *Gazella capricornis* and *G. cf. ancycensis* are present in MMTT13 and in the Site III of the KUE (Watabe 1990), suggesting their coexistence during the Middle and probably the lower part of the Upper Maragheh interval. *Gazella capricornis* may also be present in later levels as the rather rich material from MMTT37 implies (Bernor 1978).

According to the available information, *Skoufotragus* is known from the -28 m level to the top of the Maragheh section, recorded in MMTT7, 13, 27, 26, and 37 (Bernor 1978, 1986). *Skoufotragus laticeps* is present in MMTT7, 13 and in the K2 site of Bosscha-Erdbrink (1988) that likely correlates with MMTT31 (Mirzae Ataabadi pers. comm. 2009), whereas the more evolved *Sk. schlosseri* might be present in younger levels (MMTT26, 37).

Bernor (1986) originally referred *Urmiatherium polaki* to the Upper Maragheh interval but later (Bernor *et al.* 1996) he recorded it from the Middle Maragheh as well. Nevertheless, the controlled stratigraphic occurrence of *Urmiatherium polaki* is so far restricted above the -18 m interval: the holotype specimen of *U. polaki* was collected from Ilkhchi, believed to be the same locality as MMTT37, and postcranial elements attributed to the same species have been also recorded in MMTT13.

Tragoportax is known from MMTT7 and MMTT13 with *T. amalthea* whereas *Miotragoceros* might have a longer presence but with several species. Specimens in the Site III of the KUE ascribed to *Miotragoceros monacensis* (Watabe 1990) are bet-

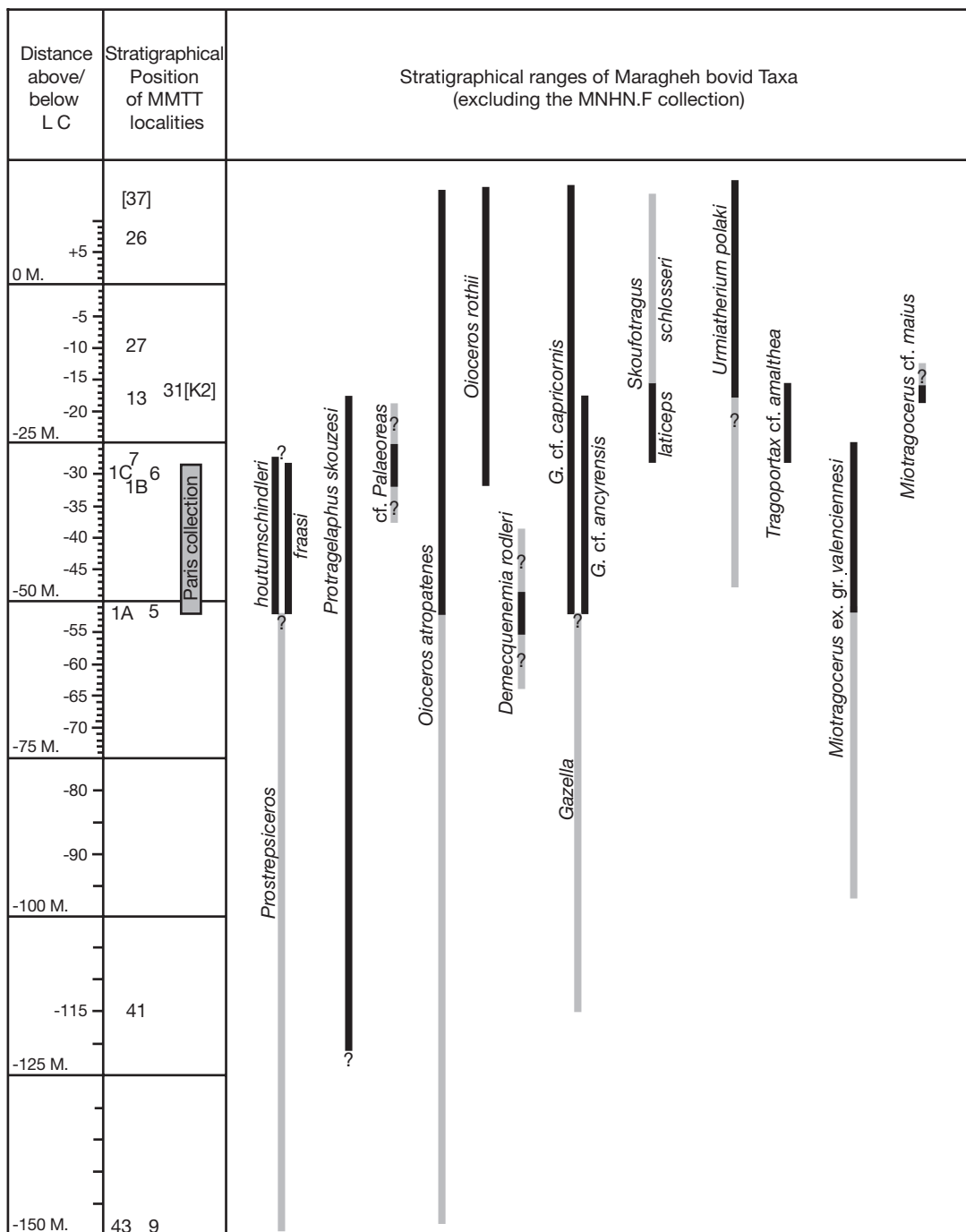


FIG. 31. — Stratigraphical distribution of Maragheh bovid taxa excluding the MNHN.F record, which range is approximately indicated at the left column. Grey lines represent uncertain ranges at the species level.

ter referred to *Miotragocerus valenciennesi*, already known from the MNHN.F and NHML collections, indicating the presence of this species during the -52 to -30 m interval. The biostratigraphic range of *Nisidorcas*, *Palaeoryx*, *Miotragocerus* cf. *maius*, and *Samokeros* remains unknown. Nevertheless, an unpublished cranium of *Miotragocerus maius* in MMTT Tehran (Z. Orak pers. comm. 2009) is probably from MMTT 7 or 13 locality. Figure 31 summarizes the biostratigraphic ranges of the Maragheh bovids. It is worth noting that, although MMTT7 and MMTT13 belong to the Middle and Upper Maragheh respectively, their updated bovid assemblages appear very similar, implying that the bovid association around the Middle/Upper Maragheh stratigraphic boundary shows no important changes in contradiction to those revealed by the hipparionine horses (Bernor 1986; Bernor *et al.* 1980).

According to the current geochronology, most of the known Maragheh is of early Turolian age and its mammal fauna is generally correlative with the European Land Mammal Age MN11 (Agustí *et al.* 2001). The bulk faunal aggregate of Middle and Upper Maragheh (8.2-7.4 Ma) are somewhat older but overlap the older portion of the main Samos fauna (7.4-6.9 Ma) (Kostopoulos *et al.* 2003; Koufos *et al.* 2009; Mirzae Ataabadi *et al.* in press). Consistent with this correlation are the less evolved Maragheh *Prostrepsiceros fraasi* compared to the Samos form, as well as the presence of *Nisidorcas* and *Gazella* cf. *ancyrensis*. Nevertheless, the available radioisotopic ages of the Maragheh succession appear older than Kostopoulos would expect based on the biochronological signal of the rest Middle and Upper Maragheh bovid taxa, which suggest a younger (i.e. middle Turolian) age. Based on the stage-of-evolution of the hipparion assemblages, and in agreement with Maragheh's radioisotopic correlation, Bernor believes, however, that Maragheh and Pikermi have genuine bases of biochronologic correlation and that both are older than the bulk of the Samos fauna. These differing scientific viewpoints are under active investigation.

The broad Old World geographic distribution of Turolian age bovid taxa, and the ecological breadth

that they certainly represent are critically depicted at the three classical faunas of Pikermi, Samos and Maragheh, located along a major longitudinal axis across Sub-Paratethyan province (henceforth, the P-S-M axis). Achieving greater clarity on the systematics, biostratigraphy, geochronology and biogeography of the faunas of these three localities will lead to a better understanding of the evolution of the structure of the Sub-Paratethyan province, as well as of the mechanisms through which the so-called Pikermian chronofauna evolved, expanded geographically and taxonomically, declined and ultimately became extinct at the end of the Miocene (e.g., Eronen *et al.* 2009).

Comparison at any taxonomic level between the faunal assemblages of these localities requires three basic assumptions: 1) the taphonomic and/or collecting bias has minor impact on the results; 2) the faunas are comparable in biological terms; and 3) the time-correlation between Samos, Pikermi and Maragheh is securely established. The first assumption is questionable because of the different sedimentologic settings of these three localities and the fact that altogether they have been collected over the last 150+ years by scores of different paleontologists. The second assumption is basically accepted because of the localities strong identity and numerous tests of commonality of their species contents. We should, however, emphasize that the mammal assemblages of Samos and Maragheh represent composite faunas of relatively long duration, whereas Pikermi is believed to sample a short temporal interval and therefore its fauna might be seen as representing a single palaeocenosis. As for the third assumption, there is chronologic precision for Samos and Maragheh but not for Pikermi that is variously correlated as old as Middle Maragheh or as young as the main Samos fauna.

Keeping these assumptions in mind, the high genus faunal similarity between Pikermi, Samos and Maragheh already showed by Bernor *et al.* (1996, 2009) and Mirzae Ataabadi *et al.* (in press) is further supported by the bovids. The Simpson genus faunal similarity index based on the Bovidae ranges from 0.78 to 0.89, indicating strong intraprovincial relationships of the P-S-M faunal group. Nevertheless, genera are logical classes and as such

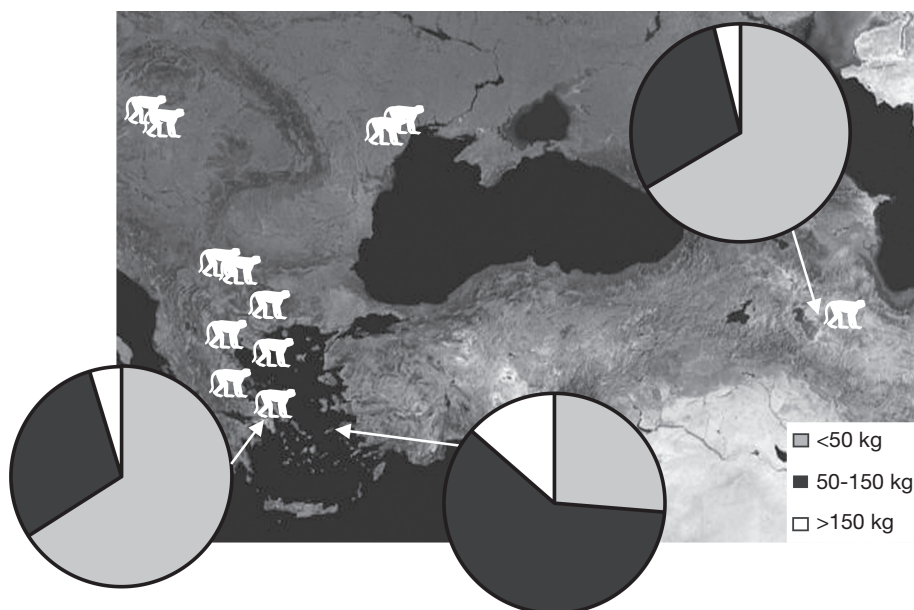


FIG. 32. — Weight spectra of the bovid assemblages of Pikermi (left), Samos (middle-down) and Maragheh (right-top) combined with the geographic distribution of Turolian *Mesopithecus* Wagner, 1939 (data from NOW 2010, <http://www.helsinki.fi/science/now>). For explanation see text.

they lack the natural (here: ecological) meaning of historical entities (i.e. the species). Despite genus-level similarity, there are substantial differences in ungulate species across the P-S-M geographic range but it remains unclear whether these differences are due to genuine chronologic differences between the faunas or whether geography, paleoenvironment and habitat construction contribute to the phenomenal species diversity. For instance, Kostopoulos (2009b) demonstrated important differences at the species level between the neighboring Greek localities of Pikermi and Samos, suggesting a distinct palaeoecological profile. It follows then that a comparison at the species level between the bovid assemblages from Pikermi, Samos and Maragheh is important in order to reveal their palaeoecologic and palaeogeographic relations.

From a total of over 40 bovid species, *Gazella capricornis*, *Protragelaphus skouzesi* and *Miotragocerus* ex. gr. *valenciennesi* are the only bovid taxa shared by Pikermi, Samos and Maragheh. *Palaeoryx palasi* and *Sporadotragus parvidens* are also present in both the Samos and Pikermi faunas, whereas

Samos and Maragheh also share *Gazella* cf. *ancyrensis*, *Prostrepsiceros fraasi*, *Skoufotragus laticeps* and *Samokeros minotaurus*. Finally, Pikermi and Maragheh have in common *Oioceros rothii*, *Tragoptax* ex. gr. *amalthea* and possibly *Prostrepsiceros rotundicornis*. Eight bovid species occurring at Maragheh are not present in Samos and 16 other species known from Samos are missing from the Maragheh faunal assemblage. Furthermore, the predominant bovid association (representing 80% of the bovid assemblage by means of MNI) in these three faunas is quite different (shown in decreasing order):

- Pikermi: *Gazella* + *Palaeoreas* + boselaphines + *O. rothii*;
- Samos: protoryxoid bovids (*Skoufotragus* + *Sporadotragus* + *Palaeoryx*) + *Gazella* + *Miotragocerus* + *Criotherium*;
- Maragheh: *Oioceros* + *Gazella* + *Prostrepsiceros* + *Demecquenemia* n. gen. + *Skoufotragus*.

Gazella represents almost 35% of the Pikermi and *Skoufotragus* almost 34% of the Samos bovid assemblage (by means of MNI), whereas in Ma-

ragheh *Oioceros* and *Prostrepsiceros* are balanced, represented by 26% each.

Although Pikermi and Maragheh are not very different from a strict taxonomic point of view, they show significant differences in the composition of their bovid assemblage and, more importantly, they are both different from the Samos bovid community in between them, implying a longitudinal diversification along the P-S-M axis. Apart, however, from taxonomic differences, Pikermi and Maragheh exhibit similar ecological spectra of their bovid assemblages with predominance of small-sized taxa. Hence, species weighing less than 50 kg represent almost 66% of the Pikermi and 66.5% of the Maragheh bovid assemblage (by means of MNI or 40% and 50% respectively by means of taxonomy), whereas in Samos medium-sized bovids (50-150 kg) clearly prevail (>60% by means of MNI or 58% of taxonomy) (Fig. 32).

There are at least two ways to interpret these results, depending on the preferred time-correlation scenario between the relevant faunas: 1) accepting the hypothesis that Pikermi and Maragheh are older than the bulk of the Samos fauna, the increase in bovid community species body mass can be related to the progressive drying trend associated with the evolution of the Pikermian chronofauna in accordance with Eronen *et al.*'s (2009) observations; and 2) accepting the hypothesis that Pikermi, Samos and Maragheh are roughly equivalent in age, an alternative explanation of the results would be that environmental conditions at the west and east edges of the P-S-M axis were more alike between them than with the center of this biogeographic province. In this case, Pikermi and Maragheh might hold ecologically similar but not identical faunas, notably influenced by the proximate Eastern Paratethys freshwater lacustrine system that could have had a climatic ameliorating effect. Among other evidences supporting such a scenario (see discussions in Strömberg *et al.* 2007; Kostopoulos 2009b), the most striking seems to be the Turolian distribution of cercopithecoid monkeys (Fig. 32). The single Turolian representative of this group in Eurasia, *Mesopithecus* Wagner, 1939 occurs from

the Balkans-SE Europe, to the north coasts of the Black Sea, to Iran and even to Afganistan but it is missing from the Samos-Anatolia area.

Apart from taxa with a relatively great geographic distribution such as *Protragelaphus*, *Tragoportax*, *Miotragocerus vallenciennesi* and *Oioceros rothii*, several of the Maragheh bovid elements show zoogeographic relationships with differing late Miocene areas. *Demecquenemia rodleri* n. comb., *Miotragocerus* cf. *maius* and the large *Palaeoryx* of the MNHN.F Paris collection indicate clear affinities of the Maragheh fauna with the North-East Black Sea region. On the other hand, *G.* cf. *ancyrensis*, *Prostrepsiceros fraasi*, *Prostrepsiceros houtumschindleri*, *Samokeros* and *Skoufotragus* suggest relations between Maragheh and the Samos-Anatolian domain. Some more taxa like *Prostrepsiceros* cf. *vinayaki* and possibly *Nisidorcas* might indicate relationships with Western Asia (Arabo-Afghan and the Indian subcontinent), whereas others like the large *Urmiatherium* are elements common with N China. Thus, Maragheh clearly represents a crossroads of several Late Miocene zoogeographic provinces consistent with its palaeogeographic location (Bernor *et al.* 2009; Eronen *et al.* 2009; Mizrae Ataabadi 2010).

Acknowledgements

DSK is partially supported by a Synthesys project (FR-TAF-1979). Many thanks are due to Claire Sagne and Pascal Tassy for their help during the first author's visit in MNHN. Denis Geraads, Majid Mizrae Ataabadi, Zhang Zhaoqun and Zahra Orak are deeply thanked for information and fruitful discussions on several topics of the paper. RLB wishes to also acknowledge the National Science Foundation, including EAR-0125009 (grant to R. L. Bernor and M. O. Woodburne), BCS-0321893 (grant to F. C. Howell and T. D. White) and the Sedimentary Geology and Paleobiology Program (GEO: EAR: SEP) for supporting his research on this project. DSK is also grateful to Miranda Armour-Chelu for her hospitality. We especially thank A. Ohler, M. Watabe and D. Geraads for their insights and helpful comments on earlier drafts of the manuscript.

REFERENCES

- AGUSTÍ J., CABRERA L., GARCÉS M., KRIJGSMAN W., OMS O. & PARÉS J. M. 2001. — A calibrated mammal scale for the Neogene of Western Europe: state of the art. *Earth Science Review* 52: 247-260.
- ANDREE J. 1926. — Neue Cavicornier aus dem Pliocän von Samos. *Palaeontographica* 67 (6): 135-175.
- ARAMBOURG C. & PIVETEAU J. 1929. — Les vertébrés du Pontien de Salonique. *Annales de Paléontologie* 18: 59-138.
- BERNOR R. L. 1978. — *The Mammalian Systematic, Biostratigraphy and Biochronology of Maragheh and its Importance for Understanding Late Miocene Hominoid Zoogeography and Evolution*. PhD Thesis, University of California, Los Angeles, 314 p.
- BERNOR R. L. 1983. — Geochronology and zoogeographic relationships of Miocene Hominoidea, in CIOCHON R. L. & CORRUCINI R. S. (eds), *New Interpretations of Ape and Human Ancestry*. Plenum Press, New York: 21-64.
- BERNOR R. L. 1986. — Mammalian biostratigraphy, geochronology and zoogeographic relationships of the late Miocene Maragheh fauna, Iran. *Journal of Vertebrate Paleontology* 6: 76-95.
- BERNOR R. L., ANDREWS P. J., SOLOUNIAS N. & VAN COUVERING J. 1979. — The evolution of "Pontian" mammal faunas: some zoogeographic, paleoecologic, and chronostratigraphic considerations. *Annales géologiques des Pays helléniques hors-série I*: 81-90.
- BERNOR R. L., WOODBURN M. & VAN COUVERING J. 1980. — A contribution to the chronology of some Old World Miocene faunas on hipparionine horses. *Geobios* 13: 705-739.
- BERNOR R. L., SOLOUNIAS N., SWISHER III C. C. & VAN COUVERING J. A. 1996. — The correlation of three classical "Pikermian" mammal faunas – Maragheh, Samos, Pikermi – with the European MN Unit System, in BERNOR R. L., FAHLBUSCH V. & MITTMAN H.-W. (eds), *The Evolution of Western Eurasian Neogene Mammal Faunas*. Columbia University Press, New York: 137-154.
- BERNOR R. L., HAILE SELASSIE Y. & ROOK L. 2009. — Paleobiogeography, in HAILE-SELASSIE Y. & WOLDEGABRIEL G. (eds), *Ardipithecus kadabba: Late Miocene Evidence from the Middle Awash, Ethiopia*. University of California Press, Berkeley: 549-563.
- BIBI F. 2008. — Bovidae (Mammalia: Artiodactyla) from the late Miocene of Sivas, Turkey. *Journal of Vertebrate Paleontology* 28: 501-519.
- BOHLIN B. 1935a. — Cavicornier der Hipparion-Fauna Nord-Chinas. *Palaeontologia Sinica* C, 9 (4): 1-166.
- BOHLIN B. 1935b. — *Tsaidamotherium hedini* n. g., n. sp. *Geografiska Annaler*, suppl.: 66-74.
- BOHLIN B. 1936. — Bemerkungen über einige pontische Antilopen-Gattungen. *Arkiv för Zoologi* 28A 18: 1-22.
- BOHLIN B. 1937. — Einige Bemerkungen über die Hörner der Ovibovinae. *Bulletin of the Geological Institution Uppsala* 27: 43-47.
- BONIS L. DE, BOUVRAIN G. & GERAADS D. 1979. — Artiodactyles du Miocène supérieur de Macédoine. *Annales géologiques des Pays helléniques hors-série I*: 167-175.
- BOSSCHA-ERDBRINK D. P. 1978. — Fossil Ovibovines from Garkin near Afyon, Turkey (I) & (II). *Proceedings of the Koninklijke Nederlandse Akademie van Wetenschappen B* 81 (2): 145-185.
- BOSSCHA-ERDBRINK D. P. 1988. — *Protoryx* from three localities East of Maragha, NW Iran. *Proceedings of the Koninklijke Nederlandse Akademie van Wetenschappen* 91 (2): 101-159.
- BOUVRAIN G. 1978. — *Protragelaphus theodori* n. sp. (Mammalia, Artiodactyla, Bovidae) du Miocène de Macédoine (Grèce). *Géologie méditerranéenne* 5: 229-236.
- BOUVRAIN G. 1979. — Un nouveau genre de bovidé de la fin du Miocène. *Bulletin de la Société géologique de France* 21: 507-511.
- BOUVRAIN G. 1982. — Révision du genre *Prostrepsicerus* Major, 1891 (Mammalia, Bovidae). *Paläontologische Zeitschrift* 56: 113-124.
- BOUVRAIN G. 1992. — Antilopes à chevilles spiralées du Miocène supérieur de la province Gréco-Iranienne: nouvelles diagnoses. *Annales de Paléontologie* 78: 49-65.
- BOUVRAIN G. 1994. — Les gisements de mammifères du Miocène supérieur de Kemiklitepe, Turquie. 9. Bovidae. *Bulletin du Muséum national d'Histoire naturelle* 16 (1): 175-209.
- BOUVRAIN G. 1996. — Les gazelles du Miocène supérieur de Macédoine, Grèce. *Neues Jahrbuch für Geologie und Paläontologie, Abhandlungen* 199: 111-132.
- BOUVRAIN G. 2001. — Les Bovidés (Mammalia, Artiodactyla) des gisements du Miocène supérieur de Vathy-lakkos (Grèce du Nord). *Neues Jahrbuch für Geologie und Paläontologie, Abhandlungen* 220: 225-244.
- BOUVRAIN G. & BONIS L. DE 1984. — Le genre *Mesembriacerus* (Bovidae, Artiodactyla, Mammalia): un ovibovin primitif du Vallésien (Miocène supérieur) de Macédoine (Grèce). *Palaeovertebrata* 14: 201-223.
- BOUVRAIN G. & BONIS L. DE 1985. — Le genre *Saomotragus* (Artiodactyla, Bovidae), une antilope du Miocène supérieur de Grèce. *Annales de Paléontologie* 71: 257-299.
- BOUVRAIN G. & BONIS L. DE 1988. — Découverte du genre *Hispanodorcas* (Bovidae, Artiodactyla) dans le Turolien de Grèce septentrionale. *Annales de Paléontologie* 74: 97-112.
- BOUVRAIN G. & THOMAS H. 1992. — Une antilope

- à chevilles spiralées: *Prostrepsiceros zitteli* (Bovidae), Miocène supérieur du Jebel Hamrin en Irak. *Geobios* 25: 525-533.
- BOUVRAIN G., SEN S. & THOMAS H. 1995. — *Parurmiatherium rugosifrons* Sickenberg, 1932, un ovibovinae (Bovidae) du Miocène supérieur d'Injana (Djebel Hamrin, Irak). *Geobios* 28: 719-726.
- CAMPBELL B. G., AMINI M. H., BERNOR R. L., DICKINSON W., DRAKE R., MORRIS R., VAN COUVERING J. A. & VAN COUVERING J. A. H. 1980. — Maragheh: a classical late Miocene vertebrate locality in northwestern Iran. *Nature* 1980: 837-841.
- CHEN G.-F. & ZHANG Z.-Q. 2004. — *Lantiantragus* g. n. (Urmiatheriinae, Bovidae, Artiodactyla) from the Bahe formation, Lantian, China. *Vertebrata Palasiatica* 42: 205-215.
- DMITRIEVA E. L. 2007. — Caprinae (Bovidae, Artiodactyla, Mammalia) from the Neogene of Mongolia. *Paleontological Journal* 41: 671-682.
- ERONEN J. T., MIRZAEI ATAABADI M., MICHEELS A., KARME A., BERNOR R. L., FORTELIUS M. 2009. — Distribution History and Climatic Controls of the Late Miocene Pikermian Chronofauna. *Proceedings of the National Academy of Sciences* 106 (29): 11867-11871.
- GAILLARD C. 1902. — Le bélier de Mendès ou le mouton domestique de l'ancienne Égypte. *Bulletin de la Société d'Anthropologie Biologique de Lyon* 20: 70-103.
- GAUDRY A. 1865. — *Animaux fossiles et Géologie de l'Attique*. Savy, Paris, 476 p.
- GENTRY A. W. 1970. — The Bovidae (Mammalia) of the Fort Ternan fossil fauna, in LEAKEY L. S. B. & SAVAGE R. J. G. (eds), *Fossil Vertebrates of Africa*. 2. Academic Press, London: 243-323.
- GENTRY A. W. 1971. — The earliest goats and other antelopes from the Samos *Hipparion* Fauna. *Bulletin of the British Museum (Natural History), Geology* 20: 229-296.
- GENTRY A. W. 1996. — A fossil *Budorcas* (Mammalia, Bovidae) from Africa, in STEWART K. M. & SEYMOUR K. L. (eds), *Paleoecology and Palaeoenvironments of Late Cenozoic Mammals*. University of Toronto Press, Toronto: 571-587.
- GENTRY A. W. 1999. — Fossil Pecorans from the Baynunah Formation, Emirate of Abu Dhabi, United Arab Emirates, in WHYBROW P. & HILL A. (eds), *Fossil Vertebrates of Arabia*. Yale University Press, New Haven: 290-316.
- GENTRY A. W. 2003. — Ruminantia (Artiodactyla), in FORTELIUS M., KAPPELMAN J., SEN S. & BERNOR R. (eds), *Geology and Paleontology of the Miocene Sinap Formation, Turkey*. Columbia University Press, New York: 332-379.
- GENTRY A. & HEIZMANN E. P. J. 1996. — Miocene Ruminants of central and eastern Tethys and Paratethys, in BERNOR R., FAHLBUSH V. & MITTMANN H.-W. (eds), *The Evolution of Western Eurasian Neogene Mammal Faunas*. Columbia University Press, New York: 378-391.
- GENTRY A. W., RÖSSNER G. E. & HEIZMANN P. J. 1999. — Suborder Ruminantia, in RÖSSNER G. & HEISSIG K. (eds), *The Miocene Land Mammals of Europe*. Verlag Dr F. Pfeil, Munich: 225-258.
- GERAADS D. 1974. — *Les giraffidés du Miocène supérieur de la région de Thessalonique (Grèce)*. PhD Thesis, Université Paris VI, 103 p.
- GERAADS D. & GÜLEÇ E. 1999. — On some spiral-horned antelopes (Mammalia: Artiodactyla: Bovidae) from the late Miocene of Turkey, with remarks on their distribution. *Paläontologische Zeitschrift* 73 (3/4): 403-409.
- GERAADS D. & SPASSOV N. 2008. — A new species of *Criotherium* (Bovidae, Mammalia) from the late Miocene of Bulgaria. *Hellenic Journal of Geosciences* 43: 21-27.
- GERAADS D., GÜLEÇ E. & KAYA T. 2002. — *Sinotragus* (Bovidae, Mammalia) from Turkey and the late Miocene Middle Asiatic Province. *Neues Jahrbuch für Geologie und Paläontologie, Monatshefte* 8: 477-489.
- GERAADS D., SPASSOV N. & KOVACHEV D. 2003. — *Palaeoreas lindermayeri* (Wagner, 1848) (Mammalia, Bovidae) from the upper Miocene of Bulgaria, and a revision of the species. *Geodiversitas* 25 (2): 405-415.
- HEINTZ E. 1963. — Complément d'étude sur *Oioceros atropatenes* (Rod. et Weith.), antilope du Pontien de Maragha (Iran). *Bulletin de la Société géologique de France* 5: 109-116.
- HEINTZ E. 1970. — Les Cervidés villafranchiens de France et d'Espagne. Volume II: figures et tableaux. *Mémoires du Muséum national d'Histoire naturelle sér. C*, 22: 1-205.
- HEINTZ E. 1971. — *Gazella deperdita* (Gervais) 1847 (Bovidae, Artiodactyla, Mammalia) du Pontien du Mont Luberon, Vaucluse, France. *Annales de Paléontologie* 57 (2): 209-229.
- KÖHLER M. 1987. — Boviden des türkischen Miozäns (Känozoikum und Braunkohlen der Türkei). *Paleontologia i Evolucio* 21: 133-246.
- KÖHLER M. 1993. — Skeleton and habitat of recent and fossil ruminants. *Münchner Geowissenschaftliche Abhandlungen*, A 25: 1-88.
- KOROTKEVICH E. L. 1976. — [*The Late Neogene Gazelles*]. Naukova Doumka, Kiev, 251 p. (in Russian).
- KOSTOPOULOS D. S. 2005. — The Bovidae (Artiodactyla, Mammalia) from the Late Miocene mammal locality of Akkaşdağı (Central Anatolia, Turkey). *Geodiversitas* 27 (4): 747-791.
- KOSTOPOULOS D. S. 2006. — The late Miocene vertebrate locality of Perivolaki, Thessaly, Greece. 9. Cervidae and Bovidae. *Palaeontographica* Abt. A 276 (1-6): 151-183.
- KOSTOPOULOS D. S. 2009a. — The Late Miocene Mam-

- mal Faunas of the Mytilinii Basin, Samos Island, Greece: new collection. 13. Bovidae. *Beiträge zur Paläontologie* 31: 345-389.
- KOSTOPOULOS D. S. 2009b. — The Pikermian Event: temporal and spatial resolution of the Turolian large mammal fauna in SE Europe. *Palaeogeography, Palaeoclimatology, Palaeoecology* 274: 82-95.
- KOSTOPOULOS D. S. & KOUFOS G. D. 1999. — The Bovidae (Mammalia, Artiodactyla) of the Nikiti-2 (NIK) faunal assemblage (Chalkidiki peninsula, N. Greece). *Annales de Paléontologie* 85: 193-218.
- KOSTOPOULOS D. S., SEN S. & KOUFOS G. D. 2003. — Magnetostratigraphy and revised chronology of the late Miocene mammal localities of Samos, Greece. *International Journal of Earth Sciences* 92: 779-794.
- KOUFOS G. D., KOSTOPOULOS D. S. & VLACHOU T. 2009. — The Late Miocene Mammal Faunas of the Mytilinii Basin, Samos Island, Greece: new collection. 16. Chronology. *Beiträge zur Paläontologie* 31: 397-408.
- KRAKHMALNAYA T. V. 1996. — [*The Old Meotian Hipparion Fauna from the North of the Black Sea*]. Naukova Dumka, Kiev, 225 p. (in Russian).
- LI C. K., WU W. Y. & QIU Z. D. 1984. — Chinese Neogene subdivision and correlation. *Vertebrata Palasiatica* 22 (3): 163-178 (in Chinese with English summary).
- LYDEKKER R. 1886. — On the fossil mammalia of Maragha in Northwest Persia. *Quarterly Journal of the Geological Society* 42: 173-176.
- MADE J. VAN DER & HUSSAIN S. T. 1994. — Horn-cores of *Sivoreas* (Bovidae) from the Miocene of Pakistan and utility of their torsion as a taxonomic tool. *Geobios* 27: 103-111.
- MECQUENEM R. DE 1908. — Contribution à l'étude du gisement des vertébrés de Maragha et de ses environs, in MORGAN J. DE (ed.), Délégation scientifique en Perse. *Annales d'Histoire Naturelle*, I, *Paléontologie*: 27-79.
- MECQUENEM R. DE 1925. — Contribution à l'étude des fossiles de Maragha. *Annales de Paléontologie* 13: 135-160.
- MELADZE G. K. 1967. — *Hipparion fauna of Arkneti and Bazaleti (Georgia)*. Izdatelystvo "Mecniereba", Tbilisi, 168 p. (in Russian).
- MIZRAE ATAABADI M. 2010. — *The Miocene of Western Asia; Fossil Mammals at the Crossroads of Faunal Provinces and Climate Regimes*. PhD Thesis, University of Helsinki, Helsinki University Press, 65 p.
- MIZRAE ATAABADI M., BERNOR R. L., KOSTOPOULOS D. S., WOLF D., ORAK Z., ZAREE GH., NAKAYA H., WATABE M. & FORTELIUS M. in press. — Recent advances in paleobiological research of the late Miocene Maragheh fauna, Northwest Iran, in XIAOMING W., FORTELIUS M., FLYNN L. (eds), *Asian Neogene Mammal Biostratigraphy and Chronology*. Columbia University Press, New York.
- PILGRIM G. E. 1934. — Two species of sheep-like antelopes from the Miocene of Mongolia. *American Museum Novitates* 716: 1-29
- PILGRIM G. E. 1939. — The fossil Bovidae of India. *Paleontologia Indica* n.s. 1: 1-365.
- PILGRIM G. E. & HOPWOOD A. 1928. — *Catalogue of the Pontian Bovidae of Europe*. British Museum (Natural History), London, 106 p.
- POHLIG H. 1886. — On the Pliocene of Maragha, Persia and its resemblance to that of Pikermi in Greece: on fossil elephant remains of Caucasia and Persia and on the results of a monograph of the fossil elephants of Germany and Italy. *Quarterly Journal of the Geological Society* 42: 177-182.
- QIU Z.-X., WANG B. Y. & XIE G. P. 2000. — Preliminary report on new genus of Ovibovinae from Hezheng district, Gansu, China. *Vertebrata Palasiatica* 38: 128-134 (in Chinese with English summary).
- RODLER A. 1885. — Das Knochenlager und die Fauna von Maragha. *Verhandlungen der k.k. geologische Reichsanstalt*: 333-337.
- RODLER A. 1888. — Notiz über ein Besitze des Dr J.E. Polak befindliches Schädelfragment eines Sivatheriden vom Knochenfelde von Maragha am Urmiassee in Nordpersien. *Anzeiger Österreichische Akademie der Wissenschaften Mathematisch naturwissenschaftliche Klasse* 25: 114-115.
- RODLER A. 1889. — Über *Urmiatherium polaki* n. g., n. sp., einen neuen Sivatheriiden aus dem Knochenfelde von Maragha. *Denkschriften der Kaiserlichen Akademie der Wissenschaften, Mathematisch-Naturwissenschaftliche Klasse* 56: 315-322.
- RODLER A. & WEITHOFER K. A. 1890. — Die Wiederkäuer der Fauna von Maragha. *Denkschriften der Kaiserlichen Akademie der Wissenschaften, Mathematisch naturwissenschaftliche Klasse* 57: 753-771.
- ROUSSIAKIS S. 2003. — *Oioceros rothii* (Wagner, 1857) from the late Miocene of Pikermi (Greece): cranial and dental morphology, comparison with related forms. *Geobios* 25 (4): 717-735.
- ROUSSIAKIS S. 2009. — *Prostrepsiceros* and *Protragelaphus* (Artiodactyla, Mammalia) from the late Miocene locality of Chomateri (Attica, Greece). *Annales de Paléontologie* 95: 181-195.
- SCOTT K. M. 1979. — *Addaptation and Allometry in Bovid Postcranial Proportions*. PhD Thesis, Yale University, New Haven, 493 p.
- SICKENBERG O. 1933. — *Parurmiatherium rugosifrons* ein neuer Bovide aus dem Unterpliozän von Samos. *Palaeobiologica* 5: 81-102.
- SOLOUNIAS N. 1981. — The Turolian fauna from the island of Samos, Greece. *Contribution to Vertebrate Evolution* 6: 1-232.
- SPASSOV N. & GERAADS D. 2004. — *Tragoportax* Pilgrim, 1937 and *Miotragocerus* Stromer, 1928 (Mammalia,

- Bovidae) from the Turolian of Hadjidimovo, Bulgaria, and a revision of the late Miocene Mediterranean Boselaphini. *Geodiversitas* 26 (2): 339-370.
- STRÖMBERG C. A. E., WERDELIN L., FRIIS E. M. & SARAÇ G. 2007. — The spread of grass-dominated habitats in Turkey and surrounding areas during the Cenozoic: phytolith evidence. *Palaeogeography, Palaeoclimatology, Palaeoecology* 250: 18-49.
- SWISHER III C. C. 1996. — New $^{40}\text{Ar}/^{39}\text{Ar}$ dates and their contribution toward a revised chronology for the late Miocene nonmarine of Europe and West Asia, in BERNOR R. L., FAHLBUSCH V. & MITTMANN H.-W. (eds), *The Evolution of the Western Eurasian Neogene Mammal Faunas*. Columbia University Press, New York: 64-77.
- TEKKAYA I. 1973. — Une nouvelle espèce de *Gazella* de Sinap moyen. *Bulletin of the Mineral Research and Exploration* 80: 118-143.
- THOMAS H., MORALES J. & HEINTZ E. 1982. — Un nouveau bovidé (Artiodactyla, Mammalia) *Hispanodorcas torrubiae* n. g., n. sp., dans le Miocène supérieur d'Espagne. *Bulletin du Muséum national d'Histoire naturelle*, Paris, 4^e sér., section C (3-4): 209-222.
- WAGNER A. 1848. — Urweltliche Säugethier-Überreste aus Griechenland. *Abhandlungen der bayerischen Akademie der Wissenschaften Mathematisch naturwissenschaftliche Klasse* 5: 333-378.
- WAGNER A. 1857. — Neue Beiträge zur Kenntniss der fossilen Säugethier-Überreste von Pikermi. *Abhandlungen der bayerischen Akademie der Wissenschaften. Mathematisch naturwissenschaftliche Klasse* 8: 111-158.
- WATABE M. 1990. — Fossil bovids (Artiodactyla, Mammalia) from Maragheh (Turolian, late Miocene), Northwest Iran. *Annual Report Historical Museum Hokkaido* 18: 19-55.
- WATABE M. & NAKAYA H. 1991. — Phylogenetic significance of the postcranial skeletons of the hipparions from Maragheh (Late Miocene), Northwest Iran. *Memoirs of the Faculty of Science, Kyoto University, Series of Geology & Mineralogy* 56 (1-2): 11-53.
- ZHANG Z.-Q. 2003. — A new species of *Shaanxispira* (Bovidae, Artiodactyla, Mammalia) from the Bahe formation, Lantian, China. *Vertebrata Palasiatica* 41: 230-239.
- ZHANG Z.-Q., WANG B.-Y. & XIE G.-P. 2000. — Preliminary report on a new genus of Ovibovinae from Hezheng district, Gansu, China. *Vertebrata Palasiatica* 38: 128-134.

Submitted on 3 March 2010;
accepted on 17 December 2010.